

CD8 $\alpha\alpha$ dimer is a receptor for Nipah virus on porcine lymphocytes

by

Nikesh Tailor

A Thesis submitted to the Faculty of Graduate Studies of

The University of Manitoba

in partial fulfilment of the requirements of the degree of

Master of Science

Department of Medical Microbiology and Infectious Diseases

University of Manitoba

Winnipeg, Manitoba

Copyright © 2019 by Nikesh Tailor

ABSTRACT

Nipah virus (NiV) and Hendra Virus (HeV) (Paramyxoviridae; *Henipavirus*) cause severe often fatal illness in humans, but can also infect swine. The presented work compared permissibility of porcine peripheral blood mononuclear cells to NiV and to HeV. While majority of cell populations did not support replication of either HeV or NiV, monocytes were permissive to both viruses. CD8⁺ subpopulations of T and NK cells were permissive only to NiV, even though they did not express ephrin B2 (receptor for HeV and NiV) on the surface. CHO-K1 cells transfected with porcine CD8 α became permissive to NiV. Antibody against CD8 α was able to block NiV replication in CD8⁺ cells; competition assays between HeV or NiV soluble virus attachment protein (sG) suggested that NiV can bind to CD8 $\alpha\alpha$ expressing porcine cells while HeV cannot. CD8 $\alpha\beta$ cells were not permissive to NiV or HeV. The results indicate that porcine CD8 α dimer is a receptor for Nipah virus, but not for HeV on porcine lymphocytes. This work has implications in vaccine design. Development of a veterinary vaccine against NiV which elicits cell mediated immune response is needed.

ACKNOWLEDGMENTS

The work presented here would not have been possible without the help and support of numerous people. First and foremost I'd like to thank Dr. Hana Weingartl for the opportunity to carry out my research as well as guidance and mentoring. I'd also like to thank all the members of the Special Pathogen Unit for the help. I would like to thank Greg Smith, Peter Marszal, Brad Collignon, and Dr. Bradley Pickering for technical assistance, training, support, and advice that helped throughout my masters thesis work.

I thank my committee members, Dr. Michael Drebot, Dr. Xi Yang, and Dr. Charles Nfon for their advice, interest, and input in this project.

I would like to thank the staff at the National Centre for Foreign Animal Disease, Canadian Food Inspection Agency of the and University of Manitoba that has helped me throughout my program. Finally, I would like to thank my parents, brother, and friends, and Aleksandra Kaminska for the overwhelming encouragement, patience and having faith in me over the years.

The thesis research funding was provided from the NSERC grant #327187-2012. I will like to thank and the University of Manitoba for funding to support this research project.

Table of Contents

ABSTRACT.....	2
Acknowledgements.....	3
Table of contents.....	4
List of Tables.....	8
List of Figures.....	9
Abbreviations.....	11
SECTION	
1.0 Introduction.....	15
1.1 Taxonomy.....	15
1.2 Hendra Virus Outbreaks.....	16
1.3 Nipah Virus Outbreaks.....	17
1.4 Nipah and Hendra Virus Infections in Humans.....	20
1.5 Nipah and Hendra Virus Infections in Pigs.....	22
1.6 A) Genome and Virion Structure.....	26
1.6 B) Virus Replication.....	26
1.7 Nipah Virus and Hendra Virus Structural Proteins.....	30
1.8 Function of the Non-Structural Proteins.....	35
1.9 Receptors for Hendra and Nipah Virus.....	36
1.10 Binding of NiV/HeV G to Ephrin B2/B3	38
1.11 Peripheral Blood Mononuclear Cells (PBMC's).....	39
1.12 Rationale.....	45

2.0 Materials and Methods.....	47
2.1 Cell Cultivation and Passaging of continuous cell lines.....	47
2.2 Recovery of the Cells.....	49
2.3 Virus Stock.....	49
2.4 Plaque Assays.....	50
2.5 RNA Isolation.....	52
2.6 NiV and HeV Reverse Transcription (RT) PCR.....	53
2.7 Peripheral Blood Mononuclear Cells (PBMC's) Harvesting from Porcine Blood....	54
2.8 Cell Sorting from PBMC.....	55
2.9 Extraction of CD8 $\alpha\beta$ cells from the Porcine Thymus.....	59
2.10 Cell Inoculation with Virus.....	59
2.11 Preparation of Flow Cytometry Compensation Beads.....	61
2.12 Intracellular Staining for the NiV/HeV N Antigen.....	62
2.13 Flow Cytometry Protocol.....	62
2.14 Whole Cell Lysate Preparation.....	63
2.15 Protein separation by SDS-PAGE.....	63
2.16 Immunoblot to detect ephrin B2.....	64
2.17 Determining Ephrin B2, CD8 α , and CD16 Surface Expression in Cells.....	65
2.18 Transfection of CHO-K1 Cells.....	66
2.19 Immunofluorescent Staining of Cells.....	67
2.20 Receptor Blocking.....	70
2.21 Competition assay.....	71
2.22 <i>In silico</i> Modeling.....	71

2.23 Ethics Statement.....	72
3.0 Results.....	73
3.1 <i>In vitro</i> permissivity of porcine PBMC subpopulations to NiV and HeV	73
3.1a Virus Stock Preparation and titration.....	73
3.1b Cell Preparation from preprial blood.....	73
3.1c Replication of NiV and HeV in the Porcine Primary Immune cells.....	75
3.2 Detection of Ephrin B2 protein by Immunoblot and Flow Cytometry.....	83
3.3 Ephrin B2 and CD8 α Antibody Blocking Assays.....	87
3.4 CD8 $\alpha\beta$ is not a receptor for Nipah Virus.....	90
3.5 Porcine CD8 α and Ephrin B2 Transfection in Chinese Hamster Ovary Cells.....	94
3.6 Competition of the HeV or NiV Soluble G with NiV on Porcine CD8+ cells.....	100
3.7 <i>In silico</i> modelling of Porcine CD8 α -NiV Glycoprotein Interaction.....	106
4.0 Discussion.....	109
4.1 Permissibility of IPAM 3D4/31 to HeV and NiV.....	109
4.1a Virus replication in IPAM 3D4/31.....	109
4.1b Ephrin expression in IPAM 3D4/31.....	110
4.1c Competition of the HeV or NiV Soluble G with NiV on IPAM 3D4/31.....	111
4.2 CD8 $\alpha\alpha$ dimer is a second receptor for NiV	
4.2a NiV and HeV infection of porcine PBMC subpopulations <i>in vitro</i>	111
4.2b Detection of ephrin B2 in sorted porcine PBMC and cell lines	112
4.2c Blocking if NiV replication by antibody against ephrin B2 and CD8 α	113
4.2d CD8 $\alpha\beta$ is not a receptor for Nipah Virus.....	113
4.2e CD8 $\alpha\alpha$ dimer serves as a receptor for NiV.....	114

4.3 Competition of HeV/NiV Soluble G with NiV on Porcine CD8+ cell.....	115
4.4 <i>In silico</i> Modeling of Porcine CD8 α -NiV Glycoprotein Interaction.....	116
4.5 Conclusion.....	116
5.0 References.....	121

List of Tables

Table 1: CD8 α expressing cells.....	43
Table 2: Cell lines used, culture methods, and characteristics.....	48
Table 3: Antibodies and dilutions used for flow cytometry, immunoblotting, and immunofluorescence.....	57
Table 4: Nucleotide sequence of porcine CD8 α and Ephrin B2 used for cloning.....	69
Table 5: Percent purity post selection of PBMC's and the percentage of cells positive for selection antibody 24h and 48h post selection.....	74
Table 6: Ephrin B2 expression in selected cells, PBMCs and permissiveness to NiV...86	

List of Figures

Figure 1: Diagram of Nipah and Hendra genome arrangement and structure.....	28
Figure 2: NiV and HeV replication cycle.....	29
Figure 3: Structure of membrane attached and soluble forms of G protein.....	34
Figure 4: Structure and NiV/HeV fusion protein.....	34
Figure 5: Preparation of 100ml of 1.75% CMC overlay.....	51
Figure 6: Flow chart of sorting of PBMC.....	58
Figure 7: Vector maps of pCDNA3.1 (+)-pCD8 α plasmid (A) and pCDNA3.1 (+)- pEFNB2plasmid (B).....	68
Figure 8: Comparing CD8+CD16- cells inoculated with NiV at 24h and 48h post selection by (A) RT-PCR and (B) plaque assay.....	77
Figure 9: Replication of NiV in the subpopulations of porcine PBMC.....	78
Figure 10: Replication of HeV in the subpopulations of porcine PBMC.....	79
Figure 11: Flow cytometry analysis of PBMC subsets inoculated with HeV or NiV 48 hpi showing negative anti-HeV/NiV N-protein antibody staining.....	80
Figure 12: Flow cytometry analysis of PBMC subsets inoculated with HeV or NiV 48 hpi showing positive anti-HeV/NiV N-protein antibody staining.....	81
Figure 13: Flow cytometry analysis of (A) CD16+ cells, (B) CD8+CD16-, and (C) CD8+CD16+ cells inoculated with NiV 48 hpi showing positive anti-HeV/NiV N-protein antibody staining.....	82
Figure 14: Ephrin B2 immuno Blot: Ephrin B2 expression in cell lines and selected PBMC subsets.....	84
Figure 15: Flow cytometry analysis of ephrin B2 expression.....	85
Figure 16: (A) RT-PCR and (B) Plaque Assay Data of replication of NiV in porcine CD8+ cells in concentrations of non-conjugated porcine CD8 α antibody at 24 hrs.....	88
Figure 17: (A) RT-PCR and (B) Plaque Assay Data of the replication of NiV in porcine CD8+ cells in concentrations of non-conjugated ephrin B2 antibody at 24hrs.....	89
Figure 18: Flow cytometry analysis of porcine CD8 β	91
Figure 19: RT-PCR and plaque assay analysis of NiV inoculated CD8 β selected cells...	92

Figure 20: Negative Immunohistochemistry staining for NiV of <i>in vivo</i> NiV infected porcine thymus.....	93
Figure 21: Confirmation of the lack of ephrin B2 expression in CHO-K1 cells by western blot.....	96
Figure 22: Flow cytometry analysis of CHO-K1 transfected cells.....	97
Figure 23: (A) RT-PCR and (B) plaque assay analysis of CHO-K1 cells transfected with ephrinB2 and/or CD8 α	98
Figure 24: Confocal microscopy staining of receptor-negative and -positive cells.....	99
Figure 25: (A) RT-PCR and (B) Plaque Assay Data of the replication of NiV and HeV in IPAM 3D4/31 cells in various amounts of HeVsG at 24h time point.....	102
Figure 26: (A) RT-PCR and (B) Plaque Assay Data of the replication of NiV in porcine CD8+ cells in various amounts of NiV and HeV sG at 24 h time point.....	103
Figure 27: (A) RT-PCR and (B) Plaque Assay Data of the replication of NiV in porcine CD8+ cells in 6 μ l/ml of NiV and HeV sG.....	104
Figure 28: Percent inhibition of 6 μ l/ml NiV and HeVsG treatment in NiV infected porcine CD8+ cells compared to non-blocked control.....	105
Figure 29: Top three models from ClusPro ranked by ClusPro, PS-HomPPI/DockRank, and DockScore.....	108

Abbreviations

ALCAM	Activated leukocyte cell adhesion molecule
APC	Antigen presenting cell
BBB	Blood brain barrier
BSL4	Biosafety level 4
BSA	Bovine Serum Albumin
CARD	Caspase activation and recruitment domain
CD	Cluster of differentiation
CHO	Chinese Hamster Ovary cells
CMC	Carboxymethylcellulose
ConA	Concanavalin A
CPE	Cytopathic effect
CNS	Central nervous system
CO₂	Carbon Dioxide
CSF	Cerebrospinal fluid
CTL	Cytotoxic T lymphocyte
DC	Dendritic cell
DMEM	Dulbecco's modified Eagle's medium
DMSO	Dimethyl sulfoxide
dpi	Days post inoculation
DTT	Dithiothreitol
EDTA	Ethylene dinitrilotetracetic acid
EMEM	Eagle's minimal essential medium

ER	Endoplasmic reticulum
FBS	Fetal bovine serum
FITC	Fluorescein isothiocyanate
GFP	Green fluorescent protein
GTP	Guanosine-5'-triphosphate
GS	Gene start sequence
HeV	Hendra virus
HIV	Human immunodeficiency virus
hpi	Hours post inoculation
hrs	Hours
IFA	Immunofluorescence Assay
IFN	Interferon
Ig	Immunoglobulin
IL	Interleukin
IN	Intranasal
IPAM	Immortalized porcine alveolar macrophage
JAK	Janus activated kinase
MAb	Monoclonal antibody
MEK	Mitogen activated kinase
MeV	Measles virus
MHC	Major histocompatibility complex
MOI	Multiplicity of infection
Min	Minutes

mRNA	Messenger RNA
MW	Molecular Weight
N	Nucleoprotein
NES	Nuclear export sequence
NF-κB	Nuclear factor kappa B
NiV	Nipah virus
NK	Natural killer cell
NLS	Nuclear localization sequence
nt	Nucleotides
ORF	Open reading frame
PAGE	Polyacrylamide gel electrophoresis
PBMC	Peripheral blood mononuclear cell
PBS	Phosphate buffered saline
PCR	Polymerase chain reaction
PE	Phycoerythrin
PFU	Plaque forming unit
PK15	Porcine kidney cells
RdRp	RNA dependent RNA polymerase
RLR	RIG-1 like receptor
RNA	Ribonucleic acid
RNP	Ribonucleocapsid
RT	Room temperature
RTK	Tyrosine kinase receptor

RT-PCR	Reverse transcriptase-PCR
SDS	Sodium dodecyl sulfate
Ser	Serine
SH2	Tyrosine-protein kinase homology
ST	Swine testis fibroblast cells
STAT	Signal transducer and activator of transcription
TBS-T	Tris buffered saline with Tween-20
TCR	T cell receptor
Th	T helper cell subset
Vero	African green monkey kidney cell line

Introduction

1.1 Taxonomy

Nipah virus (NiV) and Hendra virus (HeV) are two highly pathogenic zoonotic viruses found in the genus *Henipavirus* which also contains Mojiang virus, Ghanaian bat virus and the non-pathogenic Cedar virus (Weatherman et al., 2018). Cedar virus was isolated from Australian flying fox (*Pteropus alecto* and *P. poliocephalus*) urine. Ferrets and guinea pigs inoculated with Cedar virus did not develop clinical disease (Marsh et al., 2012). Mojiang virus was discovered in form of RNA isolated from rat urine during a study to investigate the presence of potential zoonotic pathogens in cave dwelling animals after three people working in an abandoned mine in China acquired a fatal pneumonia of unknown origin in 2012 (Wu et al., 2012). In Ghana, a study in which the droppings of the African straw-coloured fruit bat (*Eidolon helvum*) were sampled led to the isolation of the RNA of a novel Henipavirus, which was designated Ghanaian bat virus. A follow-up study found antibodies against Ghanaian bat virus or a related henipavirus in the sera of pigs in Ghana (Drexler et al., 2009). Nipah has two genotypes: Nipah Bangladesh (NiV-B) and Nipah Malaysia (NiV-M), which have differences in infectivity and pathogenicity (Clayton et al., 2002).

NiV and HeV are very similar both in physical structure and at the genomic level. They both contain a non-segmented, negative stranded RNA genome coding for six structural proteins and three non-structural viral proteins. The viruses belong to the family Paramyxoviridae, found in the order *Mononegavirales*. The order *Mononegavirales* is host to many of the world's most deadly viruses, including rabies virus and ebola viruses (Afonso et al., 2016).

1.2 Hendra Virus Outbreaks

HeV was discovered in 1994 during an outbreak in horses and humans in the Hendra suburb of Brisbane, Australia. In this outbreak, 14 of the 20 infected horses died of the infection and the remaining 6 were euthanized. Two individuals who were in close contact with infected horses developed influenza like illness which resulted in the death of one of them (Murray et al., 1995; Murray et al., 1996). A comparison study of the virus isolated from the deceased individual and one of the infected horses concluded that both the horses and humans were infected with the same virus: The virus contained RNA with 50% homology to the morbillivirus M gene (Murray et al., 1995), but the virus was not neutralized by anti-morbillivirus serum (Murray et al., 1995; Wang L et al., 1998).

Outbreaks of HeV usually occur between the months of May and October (Smith et al., 2011). From 1994-2010, there were occasional HeV outbreaks in coastal Queensland and north-eastern New South Wales. Between 2011 and 2013, there was a spike in reports of HeV: 34 horses were reported with HeV infection (Cowled et al., 2017). The first natural canine infection also occurred during this period (Anonymous, 2011). Horses are the main species that become infected with HeV, and human HeV infections are very rare. There have been only seven reported human cases, four of which were fatal (Cowled et al., 2017). Human to human transmission has never been observed, although HeV RNA has been isolated from the nasopharyngeal aspirates of infected persons (Playford et al., 2010). There is no human vaccine for HeV but there is a horse vaccine available which is the main preventative measure against transmission of HeV to horses from the natural reservoir (Middleton et al., 2014).

Following the initial HeV outbreak, 46 animal species were screened in an attempt to determine the reservoir for HeV. Detection of HeV antibodies (including neutralizing ones) in frugivorous bats quickly led to the identification of pteropus bats (flying foxes) as the natural reservoir for HeV (Chua et al., 2002; Halpin et al., 2000; Young et al., 1996). Using virus isolation and RT-PCR, Halpin and colleagues found HeV in pteropus bat tissues, uterine fluid, and urine. However, excretion of HeV by bats is extremely low, accounting for the sporadic nature of outbreaks of HeV (Halpin et al., 2000; Halpin et al., 2001).

Bat to horse transmission of HeV was documented 32 times between 1994 and 2011. Horses are thought to get infected by consuming food that has been contaminated with bat saliva and urine (Murry et al., 2005). HeV is transmitted horse to horse through airborne transmission and direct contact (Selvey et al., 1996).

1.3 Nipah Virus Outbreaks

In 1998/1999, an outbreak of what was originally thought to be Japanese encephalitis virus (JEV) occurred in Malaysia (Chua, 2003). In this outbreak, there were a total of 265 reported human cases and 105 deaths. It was determined that close contact with pigs was the primary source of human infection (Parashar et al., 2000). It later became clear that the outbreak was caused by the previously unknown virus, which was transmitted from pigs to humans. NiV was first isolated from an ill individual from a small village in Malaysia called Sungai Nipah, after which the virus was named (Chua et al., 2000). Sequencing studies concluded that NiV isolates collected from pigs had identical sequences to the NiV isolates collected from humans during the outbreak (AbuBakar et al., 2004). The Malaysian government culled over one million pigs in order to stop the outbreak, causing severe economic loss (Uppal, 2000).

It was later discovered that urine and saliva from fruit bats (*P.hypomelanus* and *P. vampyrus*) and fruit partially eaten by these fruit bats contained NiV (Chua et al., 2002; Chua, 2003). NiV neutralizing antibodies were found in 7% to 58% of *P. vampyrus* and *P. hypomelanus* in Malaysia, depending on region (Yob et al., 2001; Daszak et al., 2006), and also in Cambodia, Bangladesh, and other Asian countries (Hsu et al, 2004; Reynes et al., 2005). When *P. poliocephalus* bats were infected experimentally with NiV, no clinical signs were present (Middleton et al., 2007).

All the cases of human NiV-Malaysia infections were in people who worked with pigs. NiV infection is thought to have occurred by ingestion of contaminated fruit; subsequently, the pigs transmitted the virus to humans and other pigs by direct exposure to bodily fluids and aerosols (Chua et al., 2000). Pig to human transmission is thought to have occurred through close range exposure to infectious respiratory secretions of pigs, especially during feeding times, when pigs squeal and aerosolize considerable amounts of these secretions (Luby et al., 2012; Tan et al., 1999). Human to human transmission was also observed in the Malaysian outbreak but infrequently (Tan & Tan., 2001; Parashar et al., 2000). There has been no occurrence of the NiV Malaysia strain since the initial 1998/1999 outbreak.

In Bangladesh, there were eight NiV outbreaks from 2001-2008 which resulted in 135 human cases and 98 human deaths (Clayton, 2017; Hsu et al., 2004; Luby et al., 2006; Montgomery et al., 2008). Since 2008, there have been NiV outbreaks nearly annually. The mode of transmission of the NiV Bangladesh to humans is by the ingestion of raw date palm sap contaminated by bats, and can be followed by human to human transmission (Luby et al., 2012; Hsu et al., 2004). Due to the respiratory distress in patients with NiV-B infection, airborne transmission to people who were in contact with an ill individual is likely. Transmission from

dead people was also observed (Chakraborty et al., 2016; Hegde et al., 2016; Weatherman et al., 2018). NiV Bangladesh also had increased viral shedding which may have led to higher human to human transmission (Pulliam et al., 2011).

A henipavirus outbreak occurred in the Philippine villages of Tinalon and Midtungok in 2014. IgM ELISA results were positive for NiV antibodies. RT-PCR analysis confirmed short NiV sequence in one serum sample five days after clinical onset. ELISA was used to confirm that 17 people and 10 horses had been infected. Of the 17 human cases, 9 had died; all 10 of the infected horses had died as well (Ching et al., 2015). Transmission to humans was from direct exposure to infected horses and consumption of undercooked horse meat. Human to human virus transmission was also evident in this outbreak (Ching et al., 2015).

In 2018, there was an outbreak of NiV in the Kozhikode and Malappuram districts of Kerala, India. There were 17 deaths and 18 confirmed cases as of June 1, 2018. NiV was confirmed as the etiological agent by testing throat swabs, urine and blood samples of ill individuals using RT-PCR and IgM ELISA for NiV by the National Institute of Virology in Pune (Arunkumar et al, 2018).

1.4 Nipah and Hendra Virus Infections in Humans

NiV can manifest as influenza like illness with consequences ranging from a simple fever to death. The virus can affect multiple organ systems and displays preferential respiratory and neurological tropism (Gurley et al., 2007). In humans, NiV infection mainly takes the form of severe acute encephalitis. Many NiV-infected patients also developed reduced levels of consciousness (Wong et al., 2002). During the Malaysian outbreak, 12 survivors of acute encephalitis later had relapse of encephalitis. Ten individuals who initially had acute, non-encephalitic or asymptomatic infection suffered from late-onset encephalitis. Of the 22 total cases of relapsing encephalitis, four died (Tan et al., 2002; Chong et al., 2003).

Respiratory disease is more common with NiV Bangladesh infection: 62% of people who were infected had cough and 69% of people had respiratory difficulty compared to 14% of people infected with NiV Malaysia who experienced cough (Hossain et al., 2008; Goh et al., 2000).

Pathology of NiV in humans:

During the first outbreak in Malaysia, patients presented primarily with encephalitis and autopsy studies revealed there was substantial central nervous system (CNS) involvement with strong immunostaining of neuronal and endothelial cells.

Pathological clinical investigations on NiV infections have determined that NiV infects multiple organ systems. Vasculitis was found in the blood vessels in the CNS, lung, heart, and kidney. Plaques of necrosis were found in both the gray and white matter of the brain with diameters that ranged from 0.2 mm to 5 mm. Severe lung involvement was described as fibrinoid necrosis, vasculitis, alveolar hemorrhage, and pulmonary edema. The spleen, lymph nodes, and

kidneys were also greatly affected, liver and skeletal muscle were not impacted (Wong et al., 2002).

Susceptible human PBMCs cells to NiV:

Research groups have contradicting results on NiV replication in human monocytes. Mathieu et al. (2011) reported that human monocytes are not permissive to NiV. Chang et al. (2006) observed that the human monocyte cell line THP-1 is permissive to NiV: however, only low level of infection was observed in these cells and CPE was not observed until 48 hpi. Whereas human lung fibroblast cells (MRC5) cells, porcine stable kidney cells (PS), and human neuronal cells (SK-N-MC) began to show CPE at 24 hpi. Gupta et al. (2013) and Mathieu et al. (2011) have determined that human dendritic cells (DCs) are permissive to NiV. Mathieu et al. (2011) also reported that NiV could bind to monocytes, macrophages, or lymphocytes which then act as a transport mechanism for the virus without any viral replication. Findings from Chang et al. (2006) indicate that since infected monocytes do not die quickly, they can effectively help in virus spread.

Hendra Infections in Humans

HeV like NiV, can manifest with consequences ranging from a simple fever to death. It has a human case fatality rate of 60% and takes form of influenza-like illnesses progressing to encephalitis (Escaffre et al., 2013).

Pathology of HeV in humans:

There have been few reports on HeV infection in humans. Pathology findings of HeV infection are similar to NiV. One case of relapsing encephalitis has been reported. Vasculitis was observed in blood vessels in the brain, lung, kidney and heart. Viral antigens were observed in

vascular endothelial cells and smooth muscle cells in the brain, lungs and kidneys. There was severe inflammation and necrosis in the lungs (Wong et al., 2009).

Clinical presentation is very similar to NiV infection (Wong et al., 2002; O'Sullivan et al., 1997). High grade fever, encephalitis, ataxia, dysarthria, and seizure are common. Multifocal lesions were found in HeV infections (Playford et al., 2010). The pathway by which HeV and NiV enter the CNS is still unknown, but studies have suggested that there is involvement of the olfactory bulb. For example, it has been shown in mice, hamsters, and swine that NiV and HeV can enter the CNS through the olfactory route (Rockx et al., 2011; Weingartl et al., 2005; Munster et al., 2012; Dups et al., 2012; Li et al., 2010). Cell culture studies have shown that human olfactory epithelial cells can be infected with HeV, NiV Malaysia, and NiV Bangladesh; these cells may serve as a site of entry into the CNS (Borisevich et al., 2017).

Human PBMCs susceptible to HeV:

Permissibility studies on human peripheral blood lymphocytes and macrophages show that HeV G and F proteins were unable to induce fusion to these cells, rendering the virus incapable of infection (Bossart et al, 2001).

1.5 Nipah and Hendra Virus Infection in Pigs

Field infections:

Respiratory distress is prevalent in NiV infection in pigs. Acute febrile illness was described in pigs. Piglets developed fever, nasal discharge, and a harsh, non-productive cough which gave rise to the name porcine respiratory and encephalitis syndrome or barking pig disease (Nor et al., 2000). Neurological signs, such as rear leg weakness, muscle fasciculation, and spastic paresis were observed. Suckling pigs showed high death rate compared to sows, boars,

and grower pigs. Lesions were found in lungs and meninges infected with NiV (Brockmeier et al., 2012).

There has been no natural HeV infection reported in pigs.

NiV Experimental infections:

NiV inoculation of pigs leads to different outcomes depending on route and dose of virus. The age of pigs used for experimental infections ranges between 5 and 9 weeks. Subcutaneous or nasal inoculations with inoculum titres between 5×10^4 and 5×10^5 pfu/pig consistently resulted in the development of advanced neurological signs, requiring euthanasia in some pigs (Middleton et al., 2002; Weingartl et al., 2005). Eight week old conventional pigs inoculated subcutaneously showed signs of disease earlier (7 dpi) than those inoculated orally, which did not develop signs of disease before the end of the study at 21 dpi (Middleton et al., 2002). In five week old crossbred Landrace female pigs, nasally or oronasally inoculated pigs may result in invasion of the central nervous system and may show neurological signs such as difficulty standing, a wide stance, restlessness, severe shivering and seizures (Weingartl et al., 2005). NiV was isolated from the upper and lower respiratory tract, submandibular lymph nodes, bronchial lymph nodes, retrobulbar lymphoid tissue, tonsil, spleen; and nervous tissue such as the trigeminal ganglion (Weingartl et al., 2005). Secondary infection by *Enterococcus faecalis*, *Streptococcus suis*, and *Staphylococcus hyicus* were detected in NiV infected piglets (Berhane et al., 2008).

Pathology:

In infected pigs, syncytia were detected in vascular, nervous, and lymphatic systems. The bronchi and trachea were filled with frothy fluid and blood. Enlarged lymph nodes were

observed and during neurological cases, the meninges were often congested. In the lungs, pneumonia with the infiltration of mononuclear cells is seen (Brockmeier et al., 2012).

Porcine PBMCs susceptible to NiV:

Previous studies showed that NiV does not replicate in porcine B cells or CD4⁻CD8⁻, and CD4⁺CD8⁻ T cells but does replicate in porcine monocytes, CD4⁻CD8⁺, CD4⁺CD8⁺ T cells, and CD16⁺ NK cells (Stachowiak & Weingartl., 2012). The authors also observed that CD8⁺ hi T cells were highly permissive to NiV with almost complete elimination of this population at 24 hours post inoculation (hpi) *in vivo*.

Immune response:

Vaccination experiments against NiV have been promising. The need for a vaccine that elicits cell-mediated and humoral immune response is critical. Weingartl et al. (2012) used a Canarypox virus-based vaccine vector carrying the gene for either NiV glycoprotein or the fusion protein were intramuscularly immunized pigs. They also immunized using both in the same animal. The pigs were then boosted 14 days post vaccination and challenged with 2.5×10^5 PFU of NiV two weeks later. The vaccinated pigs were protected from the challenge and the vaccine stimulated production of protective antibody levels, and both type 1 and type 2 cytokine responses. PBMCs from the vaccinated immunized with both F and G vaccines group produced higher IL-10, TNF- α , and IFN- γ expression when compared to the non-vaccinated group and singular F or G vaccinated pigs, indicating a requirement also for cell-mediated immune response.

Pickering et al., (2016) confirmed that a cell-mediated and humoral immune response is needed for full protection against NiV infection in swine. Pigs that had been orally inoculated with NiV had a large population of NiV memory cells (based on upregulation of the activation

IL-2 receptor (CD25) on CD4+CD8+ and CD4+CD8- cells), developed protective antibody levels and were fully protected 28 days later against nasal challenge with NiV.

Stachowiak & Weingartl (2012) noted that a decrease in the population frequency of CD4+CD8- T cells was related to pig death. In NiV-infected pigs, there was a decrease in population frequency of CD4+CD8- T cells in the piglets that succumbed to NiV infection while the CD4+CD8- T cell subset expanded in the piglets that lived. This indicated that humoral immunity is important in the clearance of NiV in pigs as well.

A humoral immune response against NiV is indicated by the development of antibodies in pigs that recovered from the clinical disease and cleared the virus. Berhane et al (2008) found that pigs started to develop neutralizing antibodies against NiV at around 7 to 10 dpi, and high neutralizing antibody titers were reached by 16 dpi.

HeV experimental infections:

Five-week-old Landrace pigs were used in the experimental infection with HeV. The pigs were inoculated oronasally with approximately 10^7 PFU/pig (Li et al., 2010). HeV-infected pigs exhibited an inability to rise from a lying position, severe depression, respiratory distress, and increased rectal temperature (Li et al., 2010). HeV was isolated from tonsils; bronchoalveolar lavage fluid (BALF); and oral, nasal and rectal swabs of pigs (Li et al., 2010). HeV can infect pigs; thus, pigs could play a role as an intermediate host for the spreading of the virus to humans.

Pathology:

HeV-infected pigs had petechial hemorrhages on kidneys and interstitial pneumonia in the lungs. A high viral dose was linked to CNS invasion and resulted in infection of the olfactory bulb. At a lower viral inoculation dose, HeV was not able to invade the CNS (Pickering et al., 2016). HeV neutralizing antibodies were detected at 5 dpi in HeV-infected pigs (Li et al., 2010).

1.6 A) Genome and Virion Structure

NiV and HeV are negative-stranded enveloped RNA viruses and have the same genome structure. HeV has a genome size of 18,234 nucleotides and NiV has one of 18,246 nucleotides (Satterfield et al., 2015). NiV and HeV genomes are approximately 15% larger than those of other viruses in the family Paramyxoviridae. NiV and HeV are enveloped and pleomorphic and are 500 nm in diameter (Hyatt et al., 2001). The genomes of both viruses are organized into six genes in the following order: 3' leader, N, P, M, F, G and L genes, and a 5' - trailer (**Figure 1**).

At the ends of the RNA genome, there is a 3' extracistronic leader sequence and a 5' extracistronic trailer sequence that are critical for transcription and replication. Each gene is flanked by intergenic regions containing transcriptional control sequences (Lamb & Parks, 2007). The N gene codes for the nucleoprotein. The P gene codes for the phosphoprotein as well as the non-structural V, W and C proteins. The C protein is encoded by an alternate open reading frame in the 5' end of the P gene and does not have any amino acid identity with the P, V, or W protein (Kulkarni et al., 2009). The M gene codes for the matrix protein; the F gene codes for the fusion protein; the G gene codes for the attachment glycoprotein; and the L (large) gene codes for the RNA-dependent RNA polymerase (Wong et al., 2002). NiV and HeV RNA are encapsidated by the N protein at a ratio of 1 N protein for every 6 nucleotides. This is called the rule of six. (Halpin et al., 2004)

1.6 B) **Virus Replication**

Figure 2 highlights the replication strategy of NiV and HeV: NiV or HeV binds to cellular receptors ephrin B2/B3 via the G glycoprotein, and the F protein mediates fusion of the viral envelope with the cell membrane. The viral ribonucleoprotein (RNP) complex is released

into the cytoplasm followed by transcription. The NiV/HeV RNA polymerase complex (P and L proteins) only transcribes or replicates encapsidated viral genomes. During transcription, the viral polymerase begins RNA synthesis at the 3' end of the genome and transcribes the gene into mRNA sequentially (N to the L gene) by terminating and reinitiating at each of the gene junctions. (Each gene has a gene start (GS) and gene end (GE) sequence.) The genes closer to the 3' end (N gene) are produced at higher copy numbers than the genes closer to the 5' end (L gene), as the polymerase may fall off the template at the end of a gene and fail to reinitiate the transcription at the next GS signal.

Following primary transcription and translation, presumably once sufficient amounts of proteins are produced, genome synthesis and secondary transcription are initiated, and complementary cRNA becomes a template for replication of more viral vRNA.

After transcription and translation, the N and P proteins form nucleocapsids (Wong et al., 2002) and the G and F proteins are transported to the cell membrane under the direction of the endoplasmic reticulum (ER) and the Golgi apparatus. The F protein is proteolytically cleaved in endosomes to become functionally mature. NiV M protein mediates virus assembly and budding of the virions (Diederich et al., 2005; Vogt et al., 2005; Pager et al., 2006).

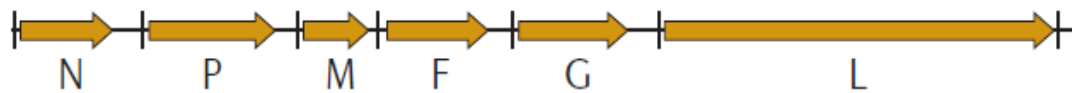
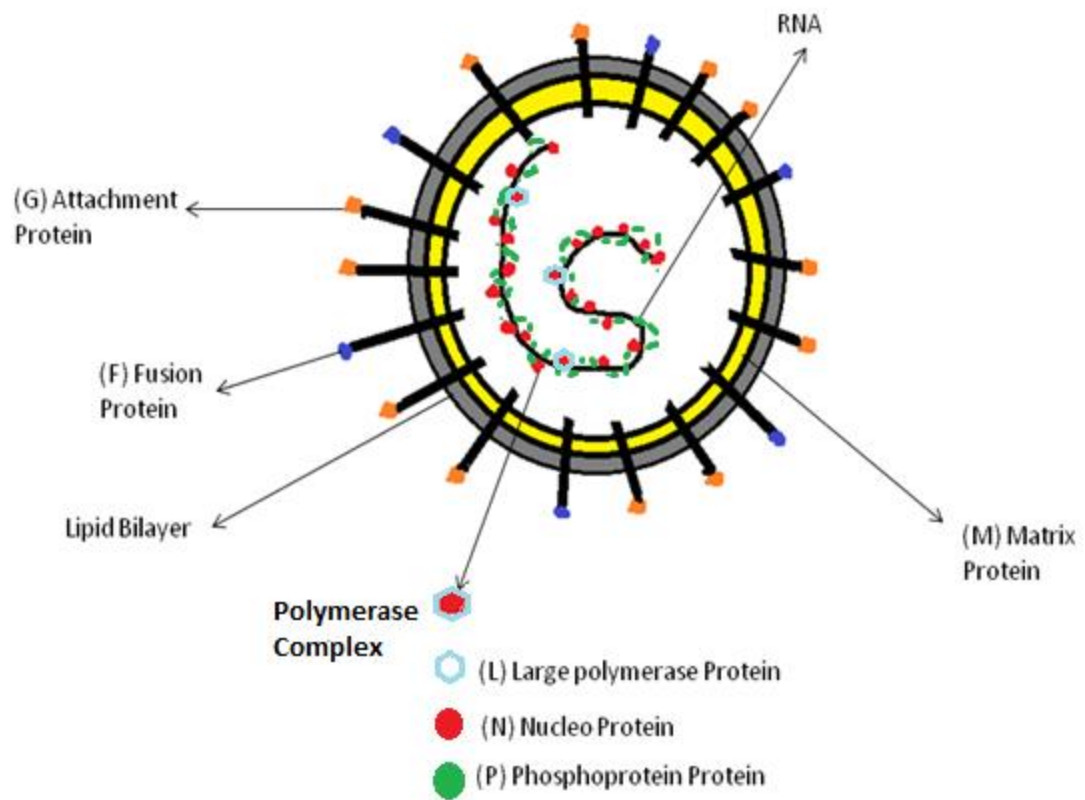


Figure 1: Diagram of Nipah virus and Hendra virus genome arrangement and virion structure.

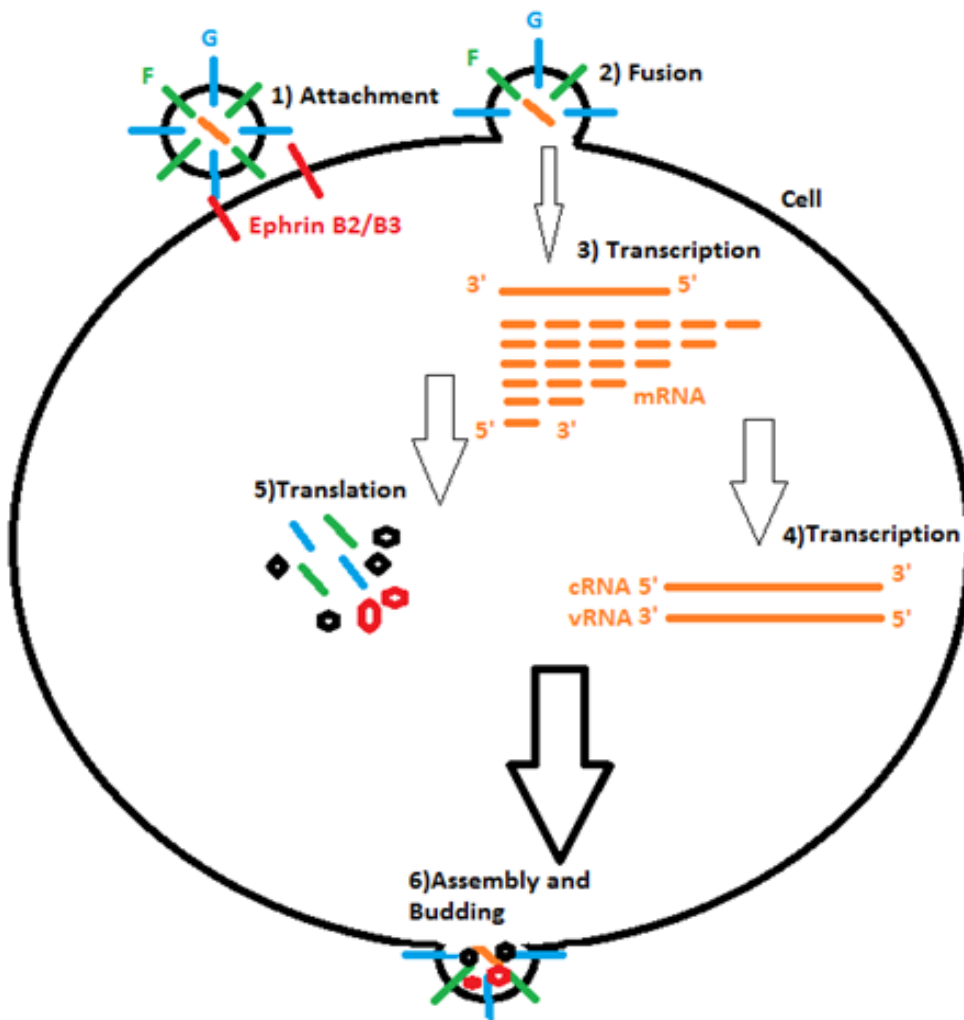


Figure 2: NiV and HeV replication cycle. 1) NiV or HeV binds to cellular receptors ephrin B2/B3 via the G glycoprotein and 2) F protein mediates fusion of the viral membrane to the cell membrane for the virus to enter the cells. The viral RNP complex is released into the cytoplasm followed by transcription and translation. 3-5) The viral polymerase begins RNA synthesis at the 3' end of the genome and transcribes the gene into mRNA sequentially (N to the L gene) by terminating and reinitiating at each of the gene junctions. Complementary cRNA becomes a template for replication of more viral vRNA. 6) Assembly and budding follow.

1.7 Nipah virus and Hendra virus Structural Proteins

Glycoprotein

The glycoprotein protein (G) is a type II membrane glycoprotein and the main virus attachment protein. Its amino terminus is on the interior of the virion and the carboxy terminus is on the exterior (**Figure 3**). The G protein is also the main antigen that elicits neutralizing antibodies. The NiV/HeV G have neither hemagglutinating nor neuraminidase activities; thus both viruses are the first identified members of the subfamily *Paramyxovirinae* whose glycoproteins have neither activity (Yu et al., 1998). The HeV G protein is 604 amino acids in length, while the NiV G protein has 602 amino acids (Wang et al., 2001). The G protein is comprised of a cytoplasmic tail, a transmembrane region which anchors the protein to the viral envelope, a stalk and a globular head (**Figure 3**). The globular head of the G protein folds into a β -propeller that consists of six blades. The blades are composed of four antiparallel beta sheets. Disulfide bonds are located between every blade and link the beta sheet from one blade to the beta sheet of the adjacent blade. There are two additional disulfide bonds: one between blades three and four, and one between the N- and C-termini of the globular head (Bowden et al., 2008). In the NiV G head domain, there are five asparagine-linked glycosylation sites (N306, N378, N417, N481 and N529) (Bowden et al., 2008; Bowden et al., 2010). The HeV G head domain has the same five predicted N-linked glycosylation sites (Xu et al., 2012).

Fusion Protein

The fusion protein (F) is a type I membrane glycoprotein that is required for the fusion of the viral and host-cell membranes. Its carboxy terminus is on the interior of the virion and its amino terminus on the exterior (**Figure 4**). The fusion process of NiV and HeV is a pH-

independent process for viral entry (Tamin et al., 2002). HeV and NiV F proteins are both 546 amino acids in length (Wang et al., 2001). The F glycoprotein consists of two alpha-helical domains, referred to as heptad repeats, which form a trimer-of-hairpins structure before entry and a six-helix bundle during and immediately following fusion (Singh et al., 1999; Hughson et al., 1997). The F protein consists of two subunits, F1 and F2, which are generated by the proteolytic cleavage of F0 (Wang et al., 2001). This cleavage is performed by cathepsin L or B (Diederich et al., 2012). The F1 subunit protein structure is comprised of an N-terminal hydrophobic peptide domain, two heptad repeat domains, a transmembrane domain, and a cytoplasmic tail. The F2 region has not been researched in depth.

The basic amino acid residue in the HeV F protein cleavage site is lysine; in NiV, it is an arginine (Michalski et al., 2000; Wang et al., 2001). Another difference between HeV and NiV is that in HeV, both the cleaved F1 and uncleaved F0 forms of the fusion protein are present in approximately equal amounts. In NiV, the F protein appears to be completely cleaved (Wang et al., 2001).

Nucleoprotein

The nucleoprotein (N) stabilizes and encapsulates the RNA of the virus. NiV and HeV N proteins are 532 amino acids in length and can self-assemble into ring-like structures (Wang et al., 2001; Eshaghi et al., 2005). The NiV and HeV N proteins are comprised of two domains. The amino-terminal domain is responsible for the specific interaction with the RNA and other N proteins. The carboxy-terminal domain interacts with the P protein of the virus (Wang et al., 2001; Chan et al., 2004; Blocquel et al., 2013).

Matrix Protein

The matrix protein or M protein provides stability to the virion by interacting with the viral envelope surface glycoproteins. Both the NiV and HeV M proteins are 352 amino acids in length (Wang et al., 2001). The N terminal domains of the NiV M protein are essential for virus budding (Bharaj et al., 2016). Expression of the whole M protein can mediate budding with or without co-expression of NiV F and G (Ciancanelli & Baseler, 2006). As a result, NiV M has a central role in the release of VLPs (Patch et al., 2007). The M protein also has IFN antagonist functions and interferes with the host antiviral response: it interacts with TRIM6 to induce TRIM6 degradation. This leads to the inactivation of IKK ϵ , which is involved in IFN-I production and IFN-I signalling (Bharaj et al., 2016).

L Protein

The L gene encodes the RNA-dependent RNA polymerase (L) protein. This protein has a size of 2244 amino acids (Wang et al., 2001). The L protein is conserved within henipaviruses (Murphy et al., 2009). The NiV and HeV L proteins form a complex with the P protein, which is required for polymerase activity (along with the N protein and RNA templates). L protein functions include initiation, elongation, and termination in both mRNA transcription and genome replication (Rota et al., 2012).

Phosphoprotein

The HeV P protein has 707 amino acids, while the NiV P protein has 709 amino acids. The P-gene encodes for the P protein and three non-structural proteins: V, W and C (Wang et al., 2001). The V and W proteins are translated from edited P gene mRNA. One or two non-templated G residues are inserted into the editing site by the polymerase protein during transcription in a mechanism called polymerase stuttering, which creates a frameshift mutation and creates a stop codon (Rodriguez et al., 2004). The V protein is created by the insertion of one

guanine base and the W protein is created by the insertion of two. The C protein has its own open reading frame that is 23 nucleotides downstream of the translation initiation site of the P ORF (Kulkarni et al., 2009). It is important to note that HeV does not have a W protein, but the NiV does. Instead, the HeV P gene contains an open reading frame that potentially encodes for a small basic (SB) protein with a very high isoelectric point. However, no function of the protein has been identified (Wang et al., 2001).

The NiV and HeV P proteins contain disordered and ordered domains that are required to form a complex with the nucleocapsid (Habchi et al., 2010). The P protein is phosphorylated on serine residues, which allows it to interact with the N protein during virus genome replication and transcription (Shiell et al., 2003).

Recombinant protein studies conducted in henipavirus infected Vero cell lines showed that the P and V proteins were detected in cytoplasm, while the W protein was found in the nucleus (Lo et al., 2009). However, in NiV infected human endothelial cell lines, the W protein is detected only in the cytoplasm (Lo et al., 2010). In NiV infected Vero cell lines, the C protein is found scattered in the perinuclear region (Lo et al., 2009). The locations of the P gene products are cell type-specific.

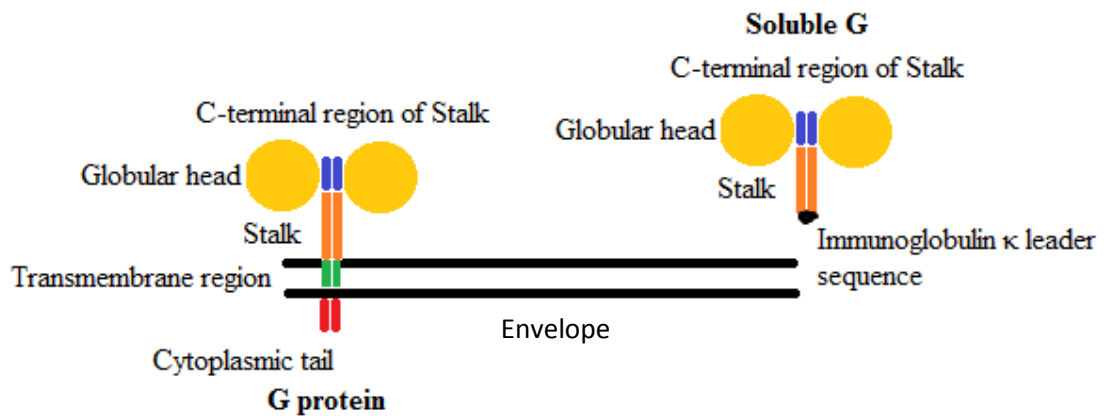


Figure 3: Structure of membrane attached (left) or soluble (right) forms of G protein. The blue stalk C-terminal region that triggers F is covered by the NiV-G head(s). Soluble G lacks the transmembrane and cytoplasmic tail regions, but it is replaced with an immunoglobulin κ leader sequence.

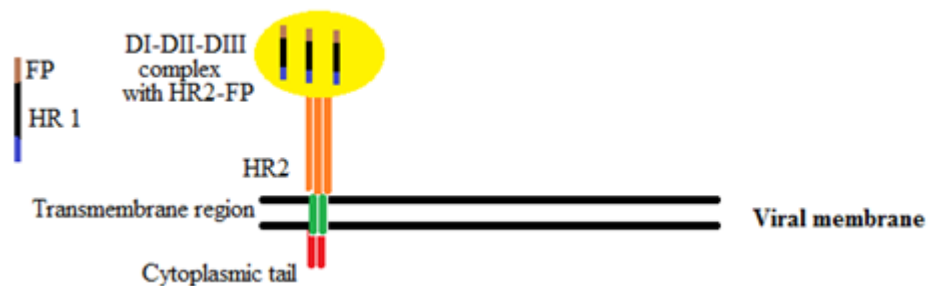


Figure 4: Structure of NiV/HeV fusion protein.

1.8 Function of the Non-Structural Proteins

The NiV and HeV non-structural proteins are involved in the henipavirus life cycle by regulating replication and evading the innate immune response by hindering the Janus kinase/signal transducers and activators of transcription (JAK/STAT) signaling pathway.

The NiV and HeV non-structural protein can alter replication of virus. In Vero cells, which do not produce IFN, growth of rNiV(Δ C) was slower and its maximum titer was lower than that of rNiV (WT) (Sleeman et al, 2008; Yoneda et al., 2010). The closely related measles virus C protein was shown to bind and decrease host protein SHCBP1 which leads to reduced RNA synthesis (Ito et al., 2013).

The JAK/STAT signalling pathway functions in immunity, cell division, and cell death (Rodriguez et al., 2002; Shaw et al., 2004). The P, V, and W proteins have a common STAT1-binding domain (Shaw et al, 2005). The N-terminal end of the P/V/W proteins binds to STAT1 and thereby interferes with the activation of the JAK/STAT pathway (Eaton et al., 2006). The W protein has the strongest interaction with STAT1 while the P protein has the weakest (Shaw et al, 2005).

The V protein is able to bind to STAT1/STAT2 and STAT1/STAT1 dimer. NiV V has been shown to bind STAT1 in porcine cells (Hagmaier et al, 2006).

The STAT pathway is not the only pathway blocked by the non-structural proteins. When in the nucleus, the NiV W protein blocks the Toll-like receptor 3/TIR-domain-containing adapter-inducing interferon- β (TLR3/TRIF) pathway which functions in innate immune response against RNA viruses. The V proteins of NiV and HeV and the W protein of NiV bind to the Melanoma Differentiation-Associated protein 5 (MDA5) helicase and Probable ATP-dependent RNA helicase DHX58 (LGP2) proteins in 293FT cells to suppress retinoic acid-inducible gene-I-

like receptor (RLR) signalling resulting in the blocking of IFN- β production (Childs et al., 2007; Parisien et al., 2009). NiV and HeV C proteins inhibit TRL7/9-dependent IFN- α induction by binding to IKKs and inhibiting phosphorylation of IRF-7 (Yamaguchi et al, 2014).

1.9 Receptors for Hendra and Nipah virus

In order to establish whether the G protein determines the known cell line tropism of NiV, Aguilar et al (2005) generated an immunoadhesin by fusing the ectodomain of NiV-G with the Fc region of human IgG1 (NiV-G-Fc). The NiV-G-Fc immunoadhesin bound to the fusion-permissive 293T, HeLa and Vero cells (Bossart et al., 2002; Guillaume et al., 2004), but not to the permissive but non-susceptible Chinese hamster ovary (CHO-pgsA 745), pig kidney fibroblast (PK13) and human Raji B cells (Bossart et al., 2002). An experiment was done in which NiV-G-Fc was used to immunoprecipitate the receptor used by NiV for entry. NiV-G-Fc immunoprecipitated a 48 kDa protein from the surface of permissive 293T and Vero cells, but not from the permissive but not susceptible CHO-pgsA 745 cells. Using mass spectrometry, ephrin B2 was identified as the receptor (Negrete et al., 2005).

The G proteins of HeV and NiV bind to ephrin B2 or ephrin B3 ligands which serve as cellular receptors for both viruses (Negrete et al., 2005; Negrete et al., 2006; Bonaparte et al., 2005). The ephrin B-ligands are highly conserved across many mammalian species including humans (Drescher, 2002; Mellott & Burke, 2008; Xu & Ma, 2016). They function with their respective receptors, Eph proteins, in cell-to-cell communication; regulation of cell attachment and repulsion; vasculogenesis; and axonal guidance (Pasquale 2008; Lisabeth et al., 2013).

Ephrin B2 is a transmembrane-anchored ligand of the receptor tyrosine kinases Eph2, Eph3 and Eph4 (Poliakov et al., 2004) and is expressed on multiple cell types such as neurons,

smooth muscle cells, and endothelial cells of arteries and capillaries (Frisén et al., 1999; Flanagan & Vanderhaeghen, 1998; Wang et al., 1998). Ephrin B2 is essential for embryo development and homeostasis of many adult organs (Pasquale, 2008). Its broad distribution corresponds with the broad cellular and tissue tropism of NiV and HeV. Surface expression of ephrin B2 was also found on human CD14 monocytes (Bennett et al., 1995) but it is not known if lymphocytes express ephrin B2 on the surface.

In order to establish that ephrin B2 is a cellular attachment receptor for NiV, Negrete et al., (2006) used a soluble HA-tagged ectodomain of NiV-G (sNiV-G-HA) in an ELISA to demonstrate that NiV-G binds directly to soluble ephrin B2-Fc but not to ephrin B1-Fc.

In addition, ephrin B2-Fc but not ephrin B1-Fc competes for sNiV-G-HA-binding on permissive 293T cells. NiV-G-Fc binds to ephrin B2-transfected CHO-pgsA 745 cells but not to non-transfected CHO-pgsA 745 cells. Additionally, fusion of NiV-F/G-expressing human microvascular endothelial cells (HMVECs) was inhibited by soluble ephrin B2 or EphB4 but not by ephrin B1. It was also shown that when Chinese hamster ovary cells (CHO) (which are negative for ephrin B2/B3 expression and not permissive to NiV) became permissive to NiV after transfection with ephrin B2 or B3 (Negrete et al., 2006). Virus replication was also blocked using an anti-ephrin B2 antibody (Bonaparte et al., 2005; Negrete et al., 2005). From these results it can be concluded that NiV fusion and infection in cell lines, including an *in vivo* target cell for NiV infection, depends on ephrin B2.

Ephrin B3 is also a receptor for NiV (Negrete et al., 2006). HeV can use ephrin B3 as well, but with much less efficiency than NiV (Negrete et al., 2007). The greater efficiency in the use of ephrin B3 by NiV may explain the differences in pathology seen in NiV infections compared to HeV infections. In mice, ephrin B3 is expressed more predominantly in the brain

stem than ephrin B2. Infection of the brain stem during NiV infection has been strongly associated with death (Negrete et al., 2007; Goh et al., 2000). Ephrin B3 is also expressed on surfaces of murine CD8⁺ and CD4⁺ T lymphocytes and monocytes/macrophages, but not B cells (Yu et al., 2003). It is not known whether human or porcine lymphocytes express ephrin B3 on their surfaces. The NiV-permissive monocyte-derived DCs of humans express ephrin B3 but not ephrin B2 on the cell surface (Gupta et al., 2013).

1.10 Binding of NiV/HeV G to Ephrin B2/B3

B-class ephrins contain a globular domain comprised of eight β -strands (referred to as A-D, F-H and K) surrounding a hydrophobic core (Toth et al., 2001). The major structural difference between ephrins B2 and B3 is the G-H loop, which is a 15 amino acid linker region between β -strands G and H. The linker is primarily responsible for the binding of ephrins to Eph receptors (Koolpe et al., 2005). Only a short stretch of amino acids within the ephrin B2/B3 G-H loop binds in the groove of the globular head of HeV and NiV-G; the only difference between ephrin B2 and ephrin B3 being F117 and Y120, respectively (Bowden et al., 2008; Xu et al., 2008).

Binding of ephrin B3 to the NiV G protein can be localized to the residue Val507 in NiV G (Negrete et al., 2007). HeV does not use ephrin B3 as effectively as ephrin B2, possibly because HeV has a serine in place of the NiV valine at amino acid 507. In an experiment by Negrete et al. (2007), changing the globular head residue 507 of the HeV G protein from serine to threonine allowed HeV to bind and enter via ephrin B3 with comparable efficiency to NiV.

Upon binding of the G protein to ephrin B2/B3, a conformational change occurs in the G tetramer that exposes the stalk domain residues (in the receptor activation site) which activates F.

Both ephrin B2 and the NiV/HeV G protein undergo conformational changes in order to form a complex. In the NiV-G-ephrin B2 complex, Isoleucine 588 and Tyrosine 581 of NiV G play a part in the formation of a binding pocket that binds to Phenylalanine 120 of ephrin B2 through hydrophobic interactions. The G-H loop (Glutamate 119 to Leucine 127) of ephrin B2 also exhibit changes in conformation. During HeV-G-Ephrin B2 binding, the only region on ephrinB2 that shows rearrangements upon HeV-G binding is the G-H loop. Ephrin-B2 attaches to the upper face of the NiV/HeV-G β -propeller and the ephrin-B2 G-H loop inserts into the NiV/HeV-G central cavity (Bowden et al., 2008).

1.11 Porcine Peripheral Blood Mononuclear Cells (PBMCs)

PBMCs are a critical component of the immune system. They are a subset of the white blood cells which have a single round nucleus. PBMCs are made up of several cell populations including monocytes, dendritic cells (DC), natural killer (NK) cells, B cells, and T-cells. These cells are a major component in the immune system (Autissier et al., 2010; Murphy et al., 2008; Corkum et al., 2015).

Monocytes and dendritic cells

Monocytes express CD14 marker, and non-conventional monocytes are also CD16+. Porcine monocytes are also identified by the expression of the SW3 (CD172a) marker (Piriou-Guzylack et al., 2008).

Monocytes function in phagocytosis, antigen presentation, chemokine and cytokine production, e.g. pro-inflammatory or CD4 Th1 and CD4 Th2 regulatory, such as IL-10 (Chaplin D., 2010). Monocytes divide and differentiate into macrophages or dendritic cells following migration into tissues. Two forms of DCs are present in the porcine immune system: conventional DC (cDC) and plasmacytoid DC (pDC) which remain in blood. DCs are potent

antigen-presenting cells that are able to prime naive T-cell responses. Porcine cDCs control T cell activation and regulation, as well as antigen presentation to B cells and induction of B-cell proliferation and isotype switching (Balázs et al., 2002; Johansson et al., 2000). Porcine pDC are important in virus infections and have the produce large quantities of IFN- α and inflammatory cytokines TNF- α , IL-6, and IL-12 (Summerfield & McCullough., 2009). Porcine dendritic cells express the SW3 (CD172a) marker similarly to monocytes (Piriou-Guzylack et al., 2008).

B cells

B cells are part of the adaptive immune system; porcine B-cells can be identified by expression of the CD21 cell surface marker (Piriou-Guzylack et al., 2008). The same five immunoglobulin (Ig) isotypes that are found in humans and mice are also found in swine: IgM, IgD, IgG, IgE and IgA. B cells are primarily involved in the production of antibodies but also secrete IFN-gamma, IL-6, and IL-10 (LeBien et al., 2008). In piglets, plasma cells mainly produce IgM (Brown and Bourne, 1976).

T cells

T-cells are a type of white blood cell that expresses the T-cell receptor. These cells mature in the thymus and can be identified by their expression of the CD3 cell surface marker (Chaplin D., 2010). When an antigen presenting cell (APC) such as a DC or macrophage encounters a foreign antigen, the antigen is phagocytosed, cleaved into peptides, and displayed on the surface of the APC in complex with an MHC molecule. The T cell receptor (TCR) (CD3) and its co-receptor CD8 interact with major histocompatibility complex I (MHC I) molecules on the cytotoxic T cells. Internalization of the CD8-MHC I-TCR complex is cell type specific: in murine fibroblasts, internalization is mediated through large cell surface invaginations; in human

T lymphocytes, internalization of the TCR-MHC occurs by clathrin-dependent endocytosis (Dietrich et al., 1994; Liu et al., 2000).

The CD8 marker also plays a role in T cell signalling by associating with Src kinase p56lck (lymphocyte-specific protein tyrosine kinase) (Zamoyska, 1994). Lck phosphorylates CD3 ζ (zeta) of the TCR complex.

Porcine CD8 molecule

The porcine CD8 is a dimeric molecule expressed on T lymphocytes and NK cells. CD8 is expressed predominantly as a $\alpha\beta$ heterodimer on rodent and human lymphocytes, while on porcine lymphocytes the CD8 molecules are predominantly $\alpha\alpha$ homodimers. Pigs have circulating pools of CD4⁺CD8 $\alpha\alpha$ ⁺ and CD4⁻CD8 $\alpha\alpha$ ⁺ cells (Summerfield et al., 1996; Lunney et al., 1996; Piriou-Guzylack & Salmon, 2009; Zuckermann et al., 1998) and porcine CD4⁺CD6⁺CD8 $\alpha\alpha$ ⁺ T cells. **Table 1** lists cell types expressing CD8 α .

Porcine CD4-CD8⁺ cells

CD4-CD8⁺ cells are called cytotoxic T cells. These cells express the CD8 $\alpha\beta$ and not CD8 $\alpha\alpha$. They can make up 8–21%, and up to 40% of the PBMCs. These cells bind to foreign antigens in an MHC class I-restricted manner and secrete cytokines that kill target cells (Saalmueller A., 1998).

Porcine CD4⁺CD8⁺ cells

The hallmark of the porcine immune system is the presence of CD4⁺CD8⁺ lymphocytes in high proportions in the peripheral blood. In pigs, it has been shown that CD4⁺ T cells can permanently express a CD8 $\alpha\alpha$ homodimer after stimulation by antigen, resulting in extrathymic CD4⁺CD8⁺ cells (Butler et al., 2006). The percentage of CD4⁺CD8⁺ cells in the peripheral blood can range from 10-60%, increasing with age of the animal. CD4⁺CD8⁺ cells can act as

memory T-helper cells in pigs and are also involved in cell proliferation; the production of cytokines like IFN α and IL-2; and the stimulation of antibody production in B cells (Saalmueller A., 1998; Ober et al., 1998). In contrast, CD4+CD8+ expressing cells are rare in healthy humans. They can be found in humans that have arthritis or some types of cancers (Saalmueller A., 1998).

Porcine CD4+CD8- T cells

CD4+CD8- cells are called T-helper cells (Saalmueller A., 1998). They recognize antigens in an MHC class II-restricted manner and proliferate in response to these antigens. These cells regulate the immune response by interacting with cytotoxic CD8+ T cells and regulating B cell activation (Gerner et al., 2009).

Porcine gamma delta ($\gamma\delta$) T cells

Swine gamma delta ($\gamma\delta$) T cells predominate in the intestinal epithelium of pigs and are a major T-cell subpopulation in the PBMCs in young pigs, which decreases with age (Chareerntanakul and Roth, 2006). They are characterized as CD2+CD4-CD8 $\alpha\alpha^{\text{lo}}$ (Gerner et al., 2009). They respond to non-peptide antigens and elicit antigen-specific proliferation and IFN- γ responses (Lee et al., 2004).

Low frequency T cells

A fourth T-cell population are CD4-CD8- cells. These cells have no known role in the porcine immune system: they do not respond to stimulation with mitogens such as concanavalin (con)-A, and they do not elicit an immune reaction in response to antigens in pigs (Gerner et al., 2009). Regulatory T cells (T_{reg}) function in down-regulating pro-inflammatory immune responses (Käser et al., 2008). T_{reg} cells are CD4+CD25+, express FoxP3, and produce IL-10 and TGF β . T_{regs} can have either low or high expression of CD25; however only CD25 (high) cells are capable of inhibiting activated T cell proliferation (Gerner et al., 2009).

Table 1: CD8 α expressing cells

Cell	Phenotype	Description	Percentage in porcine PBMCs (%)
T helper cells	CD3+CD4+CD8 α α +	MHC class II-restricted antigen-specific memory T helper cells. Secrete cytokines and stimulate antibody production in B cells	19–60% of T cells, age-dependent increase
$\gamma\delta$ T cells	CD2+CD4-CD8 α α ^{lo}	Cytokine production and cell proliferation	N/A
Cytotoxic T cells	CD3+CD4-CD8 α +CD8 β +	MHC class I-restricted cytotoxic T cells. Secrete cytokines that kill target cells	8–21%, up to 40% of T cells
Natural killer cell	Perforin+CD2+CD3-CD4-CD5-CD6-CD8 α +CD8 β -CD11 β +CD16+	Cytotoxic lymphocytes which are part of the innate immune system	2–10%, age-dependent decrease

(Gerner et al., 2009)

Natural Killer cells

Natural Killer (NK) cells are cytotoxic lymphocytes that are part of the innate immune system. NK cells in pigs are identified by their CD16 marker and non-adherent character (Sanchez et al., 1999; Wierda et al., 1993; Piriou-Guzylack et al., 2008). NK cells have the phenotype Perforin+CD2+CD3-CD4-CD5-CD6-CD8 α +CD8 β -CD11 β +CD16+. In pigs, the percentage of PBMCs that are NK cells ranges from 2-10% and decrease with age (Gerner et al., 2009). They are unique in their ability to recognize stressed cells in the absence of antibodies and MHC molecules. NK cells provide rapid responses to virus-infected cells (Chaplin D., 2010) and

readily produce cytokines such as IFN-gamma in response to stimulation with IL-12, IL-15 and IL-18 (Vivier et al., 2008). NK cells can kill immature DCs, over-stimulated macrophages, and infected cells by activating apoptosis (Piccioli et al., 2002; Zhang et al., 2007).

The flow cytometry staining of the CD8 marker has an intensity that is half of that seen on CD8+ T cells (Trinchieri et al., 1989; Morice., 2007). The function of the CD8 molecule on these NK cells has not been determined: however, it is known that the molecule is not involved in the recognition of target cells or in the control of NK-cell function (Gerner et al., 2009).

There is also a population of NKT cells that have the phenotype Perforin+CD3+CD6-CD11β+CD16+ and represent 0.5–3% of the PBMCs. There is also a small population of the iNKT (CD3+CD16+) cells expressing CD8αα or CD8αβ, with the CD8αβ population greater than the CD8αα one (Gerner et al., 2009).

Aim

The aim of this study is to determine which subsets of porcine PBMCs are permissive to NiV and HeV, and to determine why only these cell populations are permissive.

1.12.1 Rationale

Porcine lymphocytes in viral clearance. Previous studies showed that NiV replicated in monocytes, CD6+CD8+ T lymphocytes, and NK cells *in vitro* (Stachowiak & Weingartl, 2012). The hallmark of the porcine immune system is the presence of CD4+CD8+ cells, which can account for up to 60% of the T cell population. These are memory T helper cells. They secrete cytokines such as IFN- γ and stimulate antibody production in B cells. A modulation of this T cell population will delay the development of neutralizing antibodies and secondary bacterial infections could occur; this is seen, for example, in experimentally infected swine where there was a delayed neutralizing antibody development at 7-10 dpi (Berhane et al., 2008).

HeV infection of swine has been only experimental and the virus does not seem to affect the immune response in pigs the same way as NiV: neutralizing antibodies were in contrast detected already at 5 dpi in HeV infected pigs (Li et al., 2010). HeV permissibility studies on swine peripheral blood lymphocytes have never been done, however human peripheral blood lymphocytes and macrophages are not permissive (or susceptible) to HeV (Bossart et al., 2001).

1.12.2 Hypothesis

1. HeV does infect porcine lymphocytes.
2. NiV can infect leukocytes/subpopulations expressing the CD8 marker.
3. Porcine CD8 can serve as an alternative receptor for NiV or as a co-receptor/attachment factor/receptor.

1.12.3 Objectives for Hypothesis 1

1. To determine the permissibility of porcine PBMCs to HeV *in vitro*.

1.12.4 Objectives for Hypothesis 2

1. To confirm that leukocyte populations carrying the CD8+ marker are permissive to NiV *in vitro*.
2. To determine ephrin B2 expression profiles on permissive and non-permissive porcine PBMCs and cell lines by immunoblot and flow cytometry.
3. To determine the permissiveness of porcine CD8 $\alpha\alpha$ and CD8 $\alpha\beta$ cells to NiV *in vitro*.

1.12.5 Objectives for Hypothesis 3

1. To perform antibody blocking assays using non-conjugated anti porcine ephrin B2 and CD8 α antibody to block NiV replication in IPAM 3D4/31 and select CD8+ primary porcine cells.
2. To perform protein competition assays between NiV and HeV attachment protein (soluble G protein) and NiV for the receptor. The competition will be between HeV G and NiV and between NiV G and NiV on IPAM 3D4/31 and porcine CD8+ PBMCs.
3. To evaluate if the permissive but non susceptible cell line CHO-K1 can become susceptible with the transfection of CD8 α with ephrin B2 serving as a positive control.

Materials and Methods

2.1 Cell cultivation and passaging of continuous cell lines

The cell lines (listed in **Table 2**) were passaged once reaching a confluency of 100%. The selection of maintenance medium used was cell specific. **Table 2** outlines the media and addition of supplements used for each cell line. Dulbecco's Modified Eagle Medium (DMEM; MULTICELL, Cat No.319-005-CL) or Roswell Park Memorial Institute medium 1640 medium (RPMI 1640; MULTICELL, Cat No. 350-007-CL) supplemented with 10% fetal bovine serum (FBS) (MULTICELL, Cat No.080-150) was used. RPMI-1640 was developed for culture of peripheral blood lymphocytes and immune cells and thus used for lymphocytes in the study. DMEM is optimal for culture of various adherent cell lines due to high amino acid, vitamin, and glucose concentrations and thus used in our study.

First, the media was removed from the cell culture flask and the cell layer was washed once with 1x PBS (Dulbecco's phosphate buffered saline 1X) (Multicell, Cat No. 311-425-CL). This was followed by the addition of 0.25% trypsin-EDTA (Gibco, Cat No. 25200) and incubated at 37°C, 5% CO₂. Different cell lines needed different trypsinization incubation times to detach. Trypsinization times are listed in **Table 2**. The detached cells were collected in appropriate media containing 10% FBS (listed in **Table 2**) and were counted using an automated cell counter (Nexcelom Cellometer Auto T4). The resuspended cells were then seeded on new T75 culture flask (Corning, Cat No. 3276). The number of cells seeded was dependent on the cell line and type of experiment.

Table 2: Cell lines used, culture methods, and characteristics.

Cell Line	Origin	Cultivation Medium	Trypsin time
VERO 76 (ATCC® CRL1587™)	<i>Cercopithecus aethiops</i> Kidney epithelioid	DMEM with 10% FBS	4-8 minutes
PK15(ATCC® CCL-33™)	<i>Sus scrofa</i> Kidney epithelioid	DMEM with 10% FBS	8-13 minutes
IPAM 3D4/31 (Weingartl et al., 2002)*	<i>Sus scrofa</i> Immortalized alveolar macrophage - monomyeloid	RPMI 1640 with 10% FBS and Penicillin- Streptomycin	8-15 minutes
ST (ATCC® CRL-1746™)	<i>Sus scrofa</i> Testis fibroblast	DMEM with 10% FBS	5-8 minutes
CHO-K1 (ATCC® CCL- 61™)	<i>Cricetulus griseus</i> Ovary epithelioid	DMEM with 10% FBS with 1X non-Essential Amino Acids (Gibco, Cat No.11140050)	5-8 minutes

Note: * available also from ATCC (ATCC® CRL-2844™)

2.2 Recovery of the Cells

The frozen cells were recovered by placing the cryogenic vials in a 37°C water bath. Once thawed, the cells were transferred immediately to a 15 ml conical centrifuge tube (Corning, Cat No.430052), which contained approximately 10 ml of appropriate media. The cells were centrifuged at 300g for 5 min. The supernatant (media, FBS and DMSO) was removed and the cell pellet was resuspended in 5 ml of media. To assess cell viability and determine cell count, 20 µl of the cells were stained with 20 µl Trypan Blue exclusion stain and were counted in an automated cell counter (Nexcelom Cellometer Auto T4). The dead cells are blue in color and live cells have no blue color. The cells were transferred to a T25 corning culture flask (Corning, Cat No. CLS430639). The media was changed after 24 hrs. Once the cells were 100% confluent, the cells were transferred to T75 flasks.

2.3 Virus Stock

NiV-Malaysia and HeV were obtained from Dr. T. Ksiazek and Dr. P. Rollin from the Centre for Disease Control and Prevention in Atlanta Georgia, USA. Viral stocks for both viruses were grown on Vero 76 cells infected with a multiplicity of infection (MOI) of 0.1. MOI was determined by using one confluent T75 flask and trypsinizing the Vero 76 cells and counting on an automated cell counter with Trypan Blue exclusion stain. For infection, virus was added to 5ml of FBS free DMEM, with no supplements and added to the T75 flask (Corning, Cat No. 3276) containing 100% confluent cells. After 1hr of incubation, at 37°C, 5% CO₂, 5 ml of DMEM containing 4% FBS to make a 2% final concentration was added to the flask.

Cells were incubated with NiV for 3 days or incubated with HeV for 4 days at 37°C, 5%, CO₂. Supernatant was clarified by centrifugation at 3000 g for 20 min and was aliquoted and frozen at -140°C before titration of the virus by plaque assay to determine the titre of the stocks. Control Vero 76 cells were treated as described above but no virus was added to the flasks.

2.4 Plaque Assays

NiV and HeV titres were determined by plaque assays on Vero 76 cells. Vero 76 cells were grown to 100% confluency in 24 well plates (Corning, Cat No. 3524). The cells were washed with serum free DMEM (MULTICELL, Cat No.319-005-CL), and 200 µl aliquots of virus serial dilutions from 10⁻¹ to 10⁻⁵ in DMEM containing no serum or additional supplements were added in quadruplicates to the wells. Cell controls with media only were used on each plate. Inoculum was removed after 1hr incubation at 37°C, 5%, CO₂ and 1 ml of 1.75% carboxymethylcellulose (CMC) (Sigma-Aldrich, Cat No. C-4888) overlay was added to the cells and then incubated at 37°C, 5% CO₂ for 3 days for NiV and 4 days for HeV. The overlay (**Figure 5**) contains CMC, 10x DMEM (Sigma-Aldrich, Cat No. D2429-100ml), BSA Fraction V (Sigma-Aldrich, Cat No.A8412-100ml), NaHCO₃ (MULTICELL, Cat No.609-105-EL), 1M HEPES (MULTICELL, Cat No.330-050-EL), Folic Acid (MULTICELL, Cat No.609-315-QL), L-glutamine (GlutaMAX) (Gibco, Cat No.35350-061), sodium pyruvate (Sigma-Aldrich, Cat No.S8636), and Antibiotic-Antimycotic (Penicillin/ Streptomycin/Amphotericin B) (Gibco, Cat No.15240-062). Cells were fixed by addition of 10% Phosphate buffered formalin (Fisher Scientific, Cat No. SF100-4). Formalin was added directly to cells with CMC still on. Cells were fixed with formalin for 24 h at room temperature, CMC/formalin was removed, and fixed cells

were gently washed with water. Cells were stained with crystal violet (0.1% crystal violet in Milli-Q water) by incubating for 30 min and washed again with water. The titre of the virus was determined as plaque forming units per ml (PFU/ml). Plaque forming units per milliliter were calculated by taking the average number of plaques per dilution and dividing it by the dilution factor multiplied by volume added.

Preparation of	1	x CMC overlay
	100	mL required
	1.75	% final
1 Put magnetic stirring bar in a bottle		
2 Add	74.57	mL mQ water
3 Heat to almost boiling point		
4 Add slowly	1.75	g of CMC
5 Stir on a magnetic stirrer until CMC is dissolved		
6 Heat again if necessary. Do not boil		
7 Autoclave at 121C for 15'		
8 Cool to 37C		
9 Add (mL):	10.00	10X DMEM
	4.00	7.5% BSA Fraction V
	4.93	7.5% NaHCO ₃
	2.50	1M HEPES
	1.00	0.4 g/L Folic Acid (100x)
	1.00	200 mM L-Glu
	1.00	100mM (11.0 mg/mL) Sodium Pyruvate
	1.00	100x Pen/Strep
10 Mix on magnetic stirrer in 37C incubator until ready to use		

Figure 5: Preparation of 100ml of 1.75% CMC overlay.

2.5 RNA isolation

RNA isolation was performed from the supernatants of cells pelleted in a 1.5 ml Safe-Lock Eppendorf tube (Eppendorf, Cat No.022600028) by centrifugation at 300 g for 10 min. The supernatant was collected and stored at -70°C until all the samples could be processed at the same time. To remove the supernatants out of Biosafety Level 4 (BSL4), 100 µl of sample (collected supernatant) was added to 900 µl of TriPure Isolation Reagent (Roche Diagnostics Corporation), and the supernatant in TriPure was vortexed for 20 sec. As an RNA extraction and an internal exogenous control, 2 µl of Armored RNA (Enterovirus) (Asuragen, Cat No. 42050) was added to the TriPure before aliquoting into tubes. Next, 200 µl of chloroform was added to each sample. The samples were vortexed for 20 sec followed by an incubation period at room temperature for 15 min. In order to separate the solution into three phases, the samples were centrifuged at 7500 g for 10 min at 4°C. The resulting mixture separated into three phases: 1) an upper aqueous phase containing RNA, 2) white interphase and 3) an organic phenol phase. The white interphase and organic phenol phase contain DNA, proteins, and lipids. After centrifugation, the colourless upper aqueous phase was collected into a new 1.5 ml Eppendorf tube containing, 3 µl of Glycol Blue (Thermo Fisher, Cat No. AM9516) for better visualization of the RNA pellet. Then, 750 µl of isopropanol was added to the aqueous phase. The tube was inverted by hand several times and incubated for 30 min at room temperature to precipitate the RNA. After the incubation, the tubes were centrifuged at 7500 g for 10 min at 4°C and the supernatants were discarded. The RNA pellet was washed with, 500 µl of 70% ethanol followed by centrifugation at 7500 g for 5 min at 4 °C. The supernatant was discarded and the RNA pellet was air dried for 30 min. The RNA pellet was resuspended in RNase free water (Ambicon) and

frozen at -70°C or used for reverse transcription polymerase chain reaction (RT-PCR) immediately. The entire RNA extraction protocol was performed in a Biosafety Class II Cabinet.

2.6 NiV and HeV Reverse Transcription (RT) PCR

Two sets of primers and probes were used in a multiplex RT-PCR assay using a Quantitate One-Step PCR kit (QIAGEN, Cat No. 204443):

First set of primers was targeting the NiV nucleoprotein (N) gene. The NiV nucleotide sequence for the forward primer was 5'-GCA AGA GAG TAA TGT TCA GGC TAG AG-3' and reverse primer 5'-CTG TTC TAT AGG TTC TTC CCC TTC AT-3'. The probe was labelled at the 5' end with FAM (Excitation-495; Emission-520) and has the sequence of 5'-FAM -TGC AGG AGG TGT GCT CAT TGG AGG-TAMRA- 3'. The TAMRA is a 3' fluorescent quencher.

Second set of primers targeted the Hendra virus M (Matrix) protein gene. The forward primer for HeV has the sequence 5'-CTT CGA CAA AGA CGG AAC CAA-3' and reverse primer 5'-CCA GCT CGT CGG ACA AAA TT-3'. The probe for HeV was labelled with FAM and had the sequence 5'-FAM-TGG CAT CTT TCA TGC TCC ATC TCG G-TAMRA- 3'.

Armored (Enterovirus) was used for the RNA extraction control, . The forward primer was 5'-CCT GTC GTA ACGCGC AAG T-3' and reverse primer was 5'-CAG CCA CAA TAA AAT AAA AGG AAA CA-3' located within the 5'-untranslated region (UTR). The probe was labelled with TET (Excitation-521; Emission-536) labelled probe 5'-TET-CGT GGC GGA ACC GAC TAC TTT GG-NFQ- 3'. NFQ is 3' fluorescent quencher.

The reactions were run and the curves analyzed using the Rotor Gene Q thermocycler (Corbett Research, Cat. No 9001580). NiV RNA was quantitated based on the use of a known DNA quantity of a full-length NiV N plasmid. HeV RNA was quantitated based on the use of a known DNA quantity HeV M gene containing the primers and probe sequence cloned into a plasmid, and in both types of the reaction standard curve was used to estimate the copy number. Quantities were expressed either in copies/ml or converted to the log₁₀ copy value/ml. The thermo cycling conditions for both NiV and HeV were as follows: 30 min at 50°C, 15 min at 95°C, followed by 40 cycles of 95°C for 15 seconds, and 60°C for 1 min.

2.7 Peripheral blood mononuclear cells (PBMC) harvesting from porcine blood

Porcine blood was obtained by Dr. Richard Hodges from the University of Manitoba Glenlea Research Station where a pig farm is situated or from pigs kept at the NCFAD. The blood was drawn into 8 ml BD Vacutainer cell preparation tubes (CPT) (Becton Dickinson, Cat No. 362761) which uses sodium citrate as an anticoagulant and Ficoll™ Hypaque™ as the density gradient solution. The tubes were inverted 8 times immediately after blood collection and kept upright at room temperature (18-25 °C). Blood was processed within 2 hrs of collection. The blood was separated by centrifugation at 1500g for 20 min. After the centrifugation, the plasma was removed and the white PBMC layer was collected into a 15 ml conical centrifuge tube (Corning, Cat No.430052). The PBMCs in the 15 ml conical centrifuge tube were washed twice with PBS and centrifuged at 500 g for 10 min. The cells were resuspended in 1 ml RPMI and a small volume was taken, diluted, and due to the heterogeneous size of the PBMC

population, cells were counted using a hemocytometer. After counting, PBMCs were then plated in a T75 flask (Corning, Cat No. 3524) for a period of 2 days.

2.8 Cell Sorting from PBMC

Monocytes in the PBMC preparation were allowed to adhere onto flasks by overnight incubation at 37°C in a 5% CO₂ incubator and used for ephrin B2 flow cytometry. Sorting the non-adherent PBMCs was performed by magnetic separation and performed entirely in a Biosafety Class II Cabinet, employing the EasySep Magnet (STEMCELL, Cat No.18000). EasySep™ PE Positive Selection Kit (STEMCELL, Cat No. 18557) and EasySep™ FITC Positive Selection Kit (STEMCELL, Cat No. 18558) were used to separate the cells based on PE (R-phycoerythrin) or FITC (fluorescein isothiocyanate) label on the respective antibodies. The antibodies (**Table 3**) used were, PE conjugated Mouse Anti-porcine CD8 α , FITC conjugated Mouse Anti-porcine CD4, PE conjugated Mouse Anti-porcine CD21, and FITC conjugated Mouse Anti-porcine CD16. For overview of the cell separation, please, see **Figure 6**.

Single Step Positive Selection:

The cells were washed twice with sorting media (PBS with 2%FBS and 1 mM EDTA). The cells were resuspended in 1 ml of sorting media and a FITC or PE conjugated antibody was added at an optimized concentration (**Table 3** for optimized antibody concentrations) and left to incubate for 1 hr at room temperature. (Optimization was performed by titrating out the antibody at different concentrations and comparing cell harvest yields.) Next, 100 μ l/ml of FITC or PE collection cocktail was added and incubated at room temperature for 15 min, followed by addition of 50 μ l/ml of magnetic nanoparticles provided in the PE or the FITC selection kit, and incubation for 10 min at room temperature. The solution was then transferred into a 5 ml 12 x 75 mm separation tube and the cell suspension was brought to a volume of 2.5 ml with sorting

media and mixed well. The tube was placed into an EasySep Magnet and let sit for 10 min with lid off. Once the 10 min were over, the tube contents were poured off into a 15 ml conical centrifuge tube labeled “Negative” while still keeping the separation tube inside the magnet. The cells removed with the sorting media were negatively selected cells. The cells bound to the tube were the cells positively selected for the desired marker, e.g. CD8+. The separation tube was taken out of the magnet and the positively selected cells bound to the tube were resuspended once more with 2.5 ml of sorting media using the same tube and the 10 min incubation step in the magnet was repeated once more. The negatively selected cells and sorting media was poured off again into the 15 ml conical centrifuge tube labeled “Negative”. The positively selected cells were washed with 3 ml of complete media with the tube removed out of the magnet and the contents were placed in a 15 ml conical centrifuge tube labelled “Positive”. Both positively and negatively selected cells were then pelleted, washed, resuspended and counted using a haemocytometer.

Two Step positive selection:

Selection of double positive cells (CD8+CD16+ or CD4+CD8+) was performed by employing two selection kits: EasySep™ Release Human PE Positive Selection Kit (STEMCELL, Cat No.17654) with EasySep™ Releasable RapidSpheres™ magnetic beads, followed by the EasySep™FITC Positive Selection Kit (STEMCELL, Cat No. 18558).

The EasySep™ Release Human PE Positive Selection Kit allowed for the removal of the magnetic beads from the isolated cells, while the PE-antibody complex remained on the labelled cells. Cells were then labelled with FITC conjugated antibodies and selected for with the FITC selection kit as described above in the one step positive selection section.

Table 3: Antibodies and dilutions used for flow cytometry, immunoblotting, and immunofluorescence.

Antibody	Company	Cat#	Immuno blot Dilution	Flow Cytometry Dilution	Immuno-fluorescence Dilution
Mouse Anti- porcine CD8 α	Southern Biotech	4520-01	N/A	1/250	N/A
PE conjugated Mouse Anti- porcine CD8 α	Southern Biotech	4520-09	N/A	1/250	1/300
FITC conjugated Mouse Anti- porcine CD4	Southern Biotech	4515-02	N/A	1/250	N/A
FITC conjugated Mouse Anti- porcine CD16	Bio-Rad	MCA1971F	N/A	1/250	N/A
PE conjugated Mouse Anti- porcine CD21	Southern Biotech	4530-09	N/A	1/200	N/A
FITC conjugated Mouse Anti- porcine CD8 β	Mybiosource	MBS224819	N/A	1/50	N/A
Goat Anti-multispecies Ephrin B2	Novus Biologicals	NBP1-49857	1/500	N/A	N/A
Rabbit Anti-multispecies Ephrin B2	Novus Biologicals	NBP1-84830	N/A	1/250	1/250
Goat Anti-mouse Alexa-fluor 488	Thermofisher	R37120	N/A	1/250	1/250
Goat Anti-rabbit Alexa-fluor 488	Thermofisher	R37116	N/A	1/250	1/250
Goat Anti-mouse IgG1 PerCP	Santa Cruz	sc-45092	N/A	1/50	N/A
Mouse monoclonal Anti-NiV N F45G2	Berhane et al., 2006 -NCFAD	N/A	N/A	1/50	N/A
Mouse monoclonal Anti-NiV N F45G4	Berhane et al., 2006 - NCFAD	N/A	N/A	N/A	1/1000
Anti-protein G-HRP	Thermofisher	101223	1/10000	N/A	N/A
HRP conjugated Anti-beta Tubulin	Abcam	ab21058	1/5000	N/A	N/A

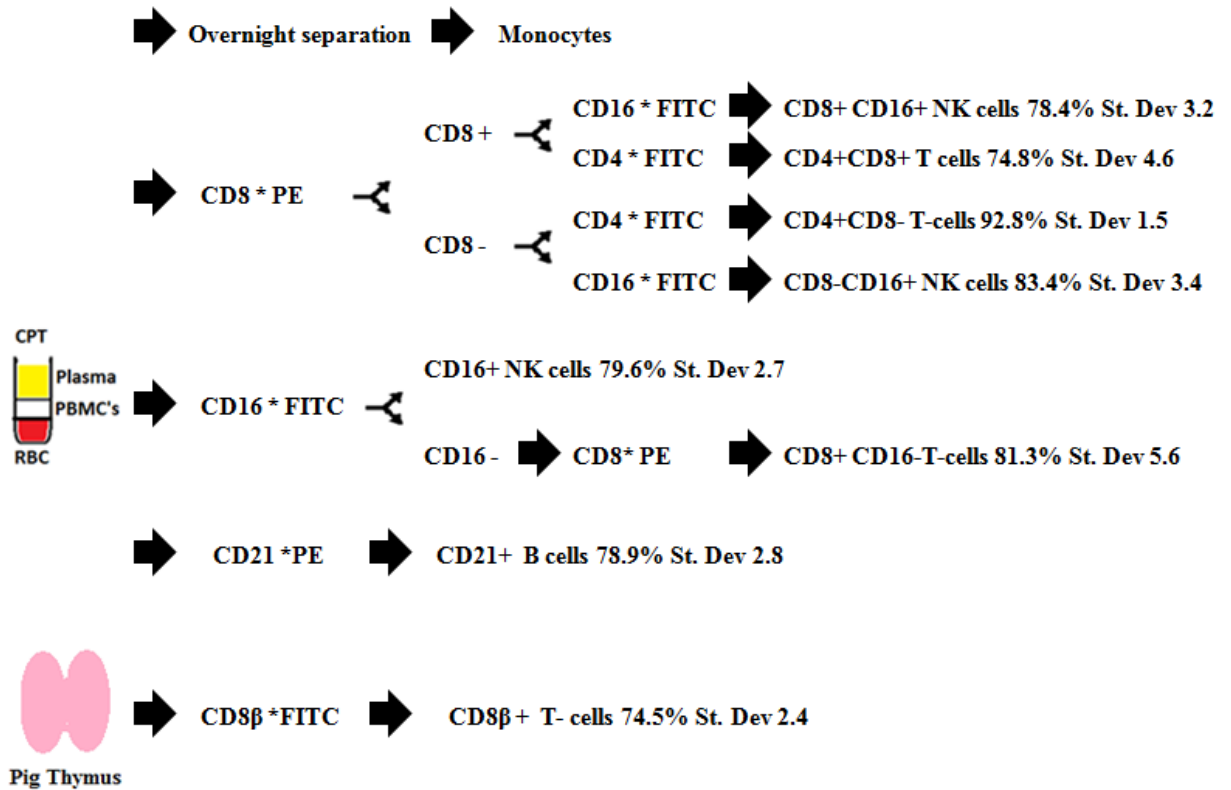


Figure 6: Flow chart of sorting of PBMC. Sorting of cell subpopulations from peripheral blood mononuclear cells (PBMC) by magnetic beads coated with antibodies against selected markers and respective obtained purities. CD8*PE=CD8 α antibody conjugated with PE fluorochrome. CD21*PE=CD21 antibody conjugated with PE fluorochrome. CD16*FITC=CD16 antibody conjugated with FITC fluorochrome. CD4*FITC=CD4 antibody conjugated with FITC fluorochrome. CD8 β *FITC=CD8 β antibody conjugated with FITC fluorochrome.

2.9 Preparation of CD8 β cells from the Porcine Thymus

Thymus was collected from pigs kept at the NCFAD, and 0.5 g was placed on a Petri dish (Falcon, Cat No. 351058). The cell extraction was performed in a Biosafety Class II Cabinet. RPMI 1640 medium containing 10% fetal bovine serum and pen/strep was placed in a 12 well plate (Corning, Cat No. 3524). The thymus was placed into a 100 μ m cell strainer (Corning, Cat No. 08-771-19) and the cell strainer was placed on top of a well in the 12 well plate. Using the plunger end of a sterile syringe, the thymus was mashed through the cell strainer into the 12 well plate. The strainer was rinsed with RPMI 1640 medium and from the 12 well plate, cells were transferred into a 15 ml conical tube (Falcon, Cat No.05-527-90). The cells were spun at 800x g for 3 min and supernatant was discarded. The pellet was resuspended in 1 ml ACK lysis buffer (Thermo Fisher, Cat No.A1049201) for red blood cell lysis and incubated at room temperature for 10 min (this will not lyse PBMCs). Next, 10 ml of RPMI 1640 medium with 10% fetal bovine serum and pen/strep was added again to the tube and spun at 800 g. Supernatant was discarded and pellet was resuspended in RPMI 1640 medium with 10% fetal bovine serum and pen/strep, counted, and CD8 β cells were selected out by magnetic separation using FITC selection kit (STEMCELL, Cat No. 18558) and Mouse Anti-porcine CD8 β -FITC (MyBioSource, Cat No.MBS224781) and analyzed by flow cytometry.

2.10 Cell inoculation with virus

After sorting the leukocytes, cells were kept in RPMI supplemented with 10% FBS at 37°C, 5% CO₂ for 24 hrs or 48 hrs prior to infection to allow time for the selection antibody to internalize or fall off. The day of infection, cells were washed with PBS and counted with a

haemocytometer. The sorted leukocytes were inoculated at 0.1 MOI with NiV or HeV at a cell count of 1×10^6 cells per well in a 48 well plate. The MOI was based on infectivity for Vero 76 cells. The cells were inoculated with virus for 1hr at 37°C, 5% CO₂ in FBS free RPMI. The cells were subsequently washed 5 times with PBS by centrifugation at 500 g for 5 min. The eluent from the last wash was kept, and RT-PCR and plaque assays were performed to determine virus amount left in the supernatant. The cells were resuspended in 500 µl of RPMI supplemented with 2.5% FBS. The cells were incubated for 1 hr, 24 hr, or 48 hrs following inoculation at 37°C, 5% CO₂. Cell populations with low harvest yield had only one well per time point.

Adherent immortalised porcine alveolar macrophages IPAM 3D4/31 were infected by first seeding the cells on a 48 well plate overnight at 10^6 cells/well (doubling time of 25.5h) in RPMI supplemented with 10% FBS. The next morning, a well was trypsinized with 0.25% trypsin/EDTA (Wisent) for 15 min at 37°C, 5% CO₂ to obtain a cell count. The IPAM 3D4/31 cells were inoculated with either NiV or HeV for 1hr at 37°C, 5% CO₂ in FBS free RPMI at a MOI of 0.1, with mock inoculated cells as a control. The cells were washed 5 times to remove virus on the plate and the eluent from the last wash was kept, and RT-PCR and plaque assays were performed to confirm no virus was left in the supernatant. Wells were filled with 500 µl of RPMI supplemented with 2% FBS.

The cell supernatants were collected at 1 hr, 24 hr, and 48 hrs post inoculation. Cells were removed by centrifugation and the infectivity in supernatants was determined by plaque assay. The amount of viral RNA was determined by RT-PCR. The cells were collected to detect the N protein in cells by flow cytometry.

2.11 Preparation of flow cytometry compensation beads

AbC™ Anti-Mouse Bead Kit (Thermofisher, Cat No. A10344) was used for compensation on the FC500 flow cytometer (Beckman-coulter, Cat No. A89264). The kit contains two components. Component A is the AbC™ capture beads and Component B is the negative beads. Component A was completely resuspended by gently vortexing for 30 seconds before use. One drop (40 µl) was added to 1.5 ml Safe-Lock Eppendorf tubes. PE conjugated Mouse Anti-porcine CD8 α , FITC conjugated Mouse Anti-porcine CD4, PE conjugated Mouse Anti-porcine CD21, or FITC conjugated Mouse Anti-porcine CD16 antibody was added to the AbC™ capture bead suspension at an optimized concentration (**Table 3**) in the designated tube and mixed well and left to incubate for 15 min at room temperature in the dark. The beads were transferred to a 15 ml conical tube (Corning) and washed with 5 ml of MACS buffer (Miltenyi Biotec, Cat No 130-091-221) and centrifuged for 5 min at 500 g. The supernatant was removed and the bead pellet was resuspended by adding 0.5 ml of MACS buffer to sample tubes. One drop (40 µl) of Component B (negative beads) was added to the tubes and mixed well. The cells were fixed overnight with Phosphate buffered formalin (Fisher Scientific, Cat No. SF100-4) before the analysis by flow cytometry to approximate cell staining protocol required for NiV infected cells. The protocol was repeated with different antibody concentrations to determine the optimal antibody concentration.

2.12 Intracellular Staining for the N antigen

The virus inoculated cells were intracellularly stained at 24 or 48 hpi, respectively, to detect the N protein of HeV or NiV. The antibody F45G2 (**Table 3**) used for staining are cross reactive and could be used to detect both HeV and NiV protein.

The cells that were in BSL4 were first fixed in 4% formaldehyde for 24 hrs in order to inactivate any virus, and the internal staining was performed in BSL3. The cells were pelleted and the formaldehyde was removed. The cells were resuspended in 250 µl of BD Cytotfix/Cytoperm (BD Pharmingen) for 20 min at 4 °C. Next, the cells were washed twice with BD Perm/Wash and resuspended in 50 µl BD Perm/Wash. An anti-N antibody F45G2 at 1:50 dilution (1 µl) against NiV and HeV nucleoprotein (N protein) was added and incubated at 4 °C for 1 h. The cells were again washed twice with BD Perm/Wash. A goat anti-mouse IgG1-PerCP secondary antibody (Santa Cruz, Cat No sc-45092) was added at 1 : 50 dilution, followed by incubation in the dark at 4 °C for 30 min. The cells were washed twice with BD Perm/Wash and resuspended in 500 µl of MACS buffer for flow cytometry analysis.

2.13 Flow Cytometry Protocol

Cells ready for flow cytometry analyses were resuspended in MACS buffer containing 0.09% azide for preventing the internalization of the antibody-antigen complexes (Miltenyi Biotec, Cat No 130-091-221). All samples were analyzed on a FC 500 Series Flow Cytometer (Beckman Coulter) using the blue 488 nm laser. The channels used were FL1 (525 nm/40) for FITC, FL2 (575 nm/40) for PE, and FL4 (675 nm/40) for PerCP. Cell populations of interest

were gated to exclude debris and doublets. The minimum number of events was 10,000 and run on a low flow rate. The data was analyzed using Kaluza software (Beckman Coulter).

2.14 Whole Cell Lysate Preparation

Cellular lysates from cell lines or sorted leukocytes were prepared by first washing the cells with PBS. Cells grown in T75 flasks to 100% confluency were scraped off, transferred to a 15 ml centrifuge tube and pelleted by centrifugation at 500 g for 5 min . Sorted leukocytes were transferred to a 1.5 ml Eppendorf tube, pelleted at 500 g for 5 min, and the supernatant was removed. The pellets were lysed by adding 1 ml of 1% SDS lysis buffer (Sigma, Cat No 71736-100ml) containing 1x HALT protease and phosphatase inhibitor (Thermo Scientific, Cat No 1861281) was added to pellets from all tested cell types. The SDS buffer and the lysed cells were vortexed and pipetted and transferred to a 1.5 ml Eppendorf tube. Subsequently, the tube was centrifuged at 1300 g for 5 min at 4 °C to pellet the cell debris. Next, the tube was heated on a heating block for 10 min at 95 °C. Samples were then cooled on ice and centrifuged at 1300 g for 5 min at room temperature before quantifying protein concentration on an Isogen Life Science Bio Drop TOUCH following manufacturer's instructions.

2.15 Protein separation by SDS-PAGE

Samples were prepared by diluting the sample 1 : 3 in 4x NuPAGE® LDS (lithium dodecyl sulfate) Sample Buffer (Invitrogen, Cat No NP0007) and (10X) NuPAGE® Sample Reducing Agent (Invitrogen, Cat No NP0004) and heated in a heating block at 70 °C for 10 min.

25 µg of protein was loaded onto the gel (different volumes of samples were loaded depending on the lysate concentration) and were separated by electrophoresis on a NuPAGE 10% 1.0 mm x 10 wells Bis-Tris gel (Invitrogen, Cat No NP0301BOX) in MOPS SDS running buffer (Invitrogen, Cat No NP0001) at 150V for 1hr. To maintain the proteins in a reduced state during protein gel electrophoresis, 500 µl of NuPAGE® Antioxidant (Invitrogen, Cat No NP0005) was added to the MOPS SDS running buffer in the upper chamber. SeeBlue® Plus2 Pre-Stained was used as the protein standard (Invitrogen, Cat No LC5925).

2.16 Immunoblot to detect ephrin

Proteins were transferred onto 0.2 µm pore nitrocellulose membrane (iBlot Gel Nitrocellulose Transfer Stack) using the iBlot Gel Transfer Device (Invitrogen). All transfers were done at 20 V for 7 min.

The nitrocellulose membrane was then blocked for 1hr at room temperature with 5% alkali-soluble casein (EMD Millipore, Cat No 70955-150ML), and then incubated with primary antibodies diluted 1 : 500 in 5% alkali-soluble casein overnight at 4 °C. The primary antibodies (**Table 3**) used were anti-ephrin B2 antibody (Novus Biologicals, Cat No NBP1-49857) and anti-ephrin B3 antibody (Abcam, Cat No ab101699). Both antibodies were diluted 1/500 in 5% alkali-soluble casein, and incubated overnight with the membranes at 4 °C on a plate rocker. The membranes were washed three times with TBST buffer and then incubated for 1 hr at room temperature with Anti-Protein G-HRP (Thermo Fisher, Cat No 101223) secondary antibody diluted 1/10000 in 5% alkali-soluble casein. The membrane was again washed three times with TBST buffer, resolved using enhanced chemiluminescence (ECL) (GE Amersham Biosciences, Cat No RPN2232) and visualized by Azure c600 imaging system.

The ECL method allows for re-probing the membrane for secondary protein by stripping the membrane with Re-Blot plus mild solution (EMD Millipore, Cat No 2502) as per manufacturer's instructions. The stripped membranes were incubated for 1 hr at room temperature with anti-beta tubulin antibody conjugated with horseradish peroxidase (HRP) (Abcam, Cat No ab21058) diluted 1/5000 in 5% alkali-soluble casein, as a loading control. The membrane was washed three times with TBST buffer and resolved using ECL.

2.17 Ephrin B2, CD8 α , and CD16 Surface Expression in Cells

Cell Preparation, adherent cells:

Cells were grown in culture flasks until 100% confluent. Monocytes in the PBMC were allowed to adhere onto flasks by overnight incubation at 37 °C in a 5% CO₂ incubator. Cells were washed once with 1x PBS and trypsinized. Cells were collected in DMEM or RPMI in a 15ml conical tube and centrifuged at 300 g for 5 minutes to pellet the cells. Trypsin containing media was removed and fresh DMEM or RPMI medium was added. The cells were incubated for at least 30 min at room temperature in the 15 ml conical tube for the surface receptors to recycle to the surface. The cells were then centrifuged and resuspended in 500 μ l of MACS buffer.

Cell Preparation, non-adherent cells:

Leukocytes were collected from a T75 plate following an overnight incubated at 37 °C at 5% CO₂ to remove adherent cells, and centrifuged at 500 g for 5 min. The cells were washed once with PBS and resuspended 500 μ l of MACS buffer.

Cell staining:

The cells were then stained with anti-porcine CD8 α -PE and/or anti-porcine CD16-FITC or rabbit anti- ephrin B2 (Novus Biologicals, Cat NoNBP1-84830) at an optimized antibody

concentration (**Table 3**) for 1 hr at 4 °C. The cells were washed 3 times using MACS buffer. For ephrin B2 expression, a goat anti-rabbit Alexa Fluor 488 conjugate (Thermo Fisher, Cat No. R37120) antibody was used as a secondary antibody and was added at an optimized concentration (**Table 3**) and incubated for 1hr at 4 °C. The cells were washed 3 times with MACS buffer and resuspended in 500 µl of MACS buffer. If cells were stained or restrained inside BSL4, the cells were resuspended in 4% formaldehyde for 24 hrs in order to inactivate any virus. Cells were then internally stained or analyzed by flow cytometry for cell-surface expression of CD8 α, CD16, and/or ephrin-B2.

2.18 Transfection of CHO-K1 Cells

CHO-K1 cells were transfected with pCDNA3.1+ vector expressing porcine CD8α (GenBank accession no.NM_001001907.1) and/or porcine ephrin-B2 (GenBank accession No. NM_001114286.1).The plasmids were custom provided by Creative Biogene. Vector maps and nucleotide sequences used are outlined in **Figure 7** and **Table 4**, respectively. One day before transfection, CHO-K1 cells were plated on 24 well plates (Corning, Cat No. 3524) at 2×10^5 cells/well (70% confluence) in 500 µl of DMEM medium supplemented with 10% fetal bovine serum (MULTICELL, Cat No.080-150) and 1x Non-Essential Amino Acids (NEAA) solution (Thermo Fisher, Cat No. 11140050). The day of transfection, the media was replaced with 500 µl fresh DMEM supplemented with 10% FBS and 1x Non-Essential Amino Acids Solution. Lipofectamine™ 3000 Transfection Reagent kit was used for the transfection (Thermo Fisher, Cat No. L3000008). Two solutions were prepared in two separate 1.5 ml Safe-Lock Eppendorf tubes (Eppendorf, Cat No.022600028). Solution A was prepared by adding 500 ng of plasmid and 2 µl of P3000 Enhancer Reagent (Thermo Fisher, Cat No. L3000008) to a final volume of 50

μ l of Opti-MEM (Thermo Fisher, Cat No. 31985062). Solution B was prepared by adding 2 μ l of Lipofectamine 3000 (Thermo Fisher, Cat No. L3000008) in 50 μ l of Opti-MEM. Contents from Tube B were added into Tube A and mixed by pipetting briefly and gently. The solution was incubated for 10 min at room temperature. The mixture was added dropwise to the well and incubated at 37 °C, 5% CO₂ for 24 hr. After 24 hr incubation, cells from one well were detached using Accutase (Thermo Fisher, Cat No. 00-4555-56) to preserve the surface receptors, and the efficiency of transfection was determined by flow cytometry by cell surface expression of CD8 α and/or ephrin B2 on cells stained with mouse Anti-porcine CD8 α -PE (Southern Biotech, Cat No.4520-09) and/or rabbit Anti- ephrin B2 (Novus Biologicals, Cat No NBP1-84830) with goat Anti rabbit Alexa Fluor 488 conjugate (Thermo Fisher, Cat No. R37120) as secondary antibodies.

2.19 Immunofluorescent Staining of Cells

One day prior to transfection, 2×10^5 cells were plated per well in 24 well plates with #1.5 coverslips at 37 °C, 5% CO₂ in DMEM (MatTek Corporation, Cat No. P24G- 1.5-13- F) to obtain 70% confluence. Once successful transfection was confirmed, cells were washed with PBS and inoculated with NiV at MOI of 0.5 based on a titer in Vero 76 cells. The cells were incubated with virus for 1hr at 37°C, 5% CO₂ in DMEM supplemented with 1x NEAA. The cells were subsequently washed 5 times with PBS and 500 μ l of DMEM supplemented with 2.5% FBS and 1x NEAA was added to the wells. The cells were incubated for 24 h at 37 °C, 5% CO₂, and following the incubation, washed with PBS and fixed overnight with 10% buffered formalin phosphate (Fisher Scientific, Cat No. SF100-4). Prior to staining, the cells were washed three times with PBS for 10 min on shaker to remove formalin. Cells were incubated at room

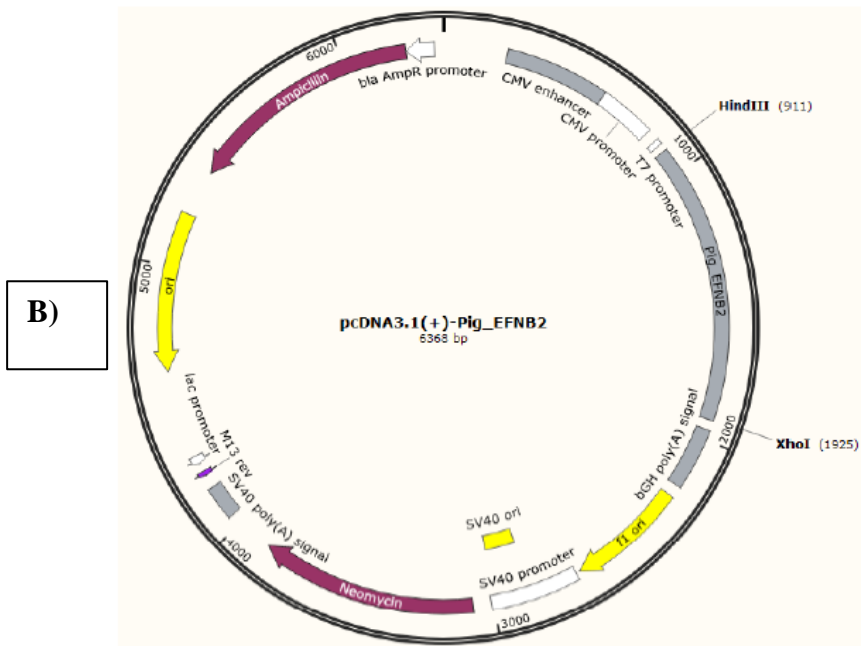
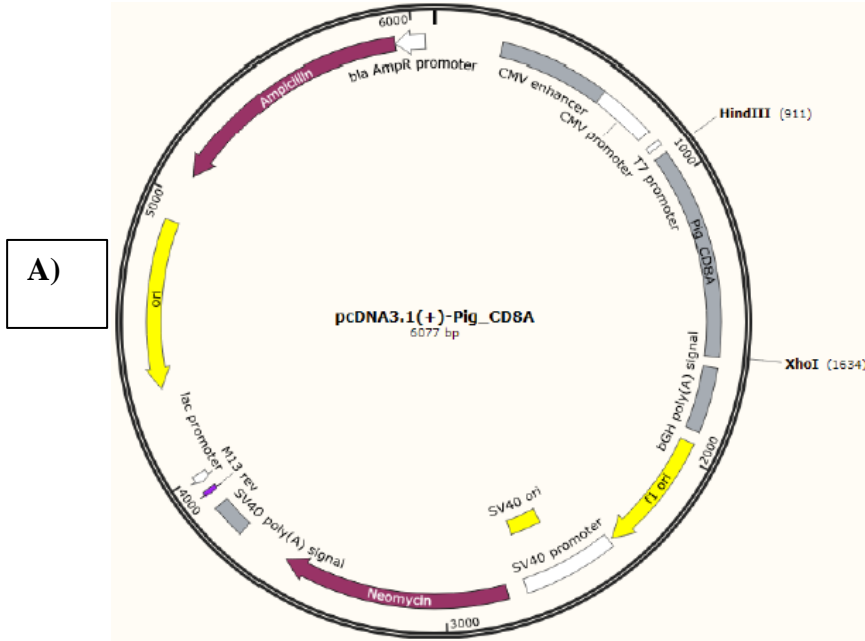


Figure 7: Vector maps of pCDNA3.1 (+)-pCD8 α plasmid (A) and pCDNA3.1 (+)-pEFNB2 plasmid (B). HindIII and XhoI restriction enzymes were used in cloning.

Table 4: Nucleotide sequence of porcine CD8 α and ephrin B2 used for cloning.

Gene	Nucleotide sequence
Sus scrofa EFNB2 Ephrin B2	aagcttgccaccatggccgagaggaggactccgtgtggaagtactgctggggagttttgatggttttatgcagaac tgcgattccagatc gatagtttagagcccatctattggaattcctcgaactctaaattctacctggacaaggactggt actataccacagataggagacaaattggatattattgccccaaagtggactctaaaactgttggccagtatgaatat tataaagtttatatggtggataaagaccaagcagacagatgcactattaagaaggaaaatacccctctcctcaactgt gccagaccagatcaagatgtaaaattcactatcaagttccaagaattcagccctaacctctggggctagaatttcag aagaacagagattattacattatctacatcaaatgggtctttggaggcctggataaccaggaggagggggtgtg ccagacaagagccatgaagatcctcatgaaagtggacaagatgcaagttctgctgggtcaaccaggcataatgag ccaacaagacgtccagaactagaagctggtacaatggaagaagttcaacaacaagccccttctgcaaaccaaatc caggtccagcacagacggcaacagcgcggacattctgggaacaatatcctcgggtccgaagtggccttattcgc agggattgcttcaggatgcatcattcctcctcctcctcctcctcctcctcctcctcctcctcctcctcctcctcct acaccgcaagcactcggcagcacacggccacgctgctgatcagcacgctggccacgccaagcgcggcgg caacaacaacggctcggagcccagtgacattatcattcccgtgaggactgcagacagtgcttctgccccactac gagaaggtcagcggggactacgggcaccgggtgtacatagtcaggagatgccccgcagagcccggcgaac atttactacaaggtctgactcgag
Sus scrofa CD8 α	aagcttgccaccatggcctcgtggtgaccgctctgctcctgccgctggtcctgcagctccatcccgccaaggtcct cgggtccagctgttccggacgtcggcggagatggtgcaggctagcctgggagagacgggtgaagctccgctgcg aggtgatgactccaacacactgacaagctgttctggctctaccagaagcgggggctgcctccaagccatctt cctcatgtacctctccaaaaccgggaataagacagccgaggggctggacaccggttacatctctggttacaaggcc aatgacaactctacctcctcctgcaccgctccgcgaggaggaccaaggctactattctgctcgttctgagcaac tcggttttgtatttcagcaactcatgtccgtcttctgcccagcaaaagccaccaagacgccgactacgccaccacc aagcggactcccacaaagcgtcgcacgccgtgtctgtggccccagaggtgtgccggccttggggcaacgcaga cccgaggaagctggacctcgcctgtgatctgtacaactgggcgccccctggttgggacctccggcatccttctcctgt cactggctaccatcatctgccaccgccaagacagacgtgttgcaaatgtcccaggcccgtggtcagaca gggaggcaaggccagccctcagagagattcatctaactcgag

CHO-K1 cells were transfected with pCDNA3.1+ vector expressing porcine CD8 α (GenBank accession no. NM_001001907.1) and/or porcine ephrin-B2 (GenBank accession no. NM_001114286.1).

temperature for 15 min with 0.25% Triton X-100 in PBS to permeabilize the cells followed by a PBS wash. Cells were then incubated for 1hr with 3% BSA in PBS to block nonspecific binding of the antibodies. Cells were incubated with primary antibody diluted in the blocking buffer at room temperature for 1hr, and washed three times for 10 min with PBS on a shaker.

The dilutions used for the primary antibodies: rabbit anti ephrin B2, mouse Anti-Pig CD8 α -PE, and mouse monoclonal antibody F45G4 (anti-N) are listed in **Table 3**. Cells were then incubated with the goat anti mouse Alexa Fluor 488 conjugated secondary antibody in 3%BSA/PBS for 1 hr at room temperature. The cells were washed with PBS and mounted with ProLong™ Diamond Antifade Mountant with DAPI (for nuclear staining) and the coverslip (Thermo Fisher, Cat No P36966) sealed with nail polish. The cells were imaged on a Zeiss LSM 710 Confocal Microscope at 630x using 63x oil immersion objective at CancerCare Manitoba by the help of Ludger Klewes.

2.20 Receptor Blocking

Sorted leukocytes were kept in RPMI supplemented with 10% FBS at 37 °C, 5% CO₂ for 24 hr or 48 hr prior to infection. IPAM 3D4/31 cells were grown to 100% confluency in 48 well plates and kept in RPMI supplemented with 10% FBS at 37 °C, 5% CO₂. Cells were washed with PBS and counted with a haemocytometer. The sorted leukocytes were incubated with non-conjugated rabbit anti ephrin B2 or anti-porcine CD8 α antibodies at concentrations ranging from 1-15 μ g/ml for 30 min at 37 °C in FBS free RPMI 1640 medium prior to infection. Cells were inoculated with NiV or HeV at a MOI of 0.1 in the presence of antibody for 1 hr at 37 °C, 5% CO₂ in FBS free RPMI. The MOI was based on infectivity for Vero 76 cells. The cells were

subsequently washed 5 times with PBS, re-suspended in 500 μ l of RPMI supplemented with 2.5% FBS and antibody for 1 hr, 24 hr, or 48 hrs following inoculation at 37 °C, 5% CO₂. Leukocytes were collected from the wells and removed by centrifugation and the infectivity in supernatants was determined by plaque assay. Quantification of viral RNA was done by RT-PCR. IPAM 3D4/31 cells were also treated with ephrin B2 antibody or HeV soluble G or NiV soluble G and infected with HeV or NiV using the protocol above.

2.21 Competition Assay

Competition assays were performed as above, employing either HeV or NiV soluble G concentrations ranging from 1-20 μ g/ml.

2.22 In silico Modeling

Crystal structures of porcine CD8 α (PDB ID: 5EDX) and NiV G (PDB ID: 3D11) were already available in the RCSB Protein Database (PDB). Protein-protein docking was performed by ClusPro 2.0 protein-protein docking server (Boston University). ClusPro 2.0 generated 30 structures. Ranking was performed by PS-HomPPI v1.3/DockRank (Pennsylvania State University) and DockScore (Malhotra et al., 2015). Molecular graphics images were generated using PyMOLv2.0 (DeLano Scientific, San Carlos, CA).

2.22 Ethics statement

The collection of non-infected blood samples was included as a component of the AUD ID#: C-15-007 (Foot-and-mouth Disease Serotype A Vaccine Efficacy in Pigs), AUD ID#: C-16-004 (Susceptibility of pigs, sheep, chickens, guinea pigs and rabbits to Zika virus infection), AUD ID#: C-16-005 (Use of IFN-expressing vectors in control of Ebola virus disease in swine), AUD ID#: C-16-006 (Use of IFN-expressing vectors in control of Nipah virus disease in swine), AUD ID#: C-16-010 (Improved vaccination for foot-and-mouth disease in pigs using intradermal application), AUD ID# C-17-001(Animal Care Training Course - Handling of Pigs in Positive Pressure Suits at the CSCHAH CL4 Animal Housing Facilities).

Results

3.1 *In vitro* permissivity of porcine PBMC subpopulations to NiV and HeV

3.1a Virus stock preparation and titration

Virus stocks were prepared and titrated on Vero 76 cells for 3 days for NiV and 4 days for HeV. The titre of the stock was 4.125×10^6 PFU/ml for NiV and 9.45×10^6 PFU/ml.

3.1b Cell preparation from peripheral blood

Adherent cells (monocytes/macrophages) were removed by overnight incubation of the swine PBMC. The cell populations of interest were harvested by magnetic sorting using PE or FITC conjugated antibodies against marker of interest. Antibodies against CD16, CD8, CD4, or CD21 markers were used. Sorting strategy is illustrated in **Figure 6**. The purity of the cells was verified immediately after sorting by flow cytometry.

The CD8+CD16- T cells had a purity of 81.3% St. Dev 5.6, CD4+CD8- T helper cells had a purity of 92.8% St. Dev 1.5, CD21+ B cells had a purity of 78.9% St. Dev 2.8, CD16+ NK cells had a purity of 79.6% St. Dev 2.7, CD8+CD16+ NK cells had a purity of 78.4 St. Dev 3.2 and CD8-CD16+ cells had a purity of 83.4% St. Dev 3.4. The selection antibody can cause steric hindrance and block virus entry. However, the percentage of antibody bound to cells dramatically decreases over time as the cell internalizes the antibody or antibody dissociates from the cell. For example, percentage of cells bound to antibody immediately after sorting CD4+CD8- cells was 92.8% St. Dev 1.5 and 48 hrs post selection, only 7.5% St. Dev 5 has the marker. **Table 5** lists the percentage of cells displaying staining for marker after sorting; 24 hrs post selection, and 48 hrs post selection.

Table 5: Percent purity post selection of PBMC's and the percentage of cells positive for selection antibody 24 hrs and 48 hrs post selection.

Cell type	Cell Purity after sorting (%)	Percent of marker after 24hrs (%)	Percent of marker after 48hrs (%)
CD16+	79.6±2.7	62.3 ± 4.4	11.5 ± 4.4
CD8+CD16+	78.4±3.2	48.2 ± 5.8	7.3 ± 4.7
CD8-CD16+	83.4±3.4	45.2 ± 6.2	2.1 ± 4.1
CD21+	78.9±2.8	58 ± 5.3	8.7 ± 3.3
CD4+CD8-	92.8±1.5	57.5± 3.6	7.5± 5
CD8+CD16-	81.3±5.6	53.6 ± 4.8	9.4 ± 6.2

3.1c Replication of NiV and HeV in the porcine primary immune cells

Leukocyte subpopulations were inoculated with HeV or NiV 24 hrs post selected at MOI of 0.1, based on titers on Vero 76 cells. The IPAM 3D4/31 cells were inoculated 24 hrs post seeding, when they reach 100% confluency. The supernatants were harvested from the inoculated cells at 24 and 48 hpi.

To determine whether steric hinderance can have an effect on virus attachment to the cells, CD8+CD16⁻ cells were inoculated with NiV at 24 h post selection (53.6% \pm 4.8 of the cells labeled) and 48 h post selection (9.4% \pm 6.2 of the cells labeled). The obtained virus yields at 24 hpi did not differ for the 2 time points of inoculation (**Figure 8**), and it was concluded that steric hinderance is not an issue, and cells can be inoculated with virus at either timepoint.

The highest NiV yield (**Figure 9**) was detected in supernatants harvested from IPAM 3D4/31. The CD8+CD16⁺ NK cells and CD8+CD16⁻ T lymphocytes, followed closely by the CD16⁺ cells were also replicating virus in contrast to the CD21⁺ B-cells, CD8-CD16⁺ NK cells, and CD4+CD8⁻ T cells. The low level of infectivity recovered from the three cell subpopulations was residual or likely due to contaminating cells from other permissive subpopulations of PBMC.

Replication of HeV was detected only in IPAM 3D4/31 cells. HeV had higher virus titres (copy numbers/ml and PFU/ml) compared to NiV (**Figure 9 vs Figure 10**). Virus was not detected in supernatants harvested from CD16⁺ NK cells, CD8+CD16⁻ T lymphocytes, CD21⁺ B-cells, or CD8-CD4⁺ T cells inoculated with HeV (**Figure 10**).

Infection of the cells with HeV or NiV was confirmed by positive internal staining for the NiV/HeV-N protein using flow cytometry (**Figure 11 and 12**). No internal staining was observed in CD21⁺ cells, CD4+CD8⁻, or CD8-CD16⁺ cells inoculated with NiV or HeV (**Figure**

11). Positive internal staining was observed in NiV inoculated IPAM 3D4/31 cells, CD8+CD16- T cells, CD8+CD16+ NK cells and CD16+ NK cells (**Figure 12**).

Contour flow cytometry plots were made to further analyze the populations of CD8+ and CD16+ cells that were infected with NiV. CD16+, CD8+CD16-, and CD8+CD16+ cells were harvested 48 hpi and surface stained for CD8 α -PE and/or CD16-FITC and internally stained with anti-NiV N-Protein antibody.

The CD16+ (**Figure 13A**) clearly separated into 3 subpopulations from those positively stained for the CD16 marker, only about 50% stained also for the NiV-N protein (Quadrant 2).

The CD8+CD16- (**Figure 13B**) cells have again quite high percentage on unlabeled cells, and only a subpopulation of the CD8+ cells showed NiV-N staining. This was an interesting finding, as the CD8+CD16- cells would comprise two populations in terms of CD4 marker: the CD4+CD8+ cells would carry CD8 $\alpha\alpha$ dimer (T memory cells), and the CD4-CD8+ cells would carry CD8 $\alpha\beta$ marker (cytotoxic T cells).

The CD8+CD16+ (**Figure 13C**) fraction was gated for only CD8 α and CD16+ positive staining cells. The population that were positive for CD8 α and CD16, all were infected with NiV. The CD8+CD16+ NK cells carry only CD8 $\alpha\alpha$ dimer.

Consequently, it appeared that the T lymphocytes and NK cells were permissive to NiV only if they carried a CD8 $\alpha\alpha$ dimer.

Positive internal staining was observed in HeV inoculated IPAM 3D4/31 cells only indicating that HeV may infect only immune cells of myeloid lineage (**Figure 12**).

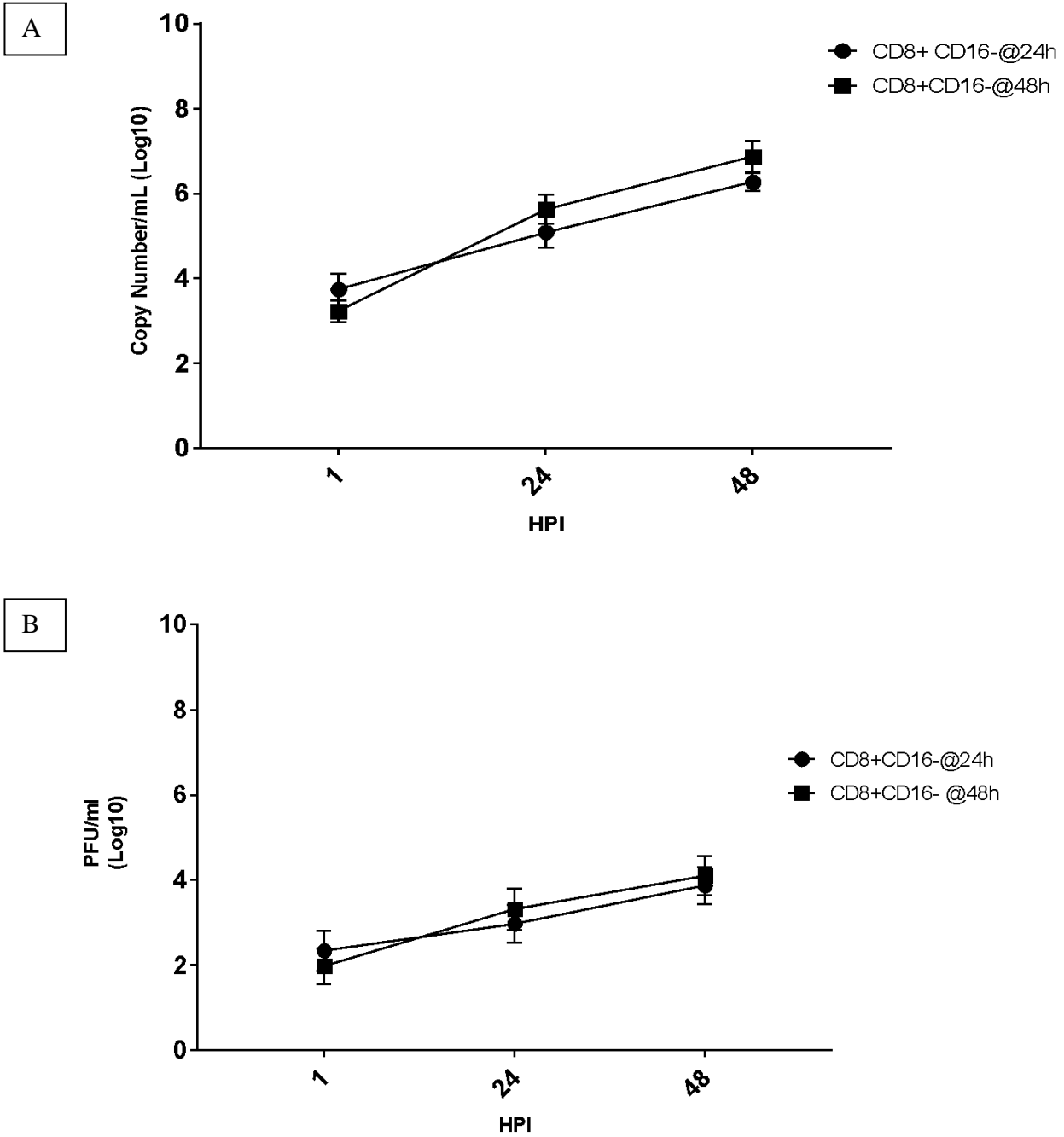


Figure 8: Comparing CD8+CD16- cells inoculated with NiV at 24 h and 48 h post selection by (A) RT-PCR and (B) plaque assay. The same pig blood was used for 24 hrs and 48 hrs inoculations but different aliquots. The values are means \pm St.Dev of 3 replicates.

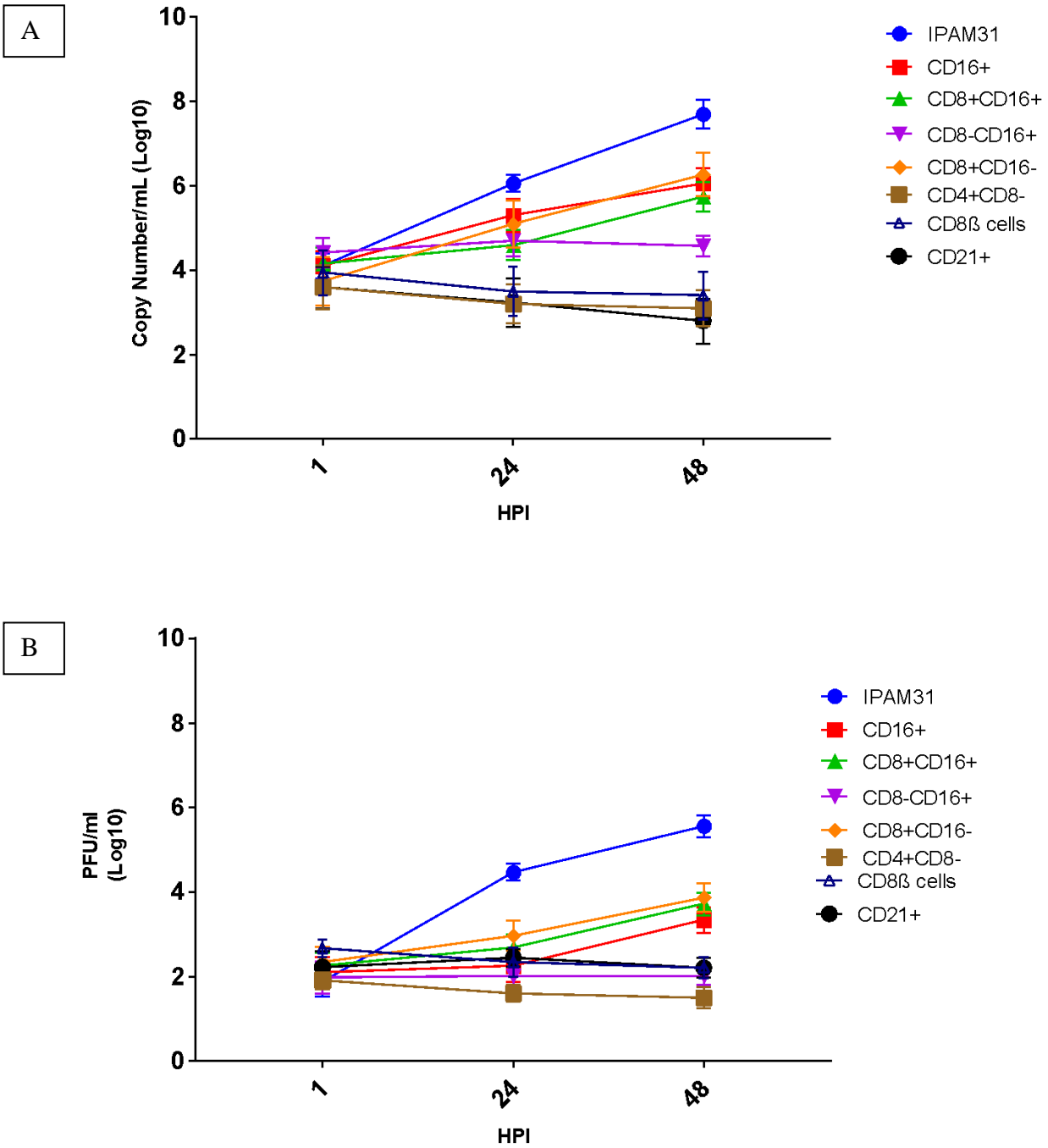


Figure 9: Replication of NiV in the subpopulations of porcine PBMC. NiV replication in the supernatant of selected cells by (A) RT-PCR and (B) plaque assay. The values are means \pm St.Dev of 3 replicates.

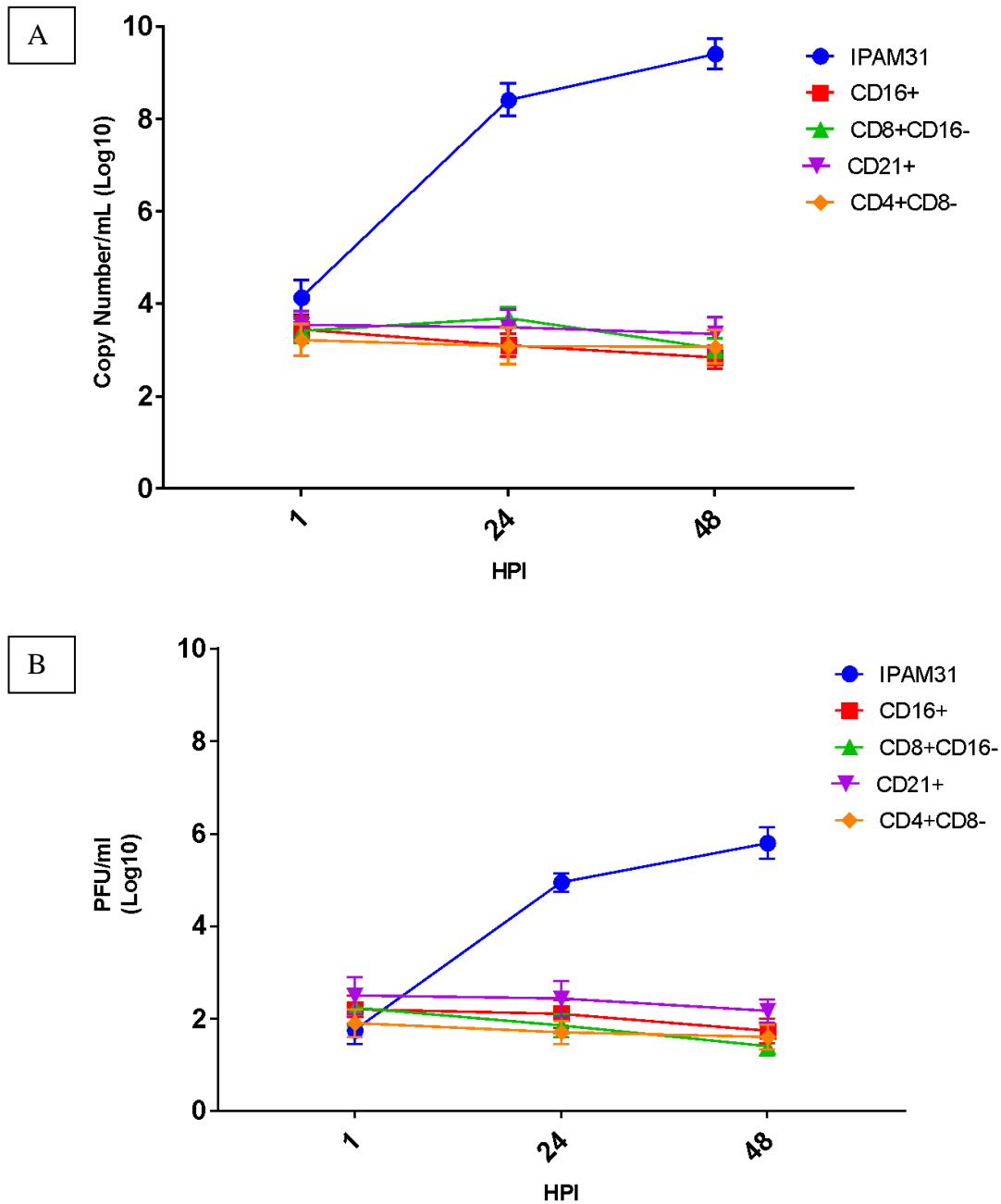


Figure 10: Replication of HeV in the subpopulations of porcine PBMC. HeV replication in the supernatant of selected cells by (A) RT-PCR and (B) plaque assay. The values are means \pm St.Dev of 3 replicates.

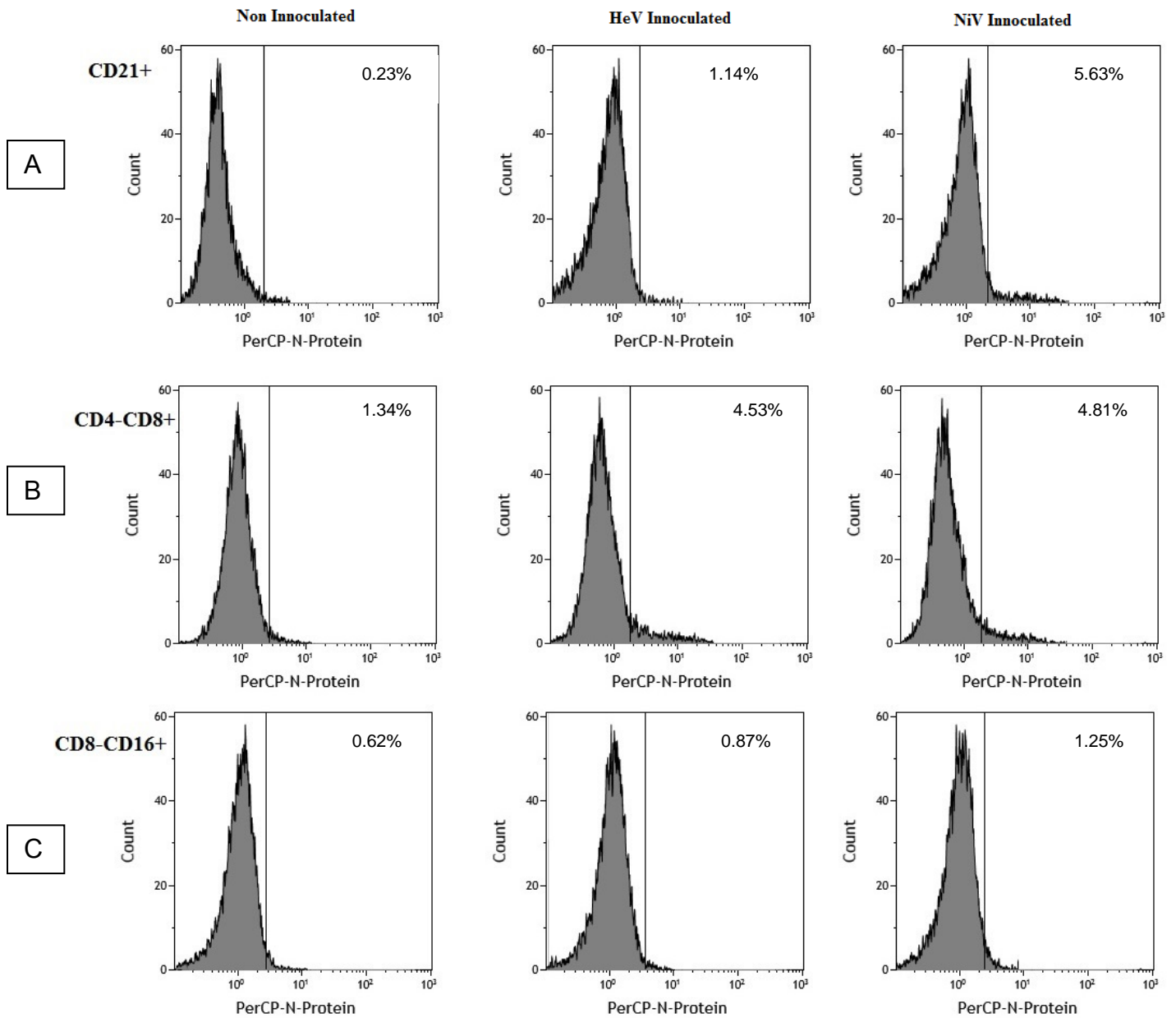


Figure 11: Flow cytometry analysis of PBMC subsets inoculated with HeV or NiV 48 hpi showing negative anti-HeV/NiV N-protein antibody staining. As a confirmation of infection, PBMCs were internally stained with anti-HeV/NiV N-protein antibody (PerCP label). Fig A, =CD21+, B=CD4+CD8-, and C=CD8-CD16+.

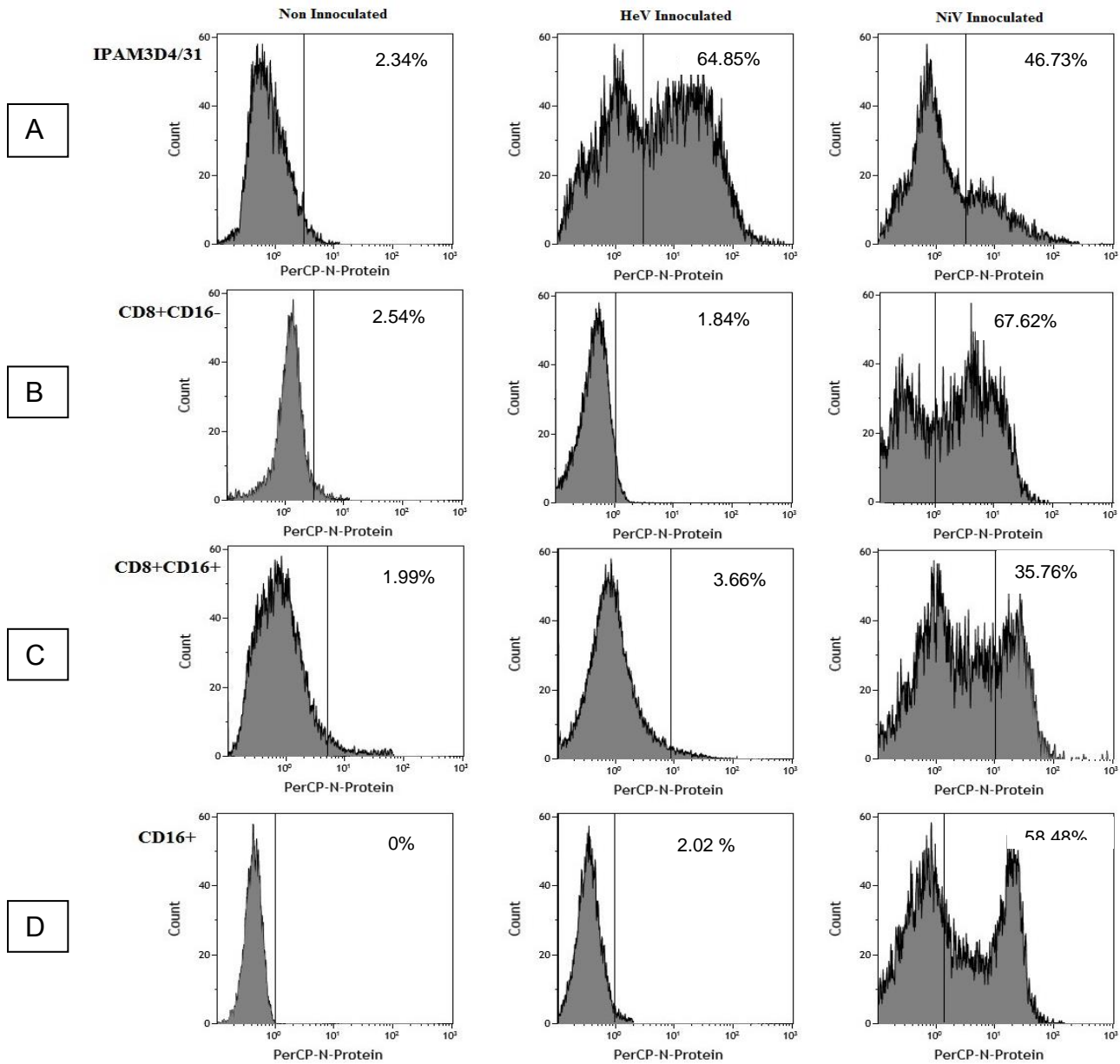


Figure 12: Flow cytometry analysis of PBMC subsets inoculated with HeV or NiV 48 hpi showing positive anti-HeV/NiV N-protein antibody staining. As a confirmation of infection, PBMCs were internally stained with anti-HeV/NiV N-protein antibody (PerCP label). Fig A=IPAM 3D4/31, B= CD8+CD16+, C=CD8+CD16-, and D=CD16+ show intracellular staining for NiV N protein at 48 hpi. Positive intracellular staining for HeV was only observed in IPAM 3D4/31 cells.

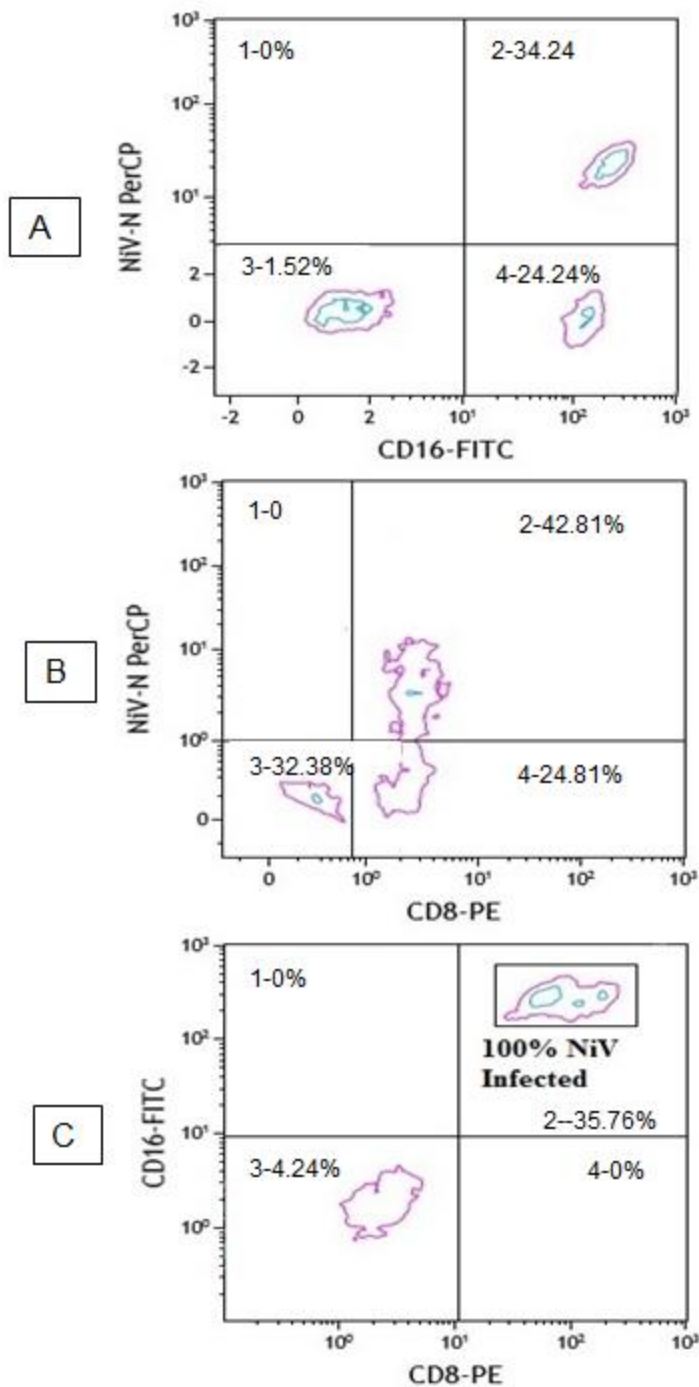


Figure 13: Flow cytometry analysis of (A) CD16+ cells, (B) CD8+CD16-, and (C) CD8+CD16+ cells inoculated with NiV 48 hpi showing positive anti-HeV/NiV N-protein antibody staining. The cells were restrained for CD8-PE and/or CD16+FITC markers and internally stained for anti-HeV/NiV N-protein antibody (PerCP label) 48 hpi.

3.2 Detection of ephrin B2 protein in cells (in IPAM 3D4/31, sorted porcine PBMC and cell lines) by immunoblot and flow cytometry

The detection of ephrin B2 on a protein level in sorted PBMC and IPAM 3D4/31 cells was used to assess whether virus replication or lack thereof was related to presence of the receptor for the virus. Ephrin B3 was not probed for because an effective antibody specific for porcine ephrin B3 was not available, and ephrin B3 was not reported to be expressed on leukocytes.

The cell lysate of the following subsets of PBMCs: CD8+CD16+, CD8-CD16+, CD4+CD8+, CD4-CD8+, and CD4-CD8+CD16- were analyzed for presence of ephrin B2 initially by immunoblot (**Figure 14**). Swine testis fibroblasts (ST), immortalized porcine alveolar macrophage cell line (IPAM 3D4/31), porcine kidney (PK15), and African green monkey kidney (Vero 76) cells were used as controls.

Whole cell lysates from all tested PBMC populations and cell lines expressed ephrin B2 protein, except for CD8-CD16+ cells. The intensity of luminescence was different for each of the lysates indicating different levels of expression. Since the lysates were not prepared from the surface fraction, we could not conclude whether there was surface expression. Cells not permissive to NiV, such as the PK15 cell line (Aljofan et al., 2009) or CD4+CD8- (Stachowiak & Weingartl et al., 2012) had also detectable ephrin B2 protein in their cell lysates (**Figure 14**), the results were inconclusive.

In course of the research work, anti-ephrin B2 antibody suitable for flow cytometry became available, and cell surface expression was then investigated using this approach.

Flow cytometry was used to confirm expression of ephrin B2 on the cell surface (**Figure 15**): Ephrin B2 was expressed on the surface in IPAM 3D4/31 cells, ST cells, Vero76 cells, and monocytes. CD8+ cells, CD8- cells, and PK15 cells did not express ephrin B2 on the cell surface (**Figure 15**). These results demonstrate (**Table 6**) that, infection of cells is either linked to expression of ephrin B2 or CD8 marker on their surface, and the permissibility of CD8+ cells to NiV is not linked to ephrin B2 expression on a cell surface.

The flow cytometry findings thus suggested presence of an alternative receptor on the leukocytes carrying the CD8 marker, and based on the permissivity findings above, specifically the CD8 $\alpha\alpha$ dimer.

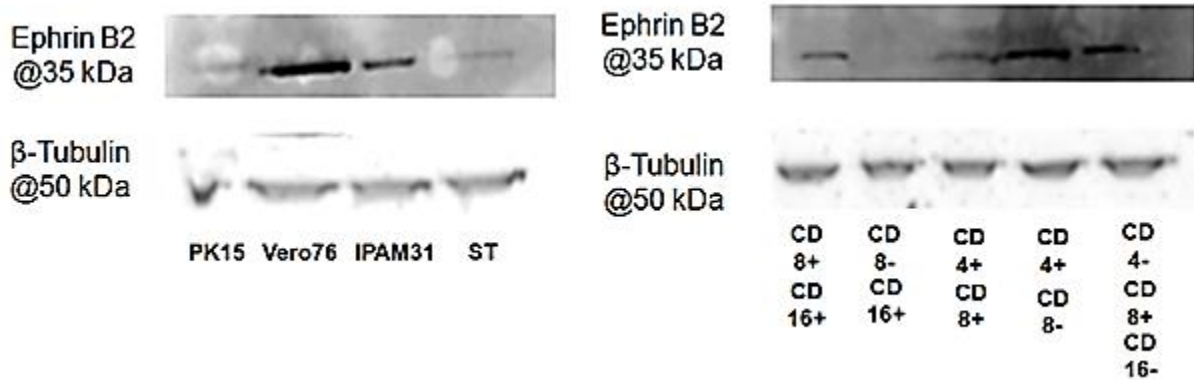


Figure 14: Ephrin B2 immuno Blot: Ephrin B2 expression in cell lines and selected PBMC subsets.

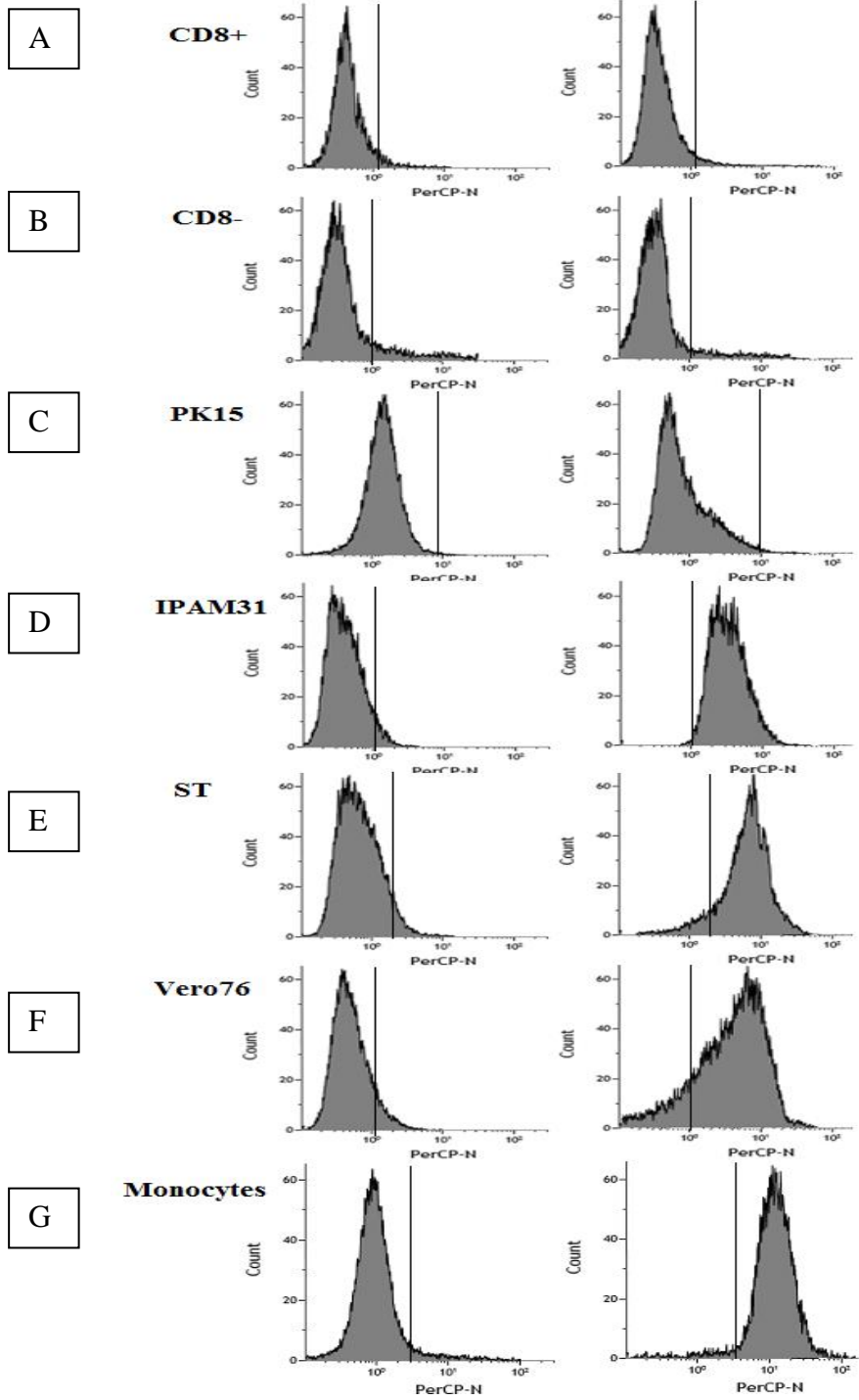


Figure 15: Flow cytometry analysis of ephrin B2 expression. PBMCs and cell lines were surface stained with anti-ephrin B2 antibody (PerCP label). Fig. A, B, C show lack of ephrin B2 staining for CD8+ fraction cells, CD8-fraction cells, and PK15 cells respectively. Fig. D, E, F and G show surface staining for ephrin B2 protein in IPAM 3D4/31, ST cells, Vero 76, porcine monocyte cells respectively.

Table 6: Ephrin B2 expression in selected cells PBMCs and permissiveness to NiV. ND-Not done

Cell Type	Permissive to NiV	CD8 Surface expression	Ephrin B2 expression in cell lysate	Ephrin B2 expression on cell surface
CD8+CD16+	+	+	+	-
CD8- CD16+	-	-	-	-
CD4+CD8+	+	+	+	-
CD4+CD8-	-	-	+	-
CD4- CD8+CD16-	+	+	+	-
Porcine monocytes	+	-	ND	+
Vero 76	+	-	+	+
IPAM 3D4/31	+	-	+	+
PK15	-	-	+	-
ST	+	-	+	+

3.3 Ephrin B2 and CD8 α Antibody Blocking Assays

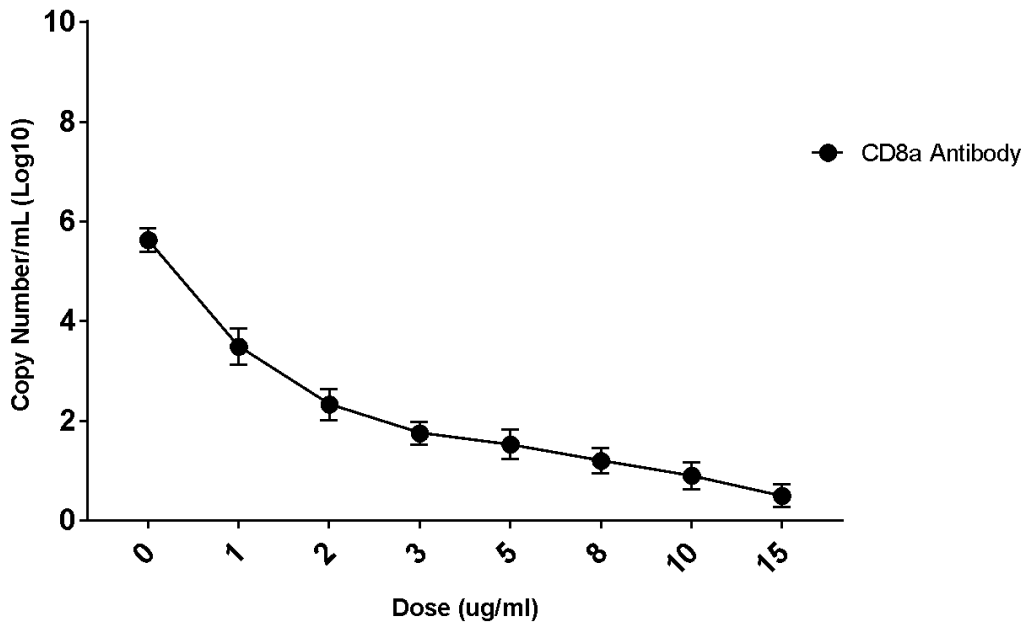
Blocking assays using the anti-ephrin B2 and anti-CD8 α antibodies were performed to determine the effect of the blocking of the ephrin B2 receptor and CD8 putative receptors on the replication of NiV. Because the leukocytes were positively sorted using the anti-CD8 α antibodies, the sorted CD8 $^{+}$ cells were expected to contain both CD8 $\alpha\alpha$ and CD8 $\alpha\beta$ expressing subpopulations.

Cells were pretreated with non-conjugated antibodies either against ephrin B2 or against CD8 α in concentrations ranging from 1-15 $\mu\text{g/ml}$, for 30 min at 37 $^{\circ}\text{C}$, 5% CO_2 in FBS free media. The cells were then inoculated with NiV at MOI 0.1, and incubated with the respective antibodies in 2% FBS medium under the same conditions for 24 hrs.

Figure 16 illustrates that, CD8 α does block NiV replication in the CD8 $^{+}$ cells. A sharp decline and near full block is achieved with CD8 α antibody. The ephrin B2 blocking curve (**Figure 17**), confirms that porcine CD8 $^{+}$ cells do not express ephrin B2. We observe non-specific binding noted by the flat line with shallow curve and full blocking is not achieved.

The ability of CD8 α antibodies to block NiV replication in CD8 $^{+}$ cells in comparison with the lack of specific block by ephrin B2 antibody indicated that CD8 α acts as a receptor on CD8 $^{+}$ porcine lymphocytes.

A



B

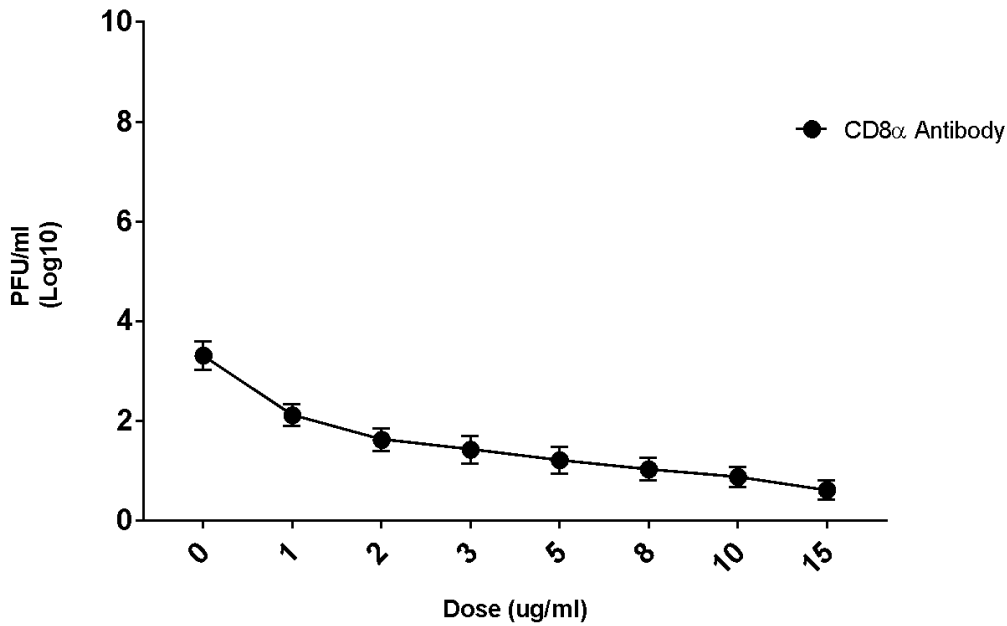
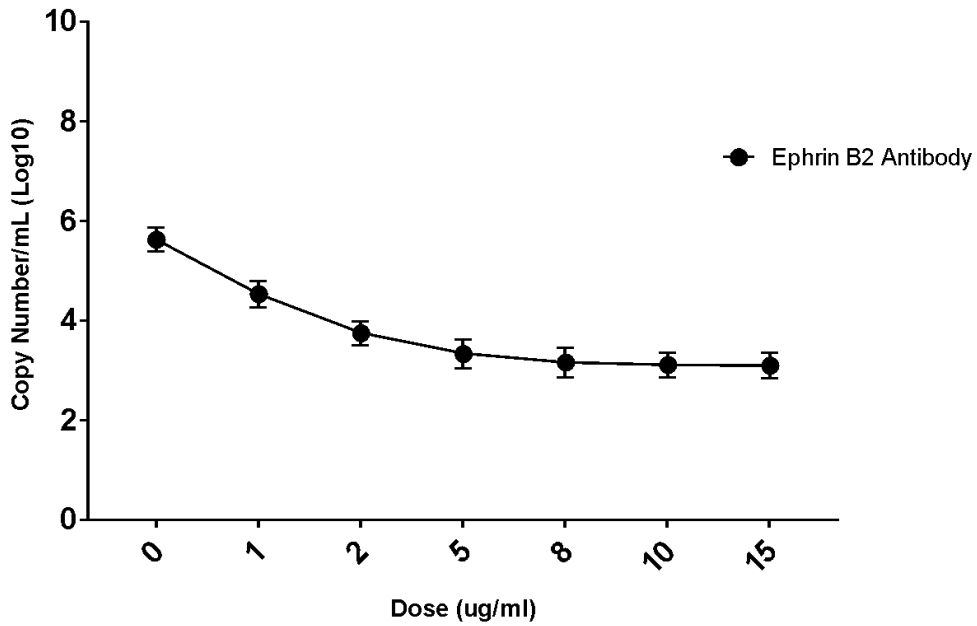


Figure 16: (A) RT-PCR and (B) Plaque Assay Data of the replication of NiV in porcine CD8+ cells in various concentrations of non-conjugated porcine CD8 α antibody at 24hrs. NiV detection in the supernatant of selected cells. The cells were inoculated 48h post selection. The values are means \pm St.Dev of 2 replicate.

A



B

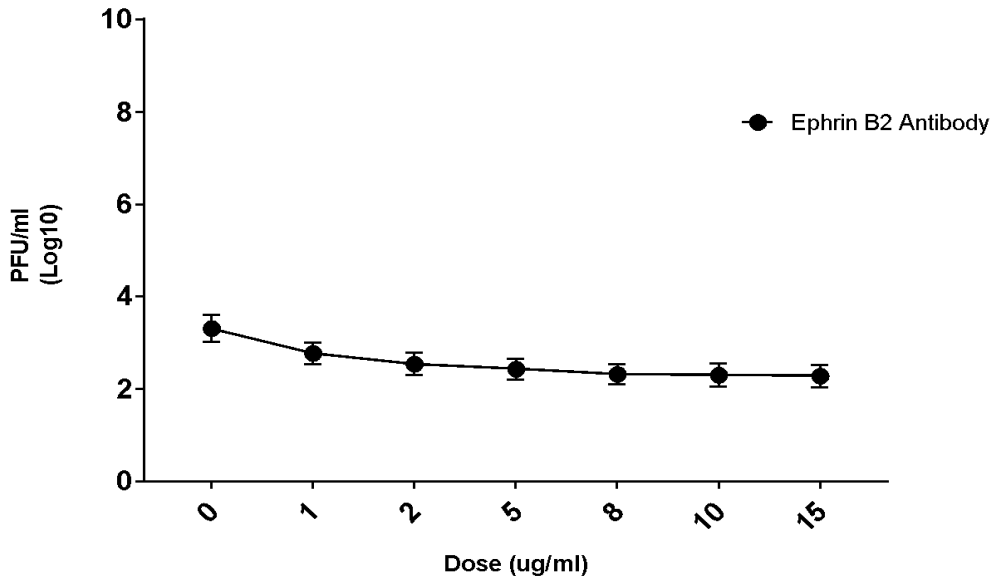


Figure 17: (A) RT-PCR and (B) Plaque Assay Data of the replication of NiV in porcine CD8+ cells in various concentrations of non-conjugated ephrin B2 antibody at 24hrs. NiV detection in the supernatant of selected cells. The cells were inoculated 48h post selection. The values are means \pm St.Dev of 2 replicate.

3.4 CD8 $\alpha\beta$ is not a receptor for Nipah Virus

To confirm that the cells expressing CD8 $\alpha\beta$ heterodimer are not permissive to NiV, and the CD8 $\alpha\beta$ molecule cannot act as a receptor, the CD8⁺ cells were harvested from the thymus using a mouse anti-porcine CD8 β -FITC antibody and FITC-sorting kit (**Figure 6**), and the cells were then inoculated with NiV as described above. The cell purity after sorting was 74.5% \pm 2.4.

RT-PCR and plaque assay data show that CD8 $\alpha\beta$ cells were not permissive to NiV (**Figure 18**). Flow cytometry analysis of the internal cellular staining for NiV-N protein confirmed that there was no NiV replication (**Figure 19**).

Immunohistochemistry was performed on *in vivo* NiV infected pig thymus (**Figure 20**). No NiV staining was observed confirming that CD8 $\alpha\beta$ cells are not permissive to NiV and only CD8 $\alpha\alpha$ acts as a receptor for NiV.

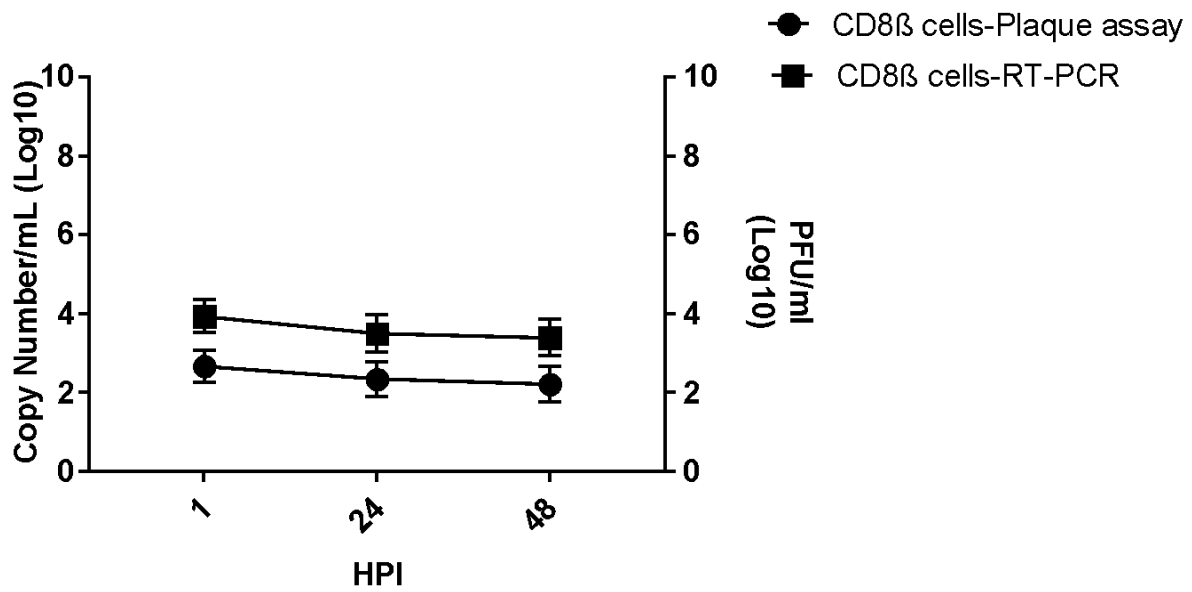


Figure 18: RT-PCR and plaque assay analysis of NiV inoculated CD8β selected cells. NiV replication in the supernatant of selected cells. The cells were inoculated 48 hrs post selection. The values are means \pm St.Dev of 2 replicates.

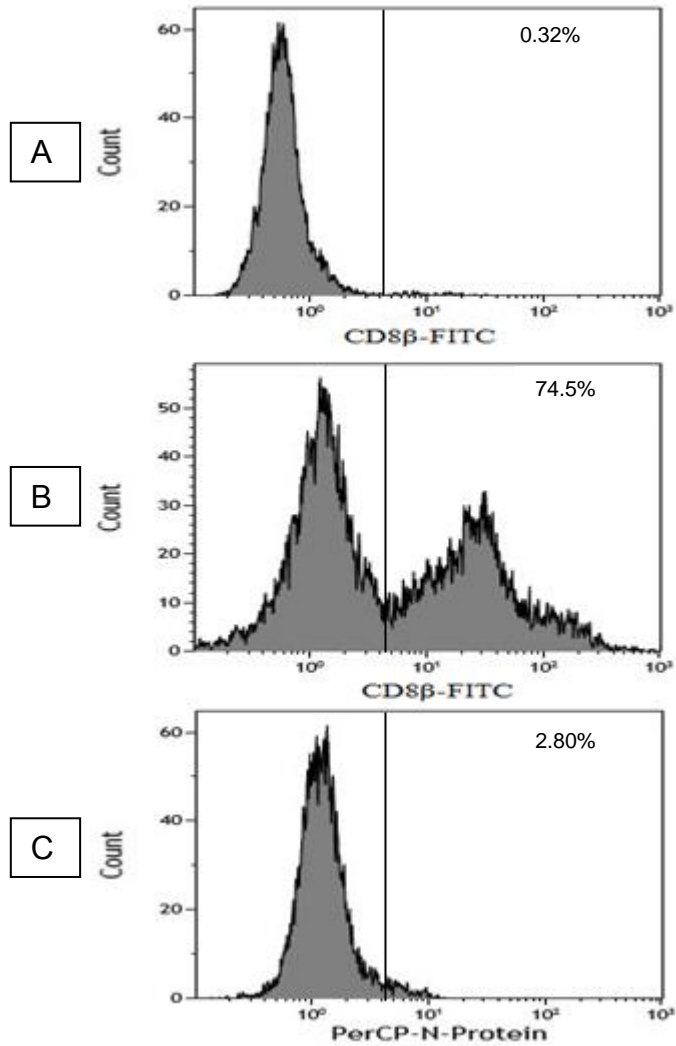


Figure 19: Flow cytometry analysis of porcine CD8β. Inoculated cells were internally stained with anti-NiV N-protein antibody (PerCP label). No positive staining was observed. **(A)** Unsorted unstained CD8β sorted cells. **(B)** CD8β sorted cells. **(C)** NiV inoculated CD8β cells at 48hrs.

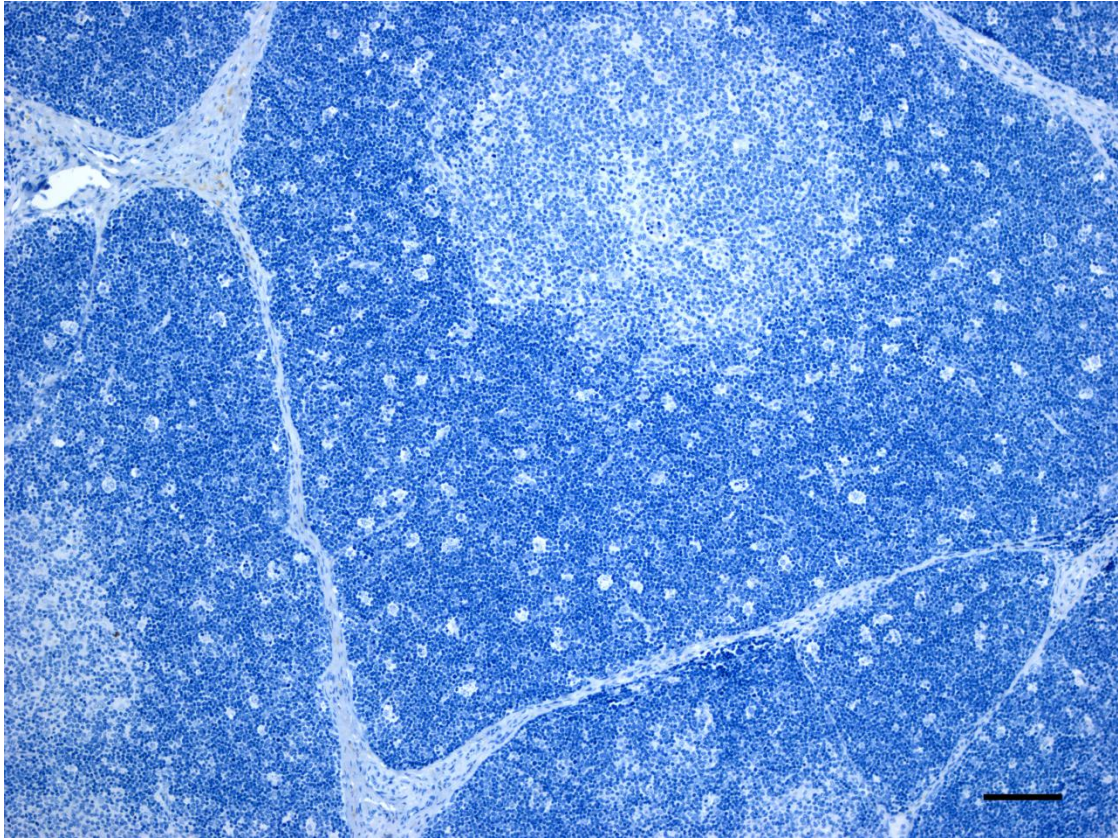


Figure 20: Negative Immunohistochemistry staining for NiV of *in vivo* NiV infected porcine thymus. Stained by Brad Collignon (CFIA) and imaged by Dr. Carissa Embury Hyatt.

3.5 Porcine CD8 α and Ephrin B2 Transfection in Chinese Hamster Ovary Cells

CHO-K1 cells are permissive but not susceptible to NiV as they do not express ephrin-B2 prior to transfection, the absence of expression of the ephrin was confirmed by immunoblot and flow cytometry (**Figure 21-22**) (Negrete et al., 2006). They also do not express CD8 α protein as confirmed by flow cytometry (**Figure 22**). To determine if CD8 α plays a role in viral entry, CHO-K1 cells were transfected with CD8 α and inoculated with NiV. Transfection of porcine ephrin B2 was used as a positive control.

Efficiency of transient transfections of porcine CD8 α (NM_001001907.1) and porcine ephrin B2 (NM_001114286.1) protein expression plasmids pCDNA3.1 into CHO-K1 cells was determined by flow cytometry (**Figure 22**). The controls were non transfected CHO-K1 cells and CHO-K1 cells mock transfected with lipofectamine 3000.

CD8 α and ephrin B2 single and co-transfections were repeated 3 times. Efficiency of transfection with CD8 α plasmid only was 61.54% St. Dev 6.1 and ephrin B2 transfection efficiency was 65.54% St. Dev 8.7 (**Figure 22**); expression of ephrin B2 in transfected CHO-K1 cells was also confirmed by immunoblot (**Figure 21**). Co- transfections did not change the transfection efficiency: in the co transfected cells, CD8 α was expressed on 62.59% St. Dev 4.2 of the cells, and ephrin B2 was expressed in 63.87 % St. Dev 6.4 of the cells. When the cells were inoculated with NiV at MOI of 0.1, virus replication was detected in ephrin B2 and/or CD8 α transfected cells by RT-PCR and plaque assay from the cell supernatants harvested at 24 hpi. The data showed that single transfected CHO-CD8 α cells and CHO-ephrin B2 cells were equally effective in NiV replication; and co- transfected cells had higher copy numbers and PFU than single transfections (**Figure 23**) likely due to a greater number of transfected cells, as some cells

were expressing ephrin B2, CD8 α , or both, although synergizing effect in double transfected cells cannot be excluded.

Infection of CD8 α + single transfected cells was confirmed by N antigen staining (**Figure 22**). The **Figure 22** shows 34% cells are infected with NiV at 24 hpi. With the MOI used (0.1), and only 61.54% St. Dev 6.1 cells were transfected, this result is expected.

NiV infection of CHO-K1 cells transfected with CD8 α was also confirmed by confocal microscopy on fixed cells (**Figure 24**). The plate was inoculated with NiV at a MOI of 0.5, and 24hrs fixed with paraformaldehyde, and the cells permeabilized with Triton X-100. The cells were then stained with anti-NiV N protein F45G4 antibody and goat anti-mouse Alexa Fluor 488 conjugate, and/or mouse anti porcine CD8 α -PE antibody, and mounted by ProLong Gold Antifade Mountant with DAPI. Cells that were expressing CD8 α were permissive to NiV, and, non-transfected cells were non permissive to NiV. Plate labeled with star in **Figure 23** illustrated that not all cells were transfected with CD8 α protein (and expected to form homodimers of CD8 $\alpha\alpha$), and only from those were some infected with NiV. Localization of both, CD8 α and NiV N F45G4 antibody was observed on a number of cells.

This data provides evidence that CD8 α can serve as a receptor for NiV independently of ephrin B2, supporting the findings in primary porcine cells: CD8 $\alpha\alpha$ T and CD8 $\alpha\alpha$ NK cells.

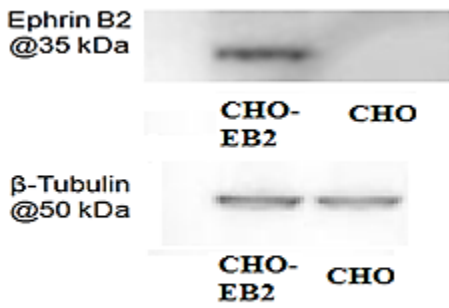


Figure 21: Confirmation of the lack of ephrin B2 expression in CHO-K1 cells by western blot. Left-CHO-K1 cells transfected with porcine ephrin B2. Right-CHO-K1 mock transfected cells.

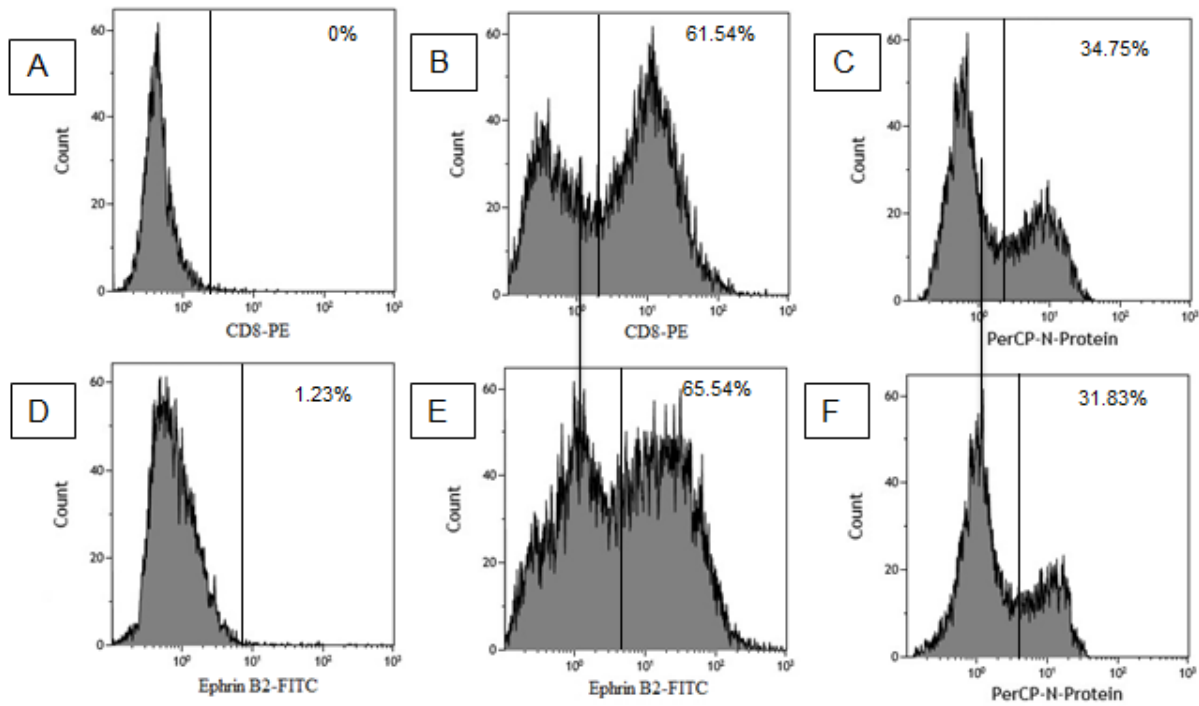


Figure 22: Flow cytometry analysis of CHO-K1 transfected cells. Fig A=Non transfected CHO cells surface stained with CD8-PE, Fig B=CHO cells transfected and surface stained with CD8 α , Fig C=CHO cells transfected with CD8 α and internally stained with anti-NiV N-protein antibody F45G2 (PerCP label), Fig D=Non transfected CHO cells surface stained with ephrin B2-FITC, Fig E=CHO cells transfected and surface stained with ephrin B2, Fig F=CHO cells transfected with ephrin B2 and internally stained with anti-NiV N-protein antibody F245G2 (PerCP label).

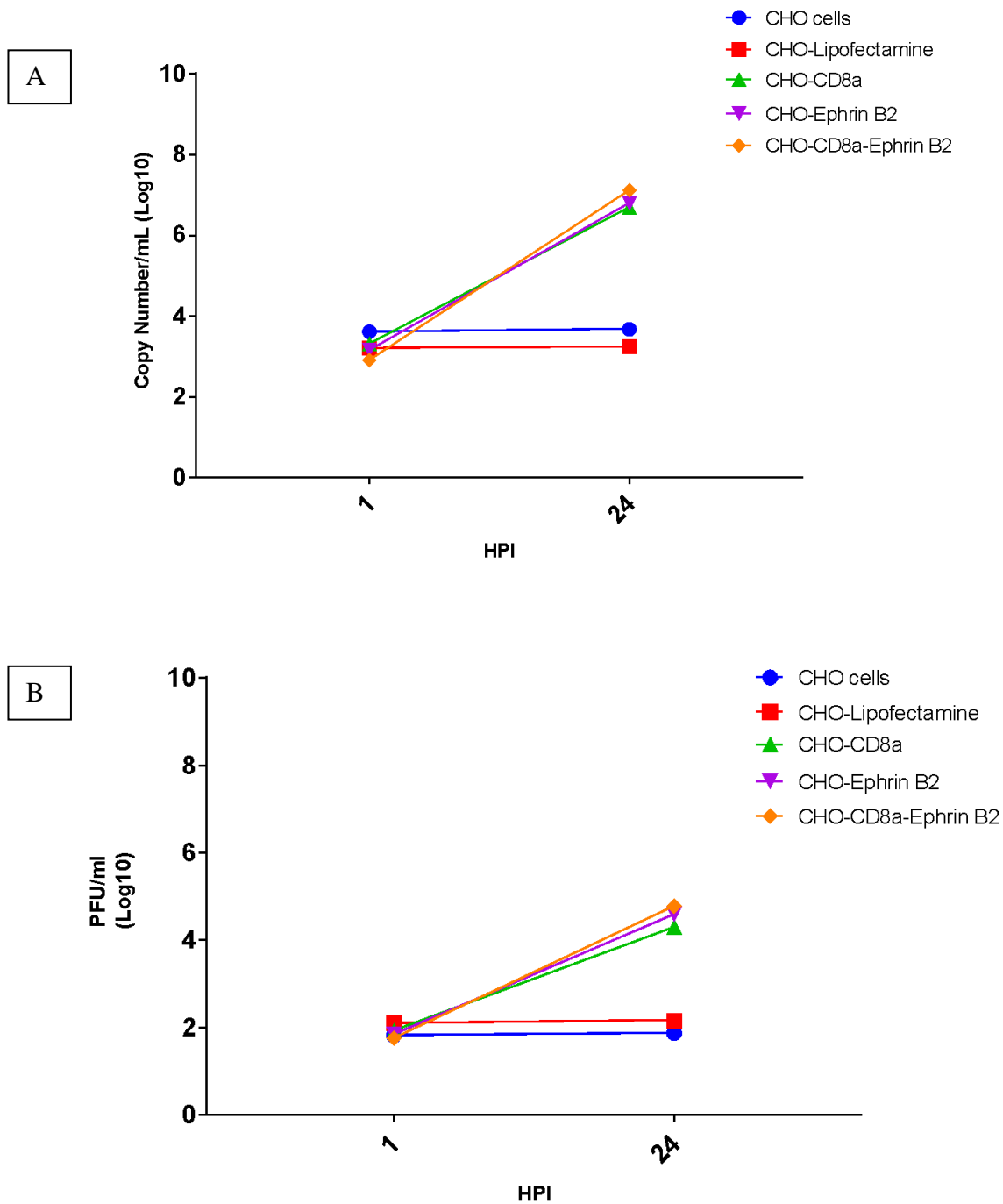


Figure 23: (A) RT-PCR and (B) plaque assay analysis of CHO-K1 cells transfected with ephrinB2 and/or CD8 α . Due to differences in transfection efficiency, runs could not be quantitatively compared, however, all runs showed that CD8 α , ephrinB2 and ephrinB2 +CD8 α transfected cells were all infected with NiV and untreated CHO cells were not permissive to NiV.

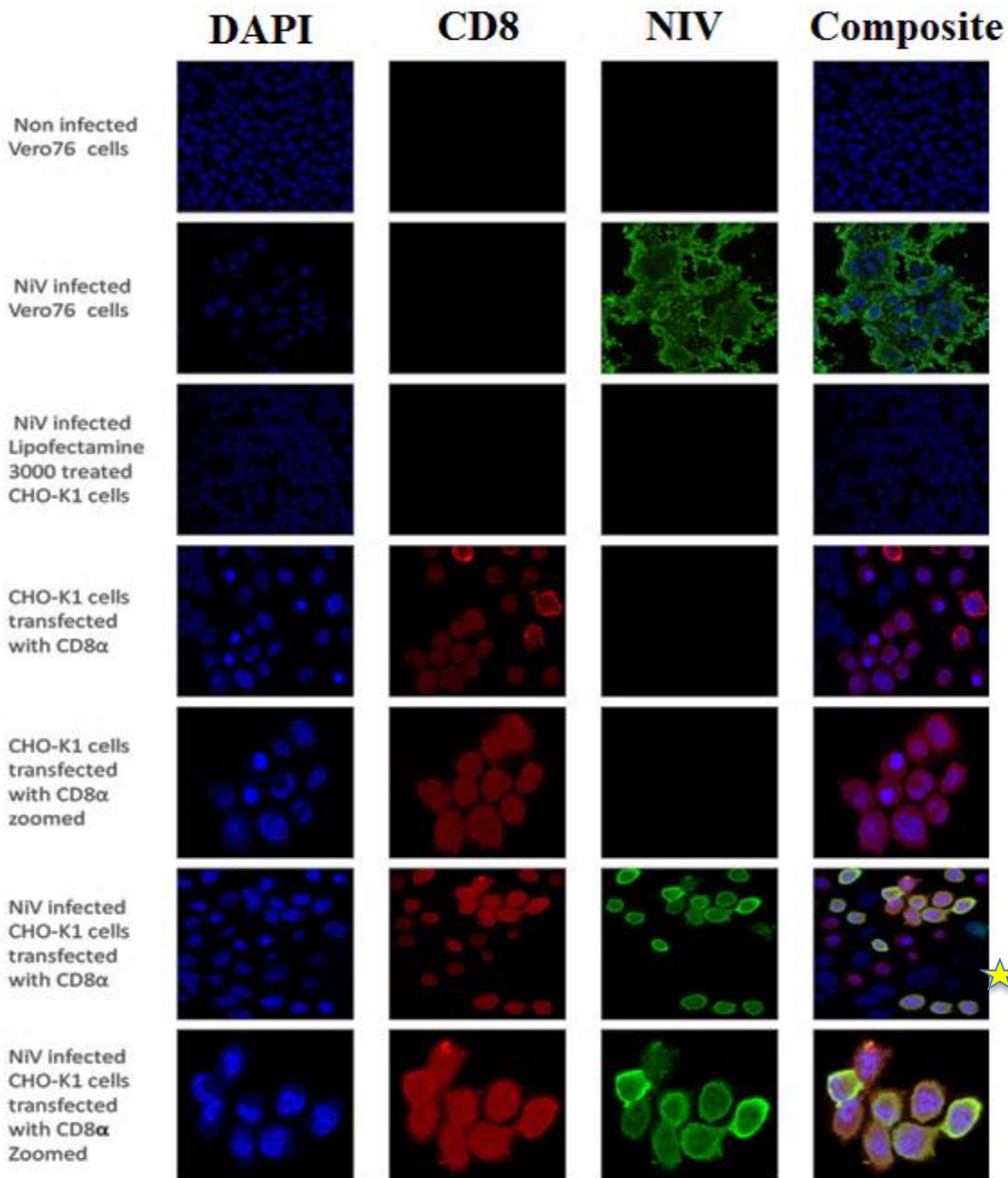


Figure 24: Confocal microscopy staining of receptor-negative and -positive cells. Cells were plated into a MatTek glass bottom 24-well plates. The plate was inoculated with NiV at a MOI of 0.5 for 24 h, fixed with paraformaldehyde, permeabilized with Triton X-100, and stained with NiV N F45G4 antibody and goat anti mouse Alexa Fluor 488 conjugate (**Green**), mouse anti-porcine CD8 α -PE antibody (**Red**), and mounted by ProLong Gold Antifade Mountant with DAPI (**Blue**). All figures were imaged at 630x (63x oil immersion objective) on a Zeiss LSM 710 confocal microscope.

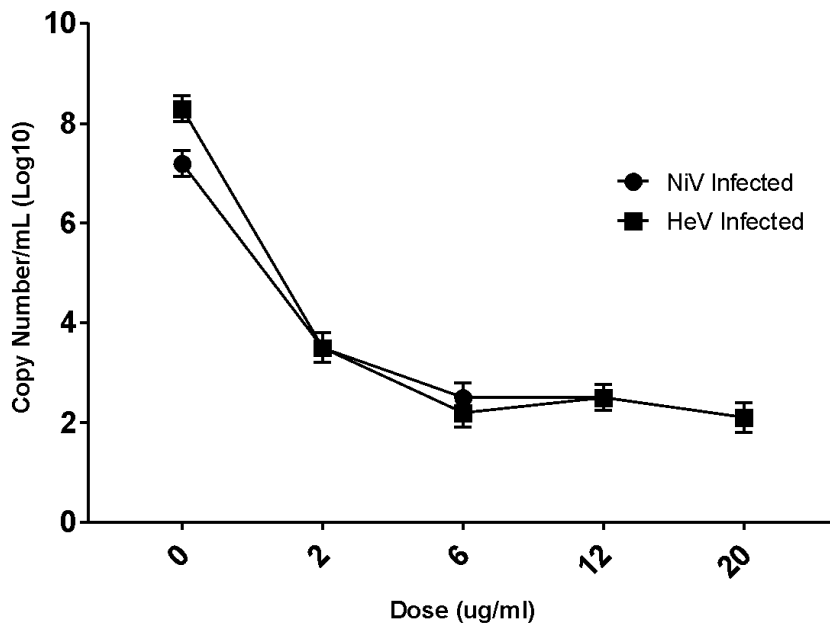
3.6 Competition of the HeV or NiV Soluble G with NiV on Porcine CD8+ cells

Because of the differences in permissivity of CD8+ cells to NiV compared to HeV, we were interested in determining whether there is a difference in binding of the virus to the cells. We assessed the effect of various HeV and NiV soluble glycoprotein (sG) concentrations on virus infection of IPAM 3D4/31 cells and primary porcine CD8+ cells *in vivo*. The method used was a modified protocol by Bossart et al. [2005]. The CD8+ cells were prepared as described in section 2.7-2.8. CD8+ porcine cells were inoculated with NiV 48 hrs post selection to eliminate the possibility of CD8-PE selection antibody participating in blocking. The CD8+ cells were pre incubated with concentrations of HeV or NiV sG ranging from 1-20 µg/ml for 30 min, then the cells were inoculated at MOI of 0.1 of HeV or NiV, in the presence of HeV or NiV sG for 1 hr, followed by removal of the virus inoculum, and incubated in media containing HeV or NiV sG. At 1 hr, 24 hr, and 48 hr time points, supernatants and cells were removed. The supernatant were used for plaque assays on Vero 76 cells to detect infectivity and for NiV RT-PCR to detect genomic RNA. The cells were internally stained for HeV/NiV N protein and flow cytometry was performed.

To determine the range of optimal concentrations of the sG required to block replication, different concentrations of HeVsG were used to assess kinetics of blocking on IPAM 3D4/31 cells (**Figure 25**). IPAM 3D4/31 cells express ephrin B2 only; therefore HeV and NiV utilize a common receptor on these cells. Inhibition of HeV and NiV infection by HeV sG protein revealed a dose-dependent response. HeV sG completely blocked HeV infection of IPAM 3D4/31 at 6µg/ml and higher, and also completely blocked NiV infection at 6 µg/ml and higher. This observation agrees with the report Bossart et al, 2005.

Porcine CD8⁺ cells were then treated with 6 µg/ml of NiV or HeV sG and infected with NiV using the same protocol used for the IPAM 3D4/31 cells. NiV sG was significantly more efficient in reducing NiV copy numbers and PFU compared to HeV sG (**Figure 26-28**), indicating that NiV is able to bind to the CD8 marker with higher affinity than HeV, explaining that lack of permissibility of porcine leukocytes to HeV. The block of NiV replication by NiV sG was not complete. The NiV sG is a truncated protein and the full protein G sequence may be required to achieve full block of NiV. See discussion in Conclusion (4.5.).

A



B

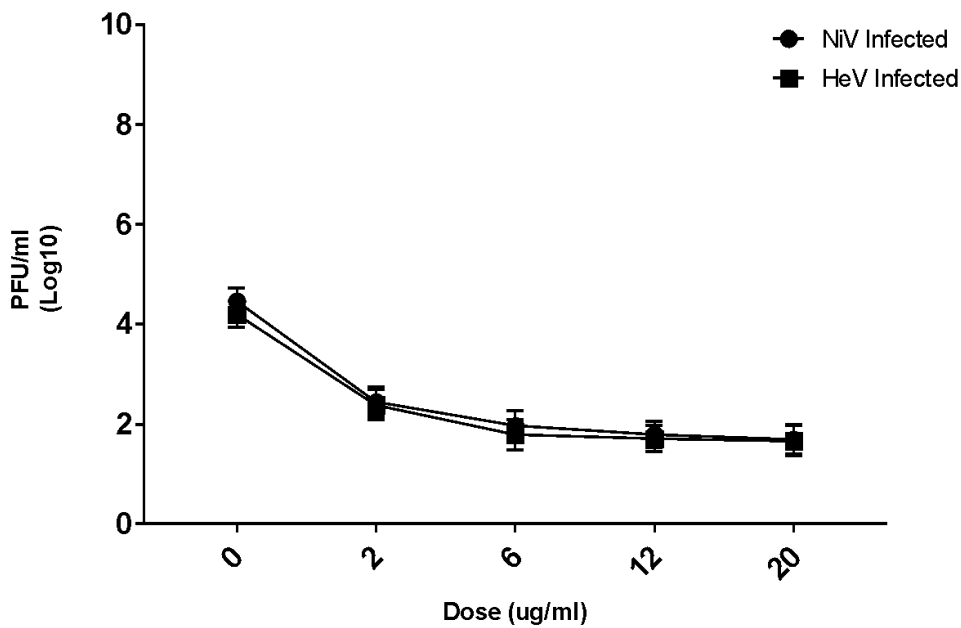


Figure 25: (A) RT-PCR and (B) Plaque Assay Data for the replication of NiV and HeV in IPAM 3D4/31 cells in various amounts of HeVsG at 24h time point. HeV and NiV yield in the supernatant of IPAM 3D4/31. The values are means \pm St.Dev of 2 replicates.

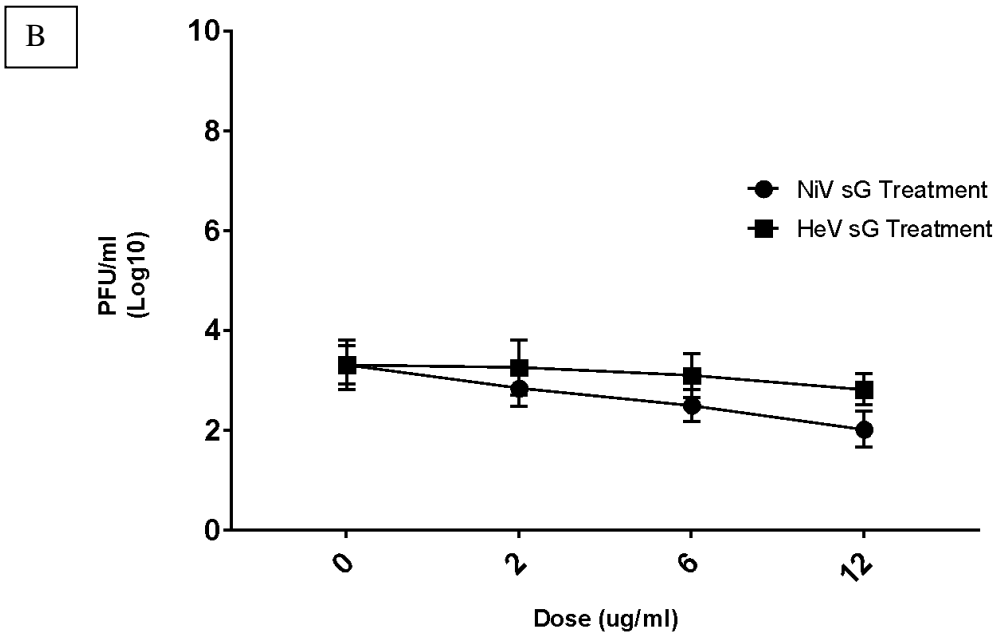
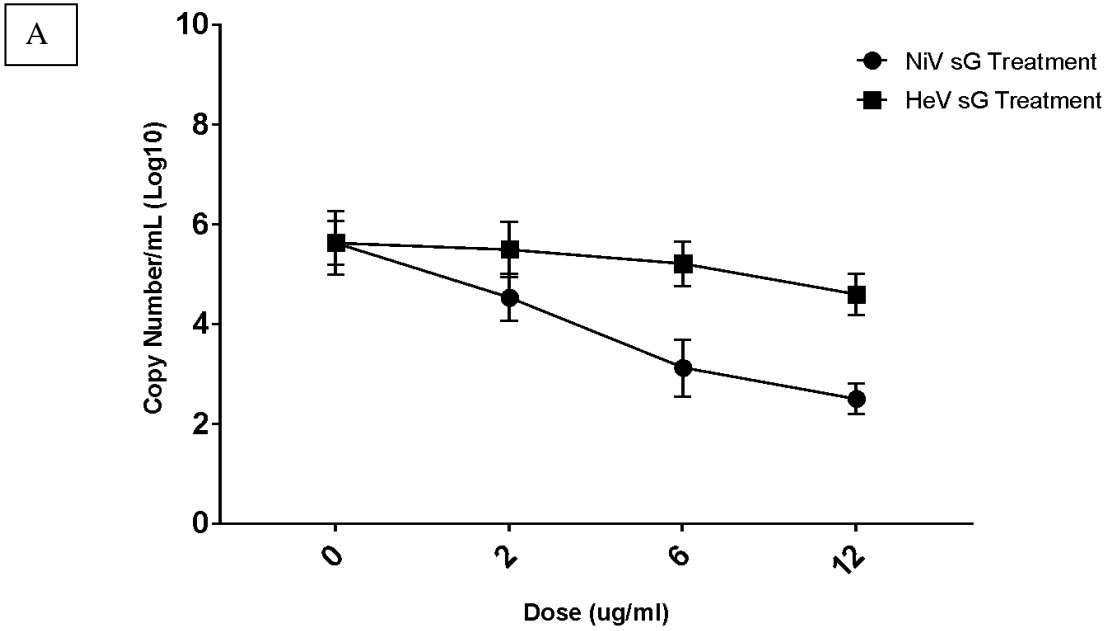


Figure 26: (A) RT-PCR and (B) Plaque Assay Data for the replication of NiV in porcine CD8+ cells in various amounts of NiV and HeV sG at 24 h time point. NiV detection in the supernatant of CD8+ cells. The cells were inoculated 48 hpi. The values are means \pm St.Dev of 2 replicate.

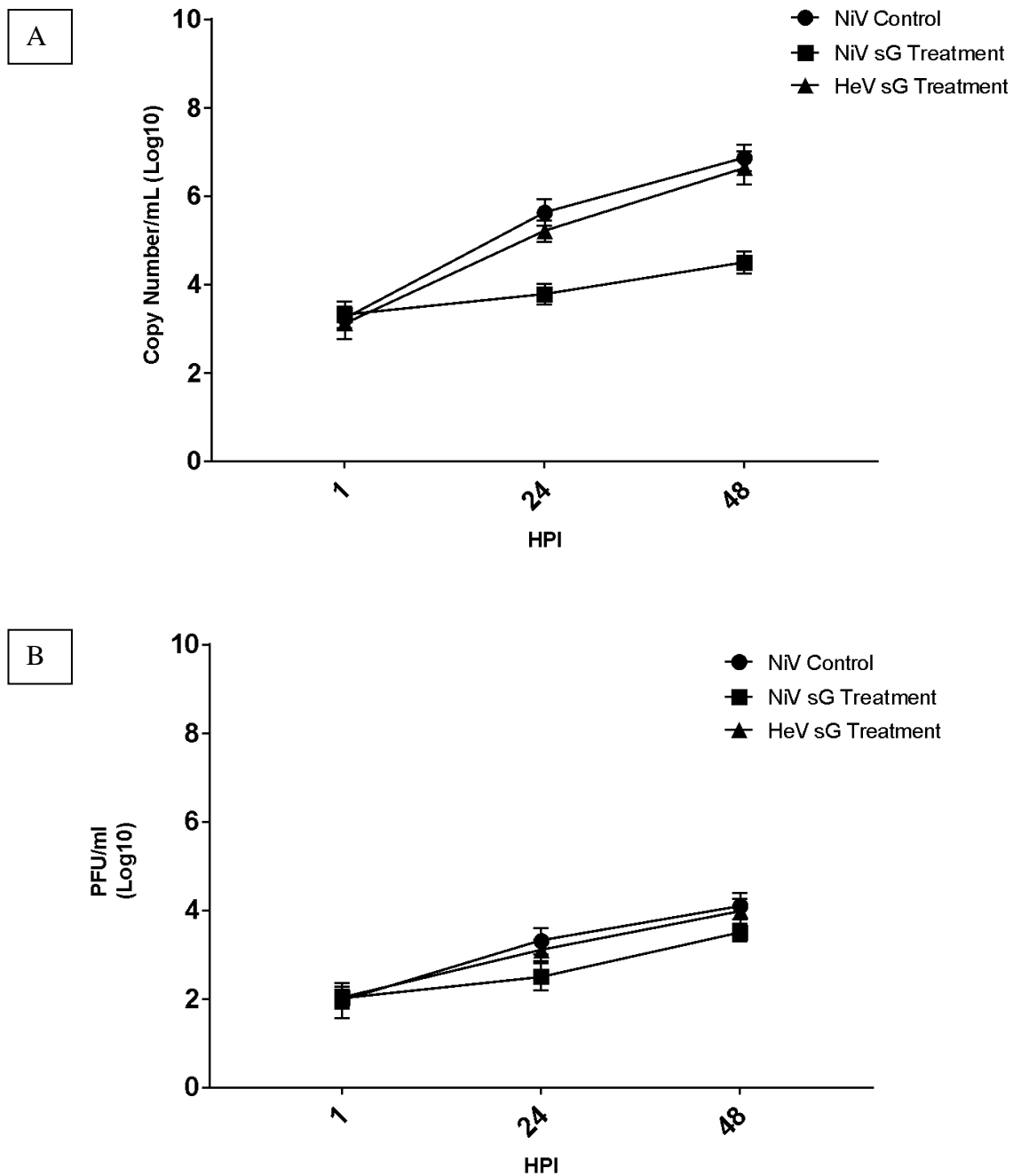


Figure 27: (A) RT-PCR and (B) Plaque Assay Data for the replication of NiV in porcine CD8+ cells in 6 μ l/ml of NiV and HeVsG. NiV yield in the supernatant of CD8+ cells. The cells were inoculated 48 hpi. The values are means \pm St.Dev of 2 replicate.

Percent Inhibition of HeV/NiV Soluble G 6 ug/ml Treatment on NiV infection of CD8+ cells Avg of 2 pigs at 24h Compared to the Control Innoculated 48h Post Selection

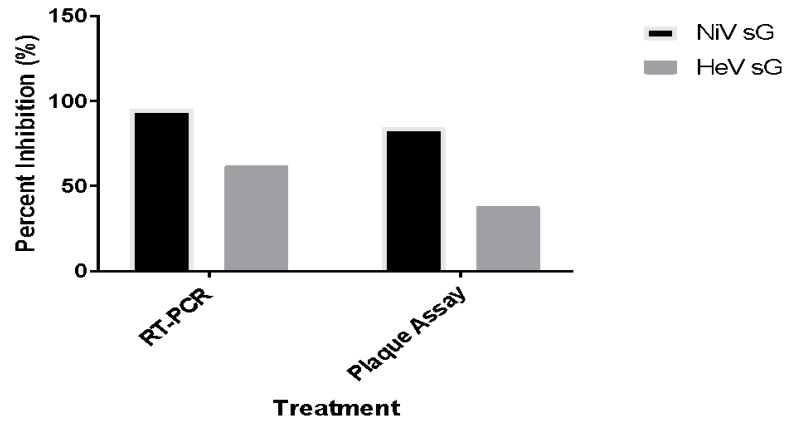


Figure 28: Percent inhibition of 6 μ l/ml NiV and HeVsG treatment in NiV infected porcine CD8+ cells compared to non-blocked control. Cells were inoculated 48 hrs post selection. Calculation used non logarithmic numbers.

3.7 *In silico* modelling of Porcine CD8 α -NiV Glycoprotein Interaction

The biological function of a protein depends upon the formation of protein-protein complexes. We attempted to model the protein-protein docking of porcine CD8 α and NiV G protein to further understand to binding of these proteins. Crystal Structures of porcine CD8 α (PDB ID: 5EDX) and NiV G (PDB ID: 3D11) were already available in RCSB Protein Database (PDB). Protein-protein docking was performed by ClusPro 2.0. ClusPro was used because it was rated first in the CAPRI (Critical Assessment of Predicted Interactions) rankings for protein docking platforms. A Balanced setting was used to generate the ClusPro models. Balanced setting optimizes van der Waals interactions, hydrophobic interactions, and electrostatic interactions. To rank the models, we used the method that was used by Xue et al, 2011. Generated ClusPro models were inputted into the program PS-HomPPI v1.3 (Partner-Specific Protein-Protein Interface Residue Predictor). PS-HomPPI predicts and optimizes the best theoretical protein binding sites. The results of the PS-HomPPI were then inputted into DockRank (Xue et al, 2014). DockRank ranks the models from PS-HomPPI. ClusPro also gives a ranking of the models. As a third way to rank the models generated by ClusPro, the models were inputted into DockScore which ranks on the basis of surface area, evolutionary conservation, hydrophobicity, short contacts and spatial clustering (Malhotra et al, 2015). Interestingly, the top 3 candidates that were generated by DockRank and DockScore coincide with the top 3 models generated by ClusPro (**Figure 27**). To visualize the models, PyMOL v2.0 Molecular Graphics System was used. **Figure 27 B** and **C** had similarities with the NiV glycoprotein-ephrin B2 interaction. During the NiV glycoprotein-ephrin B2 interaction, the residues Ile588 and Tyr581 of NiV G bind the residue Phe 120 of ephrin B2. In the NiV glycoprotein-CD8 α interaction, the residues Ile588 and Tyr581 of NiV G bind the residue

ALA43 of porcine CD8 $\alpha\alpha$ dimer. However, that would conclude that NiV G binds either ephrin B2 or CD8 α using the same binding site. If HeV, which had the same binding site for ephrin B2 as NiV, does not bind to CD8 $\alpha\alpha$ (based on competition studies), this model is not likely, and one should consider model A. Both NiV G heads are involved in binding of the CD8 α according to models A-C. Furthermore, models D-F suggest that ephrin B2 and CD8 $\alpha\alpha$ bind different regions of NiV G protein, which also negates that B and C as models. In addition, the PS-HomPPI ranking promotes A as the most probable interaction model from the evolutionally standpoint.

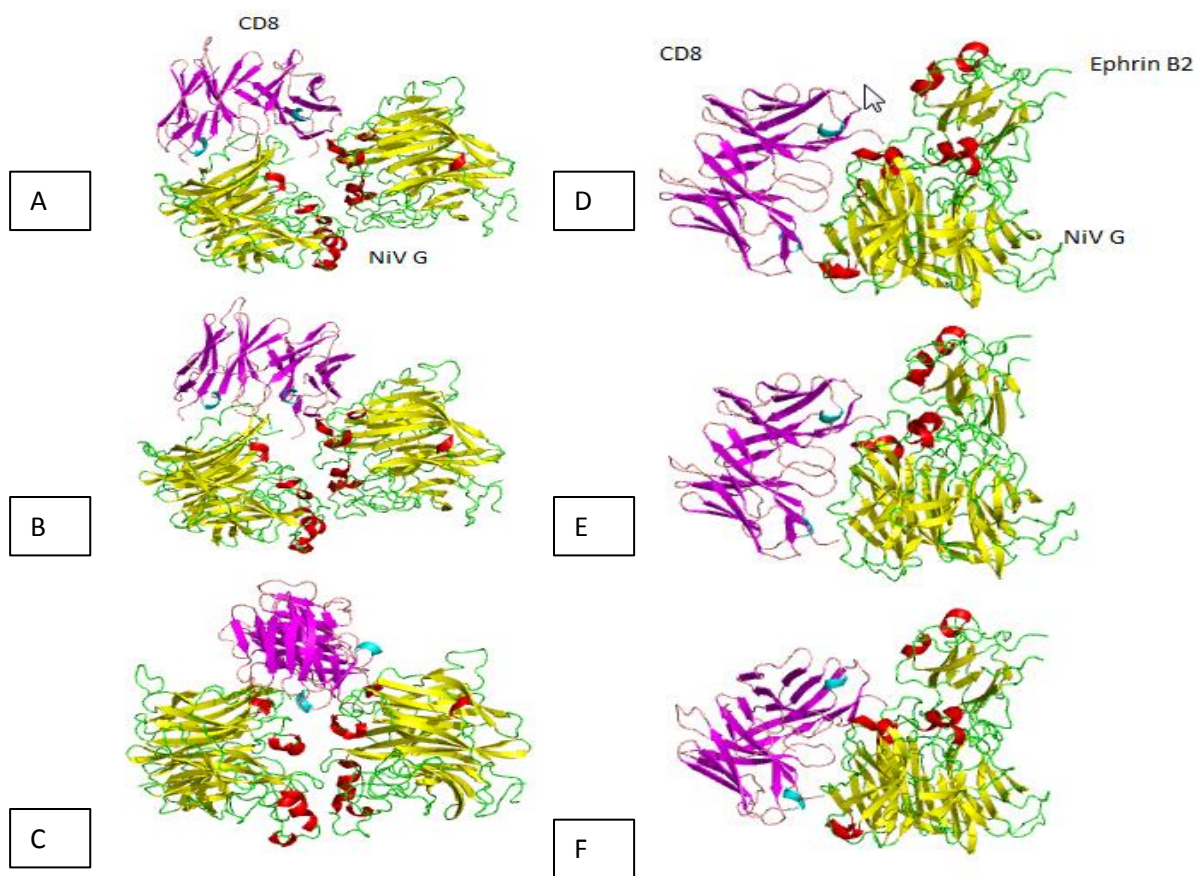


Figure 29: Top three models from ClusPro ranked by ClusPro, PS-HomPPI/DockRank, and DockScore. Models A-C are top ranking models for NiV G and CD8 $\alpha\alpha$ interaction. Models D-F are top ranking models for NiV G-Ephrin B2 complex and CD8 $\alpha\alpha$ interaction. Imaged on PyMOL v2.0

Discussion

We have confirmed the results by Stachowiak and Weingartl [2012] that NiV replicates in primary CD8⁺ T lymphocytes, NK cells, and, using an immortalized porcine alveolar macrophage cell line IPAM 3D4/31 as a surrogate for monocytes, in cells of monomyelocytic lineage. The experimental work presented here also showed that only CD8⁺ and not CD8⁻ NK cells are permissive to NiV. Furthermore, most importantly we have demonstrated that NiV can use CD8 $\alpha\alpha$ homodimer as a receptor.

This work is also the first to evaluate permissibility of primary porcine immune cells to HeV. Porcine leukocytes were not found to be permissive to HeV, and from all the tested cell populations, only the cell line IPAM 3D4/31 was permissive to HeV.

The CD8 $\alpha\alpha$ is not a shared receptor among the henipaviruses. NiV but not HeV had the ability to use CD8 $\alpha\alpha$ as a receptor. The ability of NiV to infect CD8 $\alpha\alpha$ ⁺ cells has implications in vaccine development. The CD4⁺CD8 $\alpha\alpha$ ⁺ cells are infected and play an important role in antibody development.

4.1 Permissibility of IPAM 3D4/31 to HeV and NiV

4.1.a Virus replication

Monocytes differentiate into macrophages and dendritic cells. They function in phagocytosis, antigen presentation, and cytokine production. The human monocyte cell line THP-1 was permissive to NiV, although only very low viral titres were observed, compared to MRC-5 and porcine stable kidney cells (PS) cells), and only after 48 hpi (Chang et al., 2006). Porcine monocytes were previously found to be permissive to NiV, and to produce higher titers

of NiV than porcine NK or T cells (Stachowiak & Weingartl., 2012). Similarly to what was seen for THP-1 cells, viral titers began to increase only after 48 hpi. The permissibility of porcine monocytes to HeV has never been investigated. In this study, IPAM 3D4/31 cells were used as a surrogate for monocytes and were found to be permissive to NiV and HeV with relatively high viral yields already at 24 hpi.

When comparing peak viral titres in IPAM3D4/31 cell infections, HeV ($10^{5.9}$ PFU/ml) produced similar titres to NiV ($10^{5.7}$ PFU/ml) (**Figures 9-10**). When comparing HeV and NiV infection in IPAM3D4/31 cells and Vero76 cells, titres produced by both viruses were lower in IPAM 3D4/31 cells than in Vero 76 cells. This observation is in full agreement with the observation by Stachowiak & Weingartl, (2012). The lower titres and delayed increase in virus titres in IPAM3D4/31 cells and porcine monocytes may be due to phagocytic nature of NiV monocytic cell types, where majority of attaching viral particles is phagocytized.

4.1.b Ephrin expression in IPAM 3D4/31

HeV and NiV glycoproteins (G) bind to ephrin B2 or ephrin B3. These ligands are receptors for both viruses (Negrete et al., 2005; Negrete et al., 2006; Bonaparte et al., 2005), although HeV uses ephrin B3 with much less efficiency (Negrete et al, 2007). Ephrin B2/B3 ligands function in conjunction with their respective receptors (Eph proteins) in cell-to-cell communication, regulation of cell attachment and repulsion, vasculogenesis, and axonal guidance (Pasquale 2008; Lisabeth et al., 2013).

Porcine monocytes and IPAM3D4/31 did express ephrin B2 on the cell surface observed by flow cytometry (**Figure 15**). Due to the lack of reagents, ephrin B3 expression was not

investigated; studies have found that ephrin B3 is expressed on the cell surface of murine monocytes (Yu et al., 2003); however nothing is known about expression on porcine monocytes.

4.1c Competition of the HeV or NiV Soluble G with NiV on IPAM 3D4/31

NiV and HeV replication was blocked almost 100% in IPAM3D4/31 cells at 6 µg/ml using HeV sG (**Figure 25**). These results are consistent with the soluble G studies performed by Bossart et al [2005] in which NiV and HeV infections of Vero cells were potently inhibited by HeVsG. IPAM3D4/31 (**Table 6**) did not express CD8 molecule. In light of the observation that both NiV sG and HeV sG bind to ephrin B2 (Bonaparte et al., 2005), the ability of the soluble G proteins to block NiV and HeV replication in IPAM 3D4/31 cells confirmed that NiV and HeV use ephrin B2 as a receptor for cell entry in the IPAM3D4/31 cells.

4.2 CD8αα dimer is a second receptor for NiV

4.2a NiV and HeV infection of porcine PBMC subpopulations *in vitro*

Stachowiak and Weingartl [2012] determined that NiV replicates in primary CD8+ T lymphocytes and NK cells, but not B cells, CD4-CD8-, and CD4+CD8- cells. HeV permissibility studies on swine peripheral blood lymphocytes have never been performed. Confirming the permissibility of porcine PBMCs to NiV was used as a control to determine the permissibility of porcine PBMCs to HeV.

Cell preparations highly enriched (78.9 % \pm 2.8 to 92.8 % \pm 1.5) for a specific subpopulation based on surface antigens/markers were obtained by magnetic separation using antibodies targeting the label (FITC or PE) attached to the primary antibody against the marker of interest (CD8 α , CD16, CD4 etc.).

Blocking of a viral receptor on the cell surface by the selection antibody/magnetic bead complex was thus not considered an issue at the time of inoculation with the virus, as discussed in the Results section.

We have shown that in swine peripheral blood, NiV replicated in cells carrying the CD8 marker, but there appeared to be a population of CD8⁺CD16⁻ cells refractory to NiV replication (**Figure 13**). The peripheral blood leukocytes can carry the CD8 marker either as CD8 α homodimer or CD8 $\alpha\beta$ heterodimer. **Table 1** (page 44) outlines CD8 expressing cells in peripheral blood. Since the NK cells expressing CD8 marker carry only the CD8 $\alpha\alpha$ homodimer, and they were all permissive to NiV (**Figure 9; 12; 13**), we speculated that the permissibility of CD8⁺ cells to NiV may require presence of the CD8 α homodimer on the cell surface.

4.2 B) Detection of ephrin B2 protein in sorted porcine PBMC and cell lines by immunoblot and flow cytometry

First step was to determine, whether expression of ephrin B2 on a protein level was responsible for the observed permissivity of the subpopulations of CD8⁺ cells. Although the protein was detected by immunoblotting in cell lysates of both NiV-permissive and non-permissive porcine PBMCs and cell lines (**Figure 14**), cell surface expression of the ephrin B2 using flow cytometry was not detected on CD8⁺ and CD8⁻porcine PBMCs (non-adherent cell fraction) (**Figure 15**), suggesting that peripheral blood lymphocytes of swine lack ephrin B2

surface expression. There are no reports of ephrin B3 expression on CD16+ NK cells or T cells of swine, and although it is expressed on the surface of murine CD8+ cells (Yu et al., 2003), it is not known if human or porcine CD8+ cells express ephrin B3 on their surfaces. In the absence of ephrin B2 (and B3) on the surface, the swine CD8 marker appeared to allow replication of NiV in specific subsets of CD8+ porcine lymphocytes.

4.2c Blocking of NiV replication by antibody against Ephrin B2 and CD8 α

Many studies have used antibody blocking to confirm that a virus uses a specific receptor. In our study, non-conjugated anti-porcine CD8 α antibody was able to block NiV replication in porcine CD8+ cells (**Figure 16**), while non-conjugated anti-ephrin B2 antibody was not (**Figure 17**).

The drop in NiV PFU or copies/ml with increasing anti-CD8 α antibody (**Figure 16**), but not increasing anti-ephrin B2 antibody (**Figure 17**) was comparable to blocking the virus replication in IPAM 3D4/31 cells using competition with anti-ephrin B2 antibody, with a complete block of virus production observed in both systems. The lack of ephrin B2 blocking (**Figure 17**) confirms the flow cytometry findings that porcine CD8+ cells do not express ephrin B2 on the cell surface. The slight decrease in viral titres observed with increasing anti-ephrin B2 antibody could be a result of non-specific blocking.

4.2d CD8 $\alpha\beta$ is not a receptor for Nipah Virus

While CD8⁺ cells in the porcine peripheral blood carry either the CD8 $\alpha\alpha$ homodimer, or the CD8 $\alpha\beta$ heterodimer, CD8⁺ cells in the thymus (thymocytes) express only the CD8 $\alpha\beta$ heterodimer, and were used to probe which dimer serves as a receptor for NiV. In NiV pathogenesis studies in animals, the porcine thymus was not found to be positive for infectious virus, presence of viral RNA by RT-PCR or viral antigen IHC (Middleton et al., 2002; Weingartl et al., 2005). In this study, thymocytes harvested from 4 week old pigs and inoculated *in vitro* with NiV were not found to be permissive to virus replication (**Figure 19**), and also did not show any intracellular NiV-N protein staining by flow cytometry (**Figure 18**). This confirmed the findings that no NiV staining was observed in the thymus of *in vivo* infected pigs (**Figure 20**) and ruled out the possibility that porcine CD8 $\alpha\beta$ dimer served as a receptor for NiV.

4.2e CD8 $\alpha\alpha$ dimer serves as a receptor for NiV

To confirm the results of the blocking studies suggesting that CD8 $\alpha\alpha$ is a receptor for NiV, permissive but non-susceptible Chinese Hamster Ovary (CHO) cells (which lack ephrin B2 and B3 expression) were transfected with the porcine CD8 α coding region and inoculated with NiV. Ephrin B2 was also transfected as a control. The CD8 α forms a dimer when expressed in transfected cells (Liu et al., 2016; Sun & Kavafhas., 1997), simulating the marker conformation on leukocytes.

We confirmed that CHO-K1 cells that express porcine CD8 α and/or porcine ephrin B2 are permissive to NiV (**Figure 22-24**). NiV can use the porcine CD8 $\alpha\alpha$ homodimer independently from porcine ephrin B2, agreeing with the hypothesis that CD8 $\alpha\alpha$ expression on

porcine CD8⁺ cells render these cells permissive to NiV even in the absence of ephrin B2 surface expression. No viral replication was observed in non-transfected CHO-K1 cells.

4.3 Competition of the HeV or NiV Soluble G with NiV on Porcine CD8⁺ cells

HeV sG was able to fully block replication of HeV and NiV in IPAM3D4/31 cells. In IPAM3D4/31 cells, ephrin B2 is the receptor; thus, HeV sG was able to block replication of both viruses. In porcine CD8⁺ cells, NiV sG was shown to block NiV replication substantially better than HeV sG when compared to non-blocked cells (**Figure 26-27**). We propose that NiV sG has a significantly greater affinity for the porcine CD8 α than HeV sG. HeV doesn't have adequate affinity for porcine CD8 α .

Replication of NiV in CD8⁺ cells was not blocked completely when treated with 6 μ g/ml of NiV sG (**Figure 26-27**). An incomplete block of NiV replication in CD8⁺ cells by NiV sG may be occurring because other factors are participating in the binding of NiV to CD8 α . It is to note that the sG used was truncated. The full protein G sequence may be required to achieve full block of NiV, as conformation may be critical. However, further research has to be done to verify this.

The only virus known to use CD8 as a receptor is HIV-1. Saha et al., (2001) discovered an isolate of HIV-1 from AIDS patients that maintained the ability to infect CD4⁺ cells and was able to infect CD4-CD8⁺ cells using the CD8 receptor independently of CD4, CXCR4 or CCR5. In this isolate, the HiV gp120 protein had evolved to use CD4 and CD8 as receptors for cell entry. Interestingly, use of alternative receptors is not an exception in the family Paramyxoviridae. Measles virus from the family Paramyxoviridae, has also two envelope

glycoproteins, the hemagglutinin (H) and fusion (F) proteins which are responsible for attachment and membrane fusion. Three cellular receptors for measles virus are known, CD46, CD150/SLAM, and Nectin 4 (Lin et al., 2016), and the hemagglutinin protein has likely evolved to use multiple receptors and infect more cell types.

4.4 *In silico* Modeling of Porcine CD8 α -NiV Glycoprotein Interaction

The binding affinity of the complexes in (**Figure 29**) is explained in terms of electrostatic forces, van der Waals forces, and polar and non-polar solvation energy contributions. Structural analysis of interacting porcine CD8 α and NiV G **Figure 29 B and C**, show that the same two residues (Ile588 and Tyr581) of NiV G that participate in hydrophobic interactions that bind the Phe120 of ephrin B2 can be also involved in binding the porcine CD8 α dimer (Ala43). Based on our analysis, we propose model A as a likely model for the CD8 α - NiV G interaction.

4.5) Conclusion

The work presented in this thesis provides new insight into alternate NiV receptors and permissibility of porcine PBMCs for infection by NiV and HeV. We have concluded that, HeV may infect only immune cells of myeloid lineage based on the observation that HeV only infected IPAM3D4/31 cells and not infect cells of the lymphoid lineage.

We have confirmed results published by Stachowiak & Weingartl, [2012], which documented that only CD8+ porcine PBMCs were permissive to NiV and not CD8- PBMCs, and further narrowed it to CD8+ cells carrying the CD8 α homodimer.

Interestingly, peripheral blood T cells of humans and rodents express mainly CD8 $\alpha\beta$ and not CD8 $\alpha\alpha$ on their surface (Norment & Littman., 1988; Shiue et al., 1988). Humans do have a subset of CD4+CD8 $\alpha\alpha$ + cells circulating that could be permissive, however, they are very rare and only found during heightened immune response, as observed in patients with myasthenia gravis, arthritis, and leprosy. Majority of the human T cells would therefore not be permissive to NiV replication. This is in a full agreement with the study by Mathieu et al. (2011), which concluded that human PBLs were not permissive to NiV infection but could act as a transport mechanism to other parts of the body as the virus could bind to but not internalize into the cell.

The percentage of peripheral blood T cells expressing the CD8 $\alpha\alpha$ homodimer can be in pigs very high when compared to other species, as it comprises the CD4+CD8+ cells (which represent up to 60% of the CD8+ cells, depending on age) and CD8+ NK cells and at least two minor subpopulations of NKT and iNKT. At 9 weeks of age, the percentage of porcine PBMCs that are CD8 α + is approximately 25%, however, these cells also include CD4-CD8+ $\alpha\beta$ cells (Stabel et al., 2000). The infection of a large percentage of the total PBMCs by NiV could have a profound effect on the following aspects of the immune response:

CD8- NK cells differ from the CD8+ subset in that they express higher levels of NKp46 (involved in protection against tumors and viral infections), CXCR3, IFN- γ , and TNF- α which leads to a highly activated immune state leading to higher cytokine expression (Mair et al., 2013). A lower cytotoxic activity was observed in the NKp46- cells than NKp46+ cells, however the precise role of the CD8+ NK cells is not known (Gerner et al., 2009). The effect of NiV infection of CD8 (+) NK cells on pathogenesis of NiV is unknown and future studies would be required to assess the importance of this subset in disease and immune response in NiV infected pigs.

A dramatic decrease in the CD4⁺ cells was observed in pigs requiring euthanasia due to advanced NiV infection, which was observed during the *in vitro* infection of PBMC (Stachowiak & Weingartl., 2012). The CD4⁺ T cells in swine consist of two sub populations:

CD4⁺CD8⁻ T helper cells, were found to be refractory to NiV infection in this work, confirming the previous results [Stachowiak & Weingartl., 2012], and the CD4⁺CD8⁺αα cells were found to be permissive to NiV during the course of this work.

CD4⁺CD8⁺αα cells are MHC class II-restricted antigen-specific memory T helper cells. They are involved in cell proliferation, the production of cytokines such as interferon alpha and IL-2, and the stimulation of antibody production in B cells. The prevalence of CD4⁺CD8⁺αα T cells increases upon virus infection and throughout the life time of the pigs and can reach up to 60% of T cells in the PBMCs (Saalmüller et al., 1999). Modulation of the CD4⁺CD8⁺αα cell functions and reduction of this population by NiV in the infected animals may significantly hinder the early immune response and delay the antibody development (Berhane et al., 2008). In addition to the production of IFN-γ, stimulated CD4⁺CD8⁺ T lymphocytes also produce TNF α and IL-8 (Gasser et al., 1995).

The CD4⁻CD8⁺αβ cells are MHC class I-restricted cytotoxic T cells. They secrete cytokines that kill target cells. Porcine CD8⁺ T lymphocytes are important in viral clearance as they produce IFN-γ to activate the JAK-STAT pathway to initiate antiviral state and destroy infected cells by Fas/FasL interactions and the release of cytotoxic granules (Bruin et al, 2000). Based on the results of this work this T cell population is not permissive to NiV, however Stachowiak and Weingartl [2012] observed that *in vitro*, CD4⁻CD8⁺ cell frequencies decreased in pigs that required early euthanasia due to advanced NiV infection.

Internalization of NiV by CD8 α may be occurring differently in T-lymphocytes and CHO-K1 cells. NiV has been shown to enter HeLa cells by clathrin-coated pits (Aguilar et al., 2010; Bossart et al., 2002) and, in ephrin B2-transfected CHO-K1 cells, through macropinocytosis (Pernet et al., 2009). In human T lymphocytes, internalization of CD8-TCR is through clathrin-coated pits (Liu et al., 2000), and NiV may be mimicking class I MHC molecules in the MHC I-CD8-TCR interaction. We speculate that the internalization of NiV can occur when the NiV-bound CD8 α interacts with the TCR and is subsequently internalized by coated pits. On the other hand, internalization of NiV and HeV in the monocytic cells, as shown by our studies on IPAM 3D4/31 cells, can be presumed to occur by micropinocytosis using ephrin B2 as a receptor (Pernet et al., 2009). It appears that HeV does not have the ability to bind to CD8 α and solely relies on ephrin B2 for the cell entry, since the virus was not able to replicate in primary porcine lymphocytes but was able to replicate in IPAM3D4/31 cells (**Figure 10**).

The IPAM3D4/31 cells produced more virus than CD8 $^{+}$ cells following NiV inoculation according to viral plaque and RT-PCR data (**Figures 9-11**). The higher viral titres could result from many factors. The IPAM3D4/31 population was pure which could explain the higher viral titres when compared to other permissive PBMC populations.

There could be several future directions of research resulting from the presented work: Obtaining a crystal structure of the NiV G-CD8 α interaction may allow the identification of targets for the development of antiviral agents against NiV for pigs. Additionally, analyses of these complexes will allow further insights into how CD8 α participates in binding, as there has been only one other study in which CD8 has been shown to be a receptor for a virus (Saha et al., 2001).

Since infection of lymphocytes is an important characteristic of swine disease, this work has implications in vaccine design. Development of a veterinary vaccine against NiV which elicits cell mediated immune response is needed, especially from a OneHealth perspective, as a means to further enhance protection of the human population against infections by this pathogen.

References

- AbuBakar, S., Chang, L. Y., Ali, A. M., Sharifah, S. H., Yusoff, K., & Zamrod, Z. (2004). Isolation and molecular identification of Nipah virus from pigs. *Emerging infectious diseases*, *10*(12), 2228.
- Addison, E. G., North, J., Bakhsh, I., Marden, C., Haq, S., Al- Sarraj, S., ... & Lowdell, M. W. (2005). Ligation of CD8 α on human natural killer cells prevents activation- induced apoptosis and enhances cytolytic activity. *Immunology*, *116*(3), 354-361.
- Afonso, C. L., Amarasinghe, G. K., Bányai, K., Bào, Y., Basler, C. F., Bavari, S., ... & Bukreyev, A. (2016). Taxonomy of the order Mononegavirales: update 2016. *Archives of virology*, *161*(8), 2351-2360.
- Aguilar, H. C., Ataman, Z. A., Aspericueta, V., Fang, A. Q., Stroud, M., Negrete, O. A., ... & Lee, B. (2009). A novel receptor-induced activation site in the Nipah virus attachment glycoprotein (G) involved in triggering the fusion glycoprotein (F). *Journal of biological chemistry*, *284*(3), 1628-1635..
- Aguilar, H. C., Aspericueta, V., Robinson, L. R., Aanensen, K. E., & Lee, B. (2010). A quantitative and kinetic fusion protein-triggering assay can discern distinct steps in the Nipah virus membrane fusion cascade. *Journal of virology*, *84*(16), 8033-8041.
- Aljofan, M., Saubern, S., Meyer, A. G., Marsh, G., Meers, J., & Mungall, B. A. (2009). Characteristics of Nipah virus and Hendra virus replication in different cell lines and their suitability for antiviral screening. *Virus research*, *142*(1-2), 92-99.
- Anonymous.(2011). HENDRA VIRUS, EQUINE - AUSTRALIA (21): (QUEENSLAND) CANINE. Pro-Med-mail, Archive No. 20110802.2324. International Society for Infectious Diseases: Brookline, MA, USA, 2 August 2011. Available online: <http://www.promedmail.org/> (accessed on 25 January 2018).
- Arunkumar, G., Chandni, R., Mourya, D. T., Singh, S. K., Sadanandan, R., Sudan, P., & Bhargava, B. (2018). Outbreak investigation of Nipah Virus Disease in Kerala, India, 2018. *The Journal of infectious diseases*.
- Autissier, P., Soulas, C., Burdo, T. H., & Williams, K. C. (2010). Evaluation of a 12- color flow cytometry panel to study lymphocyte, monocyte, and dendritic cell subsets in humans. *Cytometry Part A: The Journal of the International Society for Advancement of Cytometry*, *77*(5), 410-419.
- AxPyMOL The AxPyMOL Molecular Graphics Plugin for PowerPoint, Version 1.8
Schrödinger, LLC.

- Balázs, M., Martin, F., Zhou, T., & Kearney, J. F. (2002). Blood dendritic cells interact with splenic marginal zone B cells to initiate T-independent immune responses. *Immunity*, *17*(3), 341-352.
- Bender, R. R., Muth, A., Schneider, I. C., Friedel, T., Hartmann, J., Plückthun, A., ... & Buchholz, C. J. (2016). Receptor-targeted Nipah virus glycoproteins improve cell-type selective gene delivery and reveal a preference for membrane-proximal cell attachment. *PLoS pathogens*, *12*(6), e1005641.
- Berhane, Y., Berry, J. D., Ranadheera, C., Marszal, P., Nicolas, B., Yuan, X., ... & Weingartl, H. (2006). Production and characterization of monoclonal antibodies against binary ethylenimine inactivated Nipah virus. *Journal of virological methods*, *132*(1-2), 59-68.
- Binns, R. M., Duncan, I. A., Powis, S. J., Hutchings, A., & Butcher, G. W. (1992). Subsets of null and gamma delta T-cell receptor+ T lymphocytes in the blood of young pigs identified by specific monoclonal antibodies. *Immunology*, *77*(2), 219.
- Binns, R. M., & Pabst, R. (1994). Lymphoid tissue structure and lymphocyte trafficking in the pig. *Veterinary immunology and immunopathology*, *43*(1-3), 79-87.
- Bharaj, P., Wang, Y. E., Dawes, B. E., Yun, T. E., Park, A., Yen, B., ... & Rajsbaum, R. (2016). The matrix protein of Nipah virus targets the E3-ubiquitin ligase TRIM6 to inhibit the IKKε kinase-mediated type-I IFN antiviral response. *PLoS pathogens*, *12*(9), e1005880.
- Bhattacharyya, S., Warfield, K. L., Ruthel, G., Bavari, S., Aman, M. J., & Hope, T. J. (2010). Ebola virus uses clathrin-mediated endocytosis as an entry pathway. *Virology*, *401*(1), 18-28.
- Blue, M. L., Daley, J. F., Levine, H., Craig, K. A., & Schlossman, S. F. (1986). Biosynthesis and surface expression of T8 by peripheral blood T4+ cells in vitro. *The Journal of Immunology*, *137*(4), 1202-1207.
- Blocquel, D., Beltrandi, M., Eralles, J., Barbier, P., & Longhi, S. (2013). Biochemical and structural studies of the oligomerization domain of the Nipah virus phosphoprotein: evidence for an elongated coiled-coil homotrimer. *Virology*, *446*(1-2), 162-172.
- Behera, A. K., Matsuse, H., Kumar, M., Kong, X., Lockey, R. F., & Mohapatra, S. S. (2001). Blocking intercellular adhesion molecule-1 on human epithelial cells decreases respiratory syncytial virus infection. *Biochemical and biophysical research communications*, *280*(1), 188-195.
- Bochenek, M. L., Dickinson, S., Astin, J. W., Adams, R. H., & Nobes, C. D. (2010). Ephrin-B2 regulates endothelial cell morphology and motility independently of Eph-receptor binding. *Journal of cell science*, jcs-061903.
- Bowden, T. A., Aricescu, A. R., Gilbert, R. J., Grimes, J. M., Jones, E. Y., & Stuart, D. I. (2008). Structural basis of Nipah and Hendra virus attachment to their cell-surface receptor ephrin-B2. *Nature Structural and Molecular Biology*, *15*(6), 567.

- Bonaparte, M. I., Dimitrov, A. S., Bossart, K. N., Crameri, G., Mungall, B. A., Bishop, K. A., ... & Broder, C. C. (2005). Ephrin-B2 ligand is a functional receptor for Hendra virus and Nipah virus. *Proceedings of the National Academy of Sciences*, *102*(30), 10652-10657.
- Bossart, K. N., Wang, L. F., Flora, M. N., Chua, K. B., Lam, S. K., Eaton, B. T., & Broder, C. C. (2002). Membrane fusion tropism and heterotypic functional activities of the Nipah virus and Hendra virus envelope glycoproteins. *Journal of Virology*, *76*(22), 11186-11198.
- Bossart, K. N., Crameri, G., Dimitrov, A. S., Mungall, B. A., Feng, Y. R., Patch, J. R., ... & Broder, C. C. (2005). Receptor binding, fusion inhibition, and induction of cross-reactive neutralizing antibodies by a soluble G glycoprotein of Hendra virus. *Journal of virology*, *79*(11), 6690-6702.
- Bossart, K. N., Zhu, Z., Middleton, D., Klippel, J., Crameri, G., Bingham, J., ... & Hickey, A. C. (2009). A neutralizing human monoclonal antibody protects against lethal disease in a new ferret model of acute nipah virus infection. *PLoS pathogens*, *5*(10), e1000642.
- Bossart, K. N., Geisbert, T. W., Feldmann, H., Zhu, Z., Feldmann, F., Geisbert, J. B., ... & Wang, Y. (2011). A neutralizing human monoclonal antibody protects african green monkeys from hendra virus challenge. *Science translational medicine*, *3*(105), 105ra103-105ra103.
- Bossart, K. N., Rockx, B., Feldmann, F., Brining, D., Scott, D., LaCasse, R., ... & Broder, C. C. (2012). A Hendra virus G glycoprotein subunit vaccine protects African green monkeys from Nipah virus challenge. *Science translational medicine*, *4*(146), 146ra107-146ra107.
- Borisevich, V., Ozdener, M. H., Malik, B., & Rockx, B. (2017). Hendra and Nipah virus infection in cultured human olfactory epithelial cells. *mSphere*, *2*(3), e00252-17.
- Broder, C. C., Xu, K., Nikolov, D. B., Zhu, Z., Dimitrov, D. S., Middleton, D., ... & Wang, L. F. (2013). A treatment for and vaccine against the deadly Hendra and Nipah viruses. *Antiviral research*, *100*(1), 8-13.
- BRUIN, T. G. D., ROOIJ, E. M. V., VISSER, Y. E. D., & BIANCHI, A. T. (2000). Cytolytic function for pseudorabies virus-stimulated porcine CD4+ CD8dull+ lymphocytes. *Viral immunology*, *13*(4), 511-520.
- Brockmeier, S. L., Register, K. B., Nicholson, T. L., & Loving, C. L. (2012). Nipah virus. *Diseases of swine. 10th ed. Wiley-Blackwell*, 580-585.
- Cargnello, M., & Roux, P. P. (2011). Activation and function of the MAPKs and their substrates, the MAPK-activated protein kinases. *Microbiology and molecular biology reviews*, *75*(1), 50-83.
- Centers for Disease Control and Prevention (CDC). (1999). Outbreak of Hendra-like virus--Malaysia and Singapore, 1998-1999. *MMWR. Morbidity and mortality weekly report*, *48*(13), 265.

- Comeau, S. R., Gatchell, D. W., Vajda, S., & Camacho, C. J. (2004). ClusPro: an automated docking and discrimination method for the prediction of protein complexes. *Bioinformatics*, 20(1), 45-50.
- Comeau, S. R., Gatchell, D. W., Vajda, S., & Camacho, C. J. (2004). ClusPro: a fully automated algorithm for protein-protein docking. *Nucleic acids research*, 32(suppl_2), W96-W99.
- Chakraborty, A., Sazzad, H. M. S., Hossain, M. J., Islam, M. S., Parveen, S., Husain, M., ... & Daszak, P. (2016). Evolving epidemiology of Nipah virus infection in Bangladesh: evidence from outbreaks during 2010–2011. *Epidemiology & Infection*, 144(2), 371-380.
- Chaplin, D. D. (2010). Overview of the immune response. *Journal of Allergy and Clinical Immunology*, 125(2), S3-S23.
- Charerntantanakul, W., & Roth, J. A. (2006). Biology of porcine T lymphocytes. *Animal health research reviews*, 7(1-2), 81-96.
- Chan, Y. P., Koh, C. L., Lam, S. K., & Wang, L. F. (2004). Mapping of domains responsible for nucleocapsid protein-phosphoprotein interaction of Henipaviruses. *Journal of general virology*, 85(6), 1675-1684.
- Chew, M. H., Arguin, P. M., Shay, D. K., Goh, K. T., Rollin, P. E., Shieh, W. J., ... & Chew, S. K. (2000). Risk factors for Nipah virus infection among abattoir workers in Singapore. *The Journal of infectious diseases*, 181(5), 1760-1763.
- Ching, P. K. G., de Los Reyes, V. C., Sucaldito, M. N., Tayag, E., Columna-Vingno, A. B., Malbas Jr, F. F., ... & Dueger, E. (2015). Outbreak of henipavirus infection, Philippines, 2014. *Emerging infectious diseases*, 21(2), 328.
- Childs, K., Stock, N., Ross, C., Andrejeva, J., Hilton, L., Skinner, M., ... & Goodbourn, S. (2007). mda-5, but not RIG-I, is a common target for paramyxovirus V proteins. *Virology*, 359(1), 190-200.
- Chong, H. T., Kamarulzaman, A., Tan, C. T., Goh, K. J., Thayaparan, T., Kunjapan, S. R., ... & Lam, S. K. (2001). Treatment of acute Nipah encephalitis with ribavirin. *Annals of Neurology: Official Journal of the American Neurological Association and the Child Neurology Society*, 49(6), 810-813.
- Chong, H. T., & Tan, C. T. (2003). Relapsed and late-onset Nipah encephalitis, a report of three cases. *Neurol J Southeast Asia*, 8(2), 109-112.
- Chua, K. B., Bellini, W. J., Rota, P. A., Harcourt, B. H., Tamin, A., Lam, S. K., ... & Goldsmith, C. S. (2000). Nipah virus: a recently emergent deadly paramyxovirus. *Science*, 288(5470), 1432-1435.

- Chua, K. B., Koh, C. L., Hooi, P. S., Wee, K. F., Khong, J. H., Chua, B. H., ... & Lam, S. K. (2002). Isolation of Nipah virus from Malaysian Island flying-foxes. *Microbes and infection*, 4(2), 145-151.
- Chua, K. B. (2003). Nipah virus outbreak in Malaysia. *Journal of Clinical Virology*, 26(3), 265-275.
- Clayton, B. A., Middleton, D., Bergfeld, J., Haining, J., Arkininstall, R., Wang, L., & Marsh, G. A. (2012). Transmission routes for Nipah virus from Malaysia and Bangladesh. *Emerging infectious diseases*, 18(12), 1983.
- Clayton, B. A. (2017). Nipah virus: transmission of a zoonotic paramyxovirus. *Current opinion in virology*, 22, 97-104.
- Corkum, C. P., Ings, D. P., Burgess, C., Karwowska, S., Kroll, W., & Michalak, T. I. (2015). Immune cell subsets and their gene expression profiles from human PBMC isolated by Vacutainer Cell Preparation Tube (CPT™) and standard density gradient. *BMC immunology*, 16(1), 48.
- Cowled, C., Foo, C. H., Deffrasnes, C., Rootes, C. L., Williams, D. T., Middleton, D., ... & Stewart, C. R. (2017). Circulating microRNA profiles of Hendra virus infection in horses. *Scientific reports*, 7(1), 7431.
- Daszak, P., Plowright, R., Epstein, J. H., Pulliam, J., Abdul Rahman, S., Field, H. E., ... & Halpin, K. (2006). The emergence of Nipah and Hendra virus: pathogen dynamics across a wildlife-livestock-human continuum. *Disease Ecology: Community structure and pathogen dynamics*, 186-201.
- Diederich, S., Moll, M., Klenk, H. D., & Maisner, A. (2005). The nipah virus fusion protein is cleaved within the endosomal compartment. *Journal of Biological Chemistry*, 280(33), 29899-29903.
- Diederich, S., Sauerhering, L., Weis, M., Altmepfen, H., Schaschke, N., Reinheckel, T., ... & Maisner, A. (2012). Activation of the Nipah virus fusion protein in MDCK cells is mediated by cathepsin B within the endosomal-recycling compartment. *Journal of virology*, JVI-06628.
- Dietzel, E., Kolesnikova, L., Sawatsky, B., Heiner, A., Weis, M., Kobinger, G. P., ... & Maisner, A. (2015). Nipah virus matrix protein influences fusogenicity and is essential for particle infectivity and stability. *Journal of virology*, JVI-02920.
- Drescher, U. (2002). Eph family functions from an evolutionary perspective. *Current opinion in genetics & development*, 12(4), 397-402.
- Dochow, M., Krumm, S. A., Crowe, J. E., Moore, M. L., & Plemper, R. K. (2012). Independent structural domains in the paramyxovirus polymerase protein. *Journal of Biological Chemistry*, jbc-M111.

- Dups, J., Middleton, D., Yamada, M., Monaghan, P., Long, F., Robinson, R., ... & Wang, L. F. (2012). A new model for Hendra virus encephalitis in the mouse. *PloS one*, 7(7), e40308.
- Drexler, J. F., Corman, V. M., Gloza-Rausch, F., Seebens, A., Annan, A., Ipsen, A., ... & Oppong, S. (2009). Henipavirus RNA in African bats. *PloS one*, 4(7), e6367.
- Eaton, B. T., Broder, C. C., Middleton, D., & Wang, L. F. (2006). Hendra and Nipah viruses: different and dangerous. *Nature Reviews Microbiology*, 4(1), 23.
- Escaffre, O., Borisevich, V., & Rockx, B. (2013). Pathogenesis of Hendra and Nipah virus infection in humans. *The Journal of Infection in Developing Countries*, 7(04), 308-311.
- Eshaghi, M., Tan, W. S., Ong, S. T., & Yusoff, K. (2005). Purification and characterization of Nipah virus nucleocapsid protein produced in insect cells. *Journal of clinical microbiology*, 43(7), 3172-3177.
- Freiberg, A. N., Worthy, M. N., Lee, B., & Holbrook, M. R. (2010). Combined chloroquine and ribavirin treatment does not prevent death in a hamster model of Nipah and Hendra virus infection. *Journal of General Virology*, 91(3), 765-772.
- Frisén, J., Holmberg, J., & Barbacid, M. (1999). Ephrins and their Eph receptors: multitasking directors of embryonic development. *The EMBO journal*, 18(19), 5159-5165.
- Flanagan, J. G., & Vanderhaeghen, P. (1998). The ephrins and Eph receptors in neural development. *Annual review of neuroscience*, 21(1), 309-345.
- Geisbert, T. W., Daddario-DiCaprio, K. M., Hickey, A. C., Smith, M. A., Chan, Y. P., Wang, L. F., ... & Broder, C. C. (2010). Development of an acute and highly pathogenic nonhuman primate model of Nipah virus infection. *PloS one*, 5(5), e10690.
- Geisbert, T. W., Mire, C. E., Geisbert, J. B., Chan, Y. P., Agans, K. N., Feldmann, F., ... & Bossart, K. N. (2014). Therapeutic treatment of Nipah virus infection in nonhuman primates with a neutralizing human monoclonal antibody. *Science translational medicine*, 6(242), 242ra82-242ra82.
- Georges-Courbot, M. C., Contamin, H., Faure, C., Loth, P., Baize, S., Leyssen, P., ... & Deubel, V. (2006). Poly (I)-poly (C12U) but not ribavirin prevents death in a hamster model of Nipah virus infection. *Antimicrobial agents and chemotherapy*, 50(5), 1768-1772.
- Gerner, W., Käser, T., & Saalmüller, A. (2009). Porcine T lymphocytes and NK cells—an update. *Developmental & Comparative Immunology*, 33(3), 310-320.
- Gesser, B., Deleuran, B., Lund, M., Vestergard, C., Lohse, N., Deleuran, M., ... & Larsen, C. G. (1995). Interleukin-8 induces its own production in CD4+ T lymphocytes: a process regulated by interleukin 10. *Biochemical and biophysical research communications*, 210(3), 660-669.

- Goh, K. J., Tan, C. T., Chew, N. K., Tan, P. S. K., Kamarulzaman, A., Sarji, S. A., ... & Lam, S. K. (2000). Clinical features of Nipah virus encephalitis among pig farmers in Malaysia. *New England Journal of Medicine*, 342(17), 1229-1235.
- Gurley, E. S., Montgomery, J. M., Hossain, M. J., Bell, M., Azad, A. K., Islam, M. R., ... & Lowe, L. (2007). Person-to-person transmission of Nipah virus in a Bangladeshi community. *Emerging infectious diseases*, 13(7), 1031.
- Gupta, M., Lo, M. K., & Spiropoulou, C. F. (2013). Activation and cell death in human dendritic cells infected with Nipah virus. *Virology*, 441(1), 49-56.
- Halpin, K., Bankamp, B., Harcourt, B. H., Bellini, W. J., & Rota, P. A. (2004). Nipah virus conforms to the rule of six in a minigenome replication assay. *Journal of general virology*, 85(3), 701-707.
- Halpin, K., Young, P. L., Field, H. E., & Mackenzie, J. S. (2000). Isolation of Hendra virus from pteropid bats: a natural reservoir of Hendra virus. *Journal of General Virology*, 81(8), 1927-1932.
- Harcourt, B. H., Tamin, A., Halpin, K., Ksiazek, T. G., Rollin, P. E., Bellini, W. J., & Rota, P. A. (2001). Molecular characterization of the polymerase gene and genomic termini of Nipah virus. *Virology*, 287(1), 192-201.
- Habchi, J., Mamelli, L., Darbon, H., & Longhi, S. (2010). Structural disorder within Henipavirus nucleoprotein and phosphoprotein: from predictions to experimental assessment. *PLoS One*, 5(7), e11684.
- Habchi, J., Blangy, S., Mamelli, L., Jensen, M. R., Blackledge, M., Darbon, H., ... & Longhi, S. (2011). Characterization of the interactions between the nucleoprotein and the phosphoprotein of Henipaviruses. *Journal of Biological Chemistry*, jbc-M111.
- Hafner, C., Meyer, S., Hagen, I., Becker, B., Roesch, A., Landthaler, M., & Vogt, T. (2005). Ephrin-B reverse signaling induces expression of wound healing associated genes in IEC-6 intestinal epithelial cells. *World journal of gastroenterology: WJG*, 11(29), 4511.
- Hagmaier, K., Stock, N., Goodbourn, S., Wang, L. F., & Randall, R. (2006). A single amino acid substitution in the V protein of Nipah virus alters its ability to block interferon signalling in cells from different species. *Journal of general virology*, 87(12), 3649-3653.
- Hayman, D. T., Wang, L. F., Barr, J., Baker, K. S., Suu-Ire, R., Broder, C. C., ... & Wood, J. L. (2011). Antibodies to henipavirus or henipa-like viruses in domestic pigs in Ghana, West Africa. *PloS one*, 6(9), e25256.
- Hegde, S. T., Sazzad, H. M., Hossain, M. J., Alam, M. U., Kenah, E., Daszak, P., ... & Gurley, E. S. (2016). Investigating rare risk factors for Nipah virus in Bangladesh: 2001–2012. *EcoHealth*, 13(4), 720-728.

Hossain, M. J., Gurley, E. S., Montgomery, J. M., Bell, M., Carroll, D. S., Hsu, V. P., ... & Azad, A. K. (2008). Clinical presentation of Nipah virus infection in Bangladesh. *Clinical Infectious Diseases*, 46(7), 977-984.

Hughson, F. M. (1997). Enveloped viruses: a common mode of membrane fusion?. *Current Biology*, 7(9), R565-R569.

Hsu, V. P., Hossain, M. J., Parashar, U. D., Ali, M. M., Ksiazek, T. G., Kuzmin, I., ... & Breiman, R. F. (2004). Nipah virus encephalitis reemergence, Bangladesh. *Emerging infectious diseases*, 10(12), 2082.

Hyatt, A. D., & Selleck, P. W. (1996). Ultrastructure of equine morbillivirus. *Virus research*, 43(1), 1-15.

Ito, M., Iwasaki, M., Takeda, M., Nakamura, T., Yanagi, Y., & Ohno, S. (2013). Measles virus non-structural C protein modulates viral RNA polymerase activity by interacting with a host protein SHCBP1. *Journal of virology*, JVI-00714.

Jonjić, S., & Koszinowski, U. H. (1984). Monoclonal antibodies reactive with swine lymphocytes. I. Antibodies to membrane structures that define the cytolytic T lymphocyte subset in the swine. *The Journal of Immunology*, 133(2), 647-652.

JyMOL The JyMOL Molecular Graphics System, Version 1.8 Schrödinger, LLC.

Johnson, S. M., McNally, B. A., Ioannidis, I., Flano, E., Teng, M. N., Oomens, A. G., ... & Peeples, M. E. (2015). Respiratory syncytial virus uses CX3CR1 as a receptor on primary human airway epithelial cultures. *PLoS pathogens*, 11(12), e1005318.

Johansson, B., Ingvarsson, S., Björck, P., & Borrebaeck, C. A. (2000). Human interdigitating dendritic cells induce isotype switching and IL-13-dependent IgM production in CD40-activated naive B cells. *The Journal of Immunology*, 164(4), 1847-1854.

Kulkarni, S., Volchkova, V., Basler, C. F., Palese, P., Volchkov, V. E., & Shaw, M. L. (2009). Nipah virus edits its P gene at high frequency to express the V and W proteins. *Journal of virology*, 83(8), 3982-3987.

Koolpe, M., Burgess, R., Dail, M., & Pasquale, E. B. (2005). EphB receptor-binding peptides identified by phage display enable design of an antagonist with ephrin-like affinity. *Journal of Biological Chemistry*, 280(17), 17301-17311.

Kozakov, D., Hall, D. R., Xia, B., Porter, K. A., Padhorny, D., Yueh, C., ... & Vajda, S. (2017). The ClusPro web server for protein-protein docking. *Nature protocols*, 12(2), 255.

Kozakov, D., Beglov, D., Bohnuud, T., Mottarella, S. E., Xia, B., Hall, D. R., & Vajda, S. (2013). How good is automated protein docking?. *Proteins: Structure, Function, and Bioinformatics*, 81(12), 2159-2166.

Kozakov, D., Brenke, R., Comeau, S. R., & Vajda, S. (2006). PIPER: an FFT- based protein docking program with pairwise potentials. *Proteins: Structure, Function, and Bioinformatics*, 65(2), 392-406.

Lamb RA, Parks GD. Paramyxoviridae: the viruses and their replication. (2007) In: Knipe DM, Howley PM (eds) Fields virology, 5th edn. vols 1 and 2. Lippincott Williams & Wilkins, Philadelphia, 1449–1496.

LeBien, T. W., & Tedder, T. F. (2008). B lymphocytes: how they develop and function. *Blood*, 112(5), 1570-1580.

Lefevre, E. A., Carr, B. V., Inman, C. F., Prentice, H., Brown, I. H., Brookes, S. M., ... & Barclay, W. S. (2012). Immune responses in pigs vaccinated with adjuvanted and non-adjuvanted A (H1N1) pdm/09 influenza vaccines used in human immunization programmes. *PLoS One*, 7(3), e32400.

Lee, B., & Ataman, Z. A. (2011). Modes of paramyxovirus fusion: a Henipavirus perspective. *Trends in microbiology*, 19(8), 389-399.

Lee, B., Pernet, O., Ahmed, A. A., Zeltina, A., Beaty, S. M., & Bowden, T. A. (2015). Molecular recognition of human ephrinB2 cell surface receptor by an emergent African henipavirus. *Proceedings of the National Academy of Sciences*, 201501690.

Lee, J., Choi, K., Olin, M. R., Cho, S. N., & Molitor, T. W. (2004). $\gamma\delta$ T cells in immunity induced by Mycobacterium bovis Bacillus Calmette-Guérin vaccination. *Infection and immunity*, 72(3), 1504-1511.

Li, M., Embury-Hyatt, C., & Weingartl, H. M. (2010). Experimental inoculation study indicates swine as a potential host for Hendra virus. *Veterinary research*, 41(3), 33.

Liu, H., Rhodes, M., Wiest, D. L., & Vignali, D. A. (2000). On the dynamics of TCR: CD3 complex cell surface expression and downmodulation. *Immunity*, 13(5), 665-675.

Liu, Q., Stone, J. A., Bradel-Tretheway, B., Dabundo, J., Montano, J. A. B., Santos-Montanez, J., ... & Aguilar, H. C. (2013). Unraveling a three-step spatiotemporal mechanism of triggering of receptor-induced Nipah virus fusion and cell entry. *PLoS pathogens*, 9(11), e1003770.

Liu, Y., Li, X., Qi, J., Zhang, N., & Xia, C. (2016). The structural basis of chicken, swine and bovine CD8 α dimers provides insight into the co-evolution with MHC I in endotherm species. *Scientific Reports*, 6, 24788.

Lisabeth, E. M., Falivelli, G., & Pasquale, E. B. (2013). Eph receptor signaling and ephrins. *Cold Spring Harbor perspectives in biology*, 5(9), a009159.

- Lo, M. K., Harcourt, B. H., Mungall, B. A., Tamin, A., Peeples, M. E., Bellini, W. J., & Rota, P. A. (2009). Determination of the henipavirus phosphoprotein gene mRNA editing frequencies and detection of the C, V and W proteins of Nipah virus in virus-infected cells. *Journal of General Virology*, *90*(2), 398-404.
- Lo, M. K., Miller, D., Aljofan, M., Mungall, B. A., Rollin, P. E., Bellini, W. J., & Rota, P. A. (2010). Characterization of the antiviral and inflammatory responses against Nipah virus in endothelial cells and neurons. *Virology*, *404*(1), 78-88.
- Luby, S. P., Rahman, M., Hossain, M. J., Blum, L. S., Husain, M. M., Gurley, E., ... & Kenah, E. (2006). Foodborne transmission of Nipah virus, Bangladesh. *Emerging infectious diseases*, *12*(12), 1888.
- Luby, S. P., & Gurley, E. S. (2012). Epidemiology of henipavirus disease in humans. In *Henipavirus* (pp. 25-40). Springer, Berlin, Heidelberg.
- Lunney, J. K., & Pescovitz, M. D. (1987). Phenotypic and functional characterization of pig lymphocyte populations. *Veterinary immunology and immunopathology*, *17*(1-4), 135-144.
- Mair, K. H., Müllebnner, A., Essler, S. E., Duvigneau, J. C., Storset, A. K., Saalmüller, A., & Gerner, W. (2013). Porcine CD8 α dim⁻/NKp46 high NK cells are in a highly activated state. *Veterinary research*, *44*(1), 13.
- Malhotra, S., Mathew, O. K., & Sowdhamini, R. (2015). DOCKSCORE: a webserver for ranking protein-protein docked poses. *BMC bioinformatics*, *16*(1), 127.
- Mathieu, C., Pohl, C., Szecsi, J., Trajkovic-Bodennec, S., Devergnas, S., Raoul, H., ... & Horvat, B. (2011). Nipah virus uses leukocytes for efficient dissemination within a host. *Journal of virology*, JVI-00549.
- Machy, P., Truneh, A., Gennaro, D., & Hoffstein, S. (1987). Endocytosis and de novo expression of major histocompatibility complex encoded class I molecules: kinetic and ultrastructural studies. *European journal of cell biology*, *45*(1), 126-136.
- McEachern, J. A., Bingham, J., Cramer, G., Green, D. J., Hancock, T. J., Middleton, D., ... & Bossart, K. N. (2008). A recombinant subunit vaccine formulation protects against lethal Nipah virus challenge in cats. *Vaccine*, *26*(31), 3842-3852.
- Marsh, G. A., De Jong, C., Barr, J. A., Tachedjian, M., Smith, C., Middleton, D., ... & Payne, J. (2012). Cedar virus: a novel Henipavirus isolated from Australian bats. *PLoS pathogens*, *8*(8), e1002836.
- Michalski, W. P., Cramer, G., Wang, L. F., Shiell, B. J., & Eaton, B. (2000). The cleavage activation and sites of glycosylation in the fusion protein of Hendra virus. *Virus research*, *69*(2), 83-93.
- Mellott, D. O., & Burke, R. D. (2008). The molecular phylogeny of eph receptors and ephrin ligands. *BMC cell biology*, *9*(1), 27.

- Middleton, D., Pallister, J., Klein, R., Feng, Y. R., Haining, J., Arkinstall, R., ... & Elhay, M. (2014). Hendra virus vaccine, a one health approach to protecting horse, human, and environmental health. *Emerging infectious diseases*, 20(3), 372.
- Mire, C. E., Geisbert, J. B., Agans, K. N., Feng, Y. R., Fenton, K. A., Bossart, K. N., ... & Geisbert, T. W. (2014). A recombinant Hendra virus G glycoprotein subunit vaccine protects nonhuman primates against Hendra virus challenge. *Journal of virology*, JVI-00005.
- Montgomery, J. M., Hossain, M. J., Gurley, E., Carroll, D. S., Croisier, A., Bertherat, E., ... & Bell, M. R. (2008). Risk factors for Nipah virus encephalitis in Bangladesh. *Emerging infectious diseases*, 14(10), 1526.
- Morice, W. G. (2007). The immunophenotypic attributes of NK cells and NK-cell lineage lymphoproliferative disorders. *American journal of clinical pathology*, 127(6), 881-886.
- Murphy, A. M., & Grdzlishvili, V. Z. (2009). Identification of sendai virus L protein amino acid residues affecting viral mRNA cap methylation. *Journal of virology*, 83(4), 1669-1681.
- Murray, K., Selleck, P., Hooper, P., Hyatt, A., Gould, A., Gleeson, L., ... & Rodwell, B. (1995). A morbillivirus that caused fatal disease in horses and humans. *Science*, 268(5207), 94-97.
- Murray, K., Rogers, R., Selvey, L., Selleck, P., Hyatt, A., Gould, A., ... & Westbury, H. (1995). A novel morbillivirus pneumonia of horses and its transmission to humans. *Emerging infectious diseases*, 1(1), 31.
- Munster, V. J., Prescott, J. B., Bushmaker, T., Long, D., Rosenke, R., Thomas, T., ... & De Wit, E. (2012). Rapid Nipah virus entry into the central nervous system of hamsters via the olfactory route. *Scientific reports*, 2, 736.
- Montgomery, J. M., Hossain, M. J., Gurley, E., Carroll, D. S., Croisier, A., Bertherat, E., ... & Bell, M. R. (2008). Risk factors for Nipah virus encephalitis in Bangladesh. *Emerging infectious diseases*, 14(10), 1526.
- Coordinators, N. R. (2016). Database resources of the national center for biotechnology information. *Nucleic acids research*, 44(Database issue), D7.
- Nikolov, D. B., Li, C., Barton, W. A., & Himanen, J. P. (2005). Crystal structure of the ephrin-B1 ectodomain: implications for receptor recognition and signaling. *Biochemistry*, 44(33), 10947-10953.
- Negrete, O. A., Levroney, E. L., Aguilar, H. C., Bertolotti-Ciarlet, A., Nazarian, R., Tajyar, S., & Lee, B. (2005). EphrinB2 is the entry receptor for Nipah virus, an emergent deadly paramyxovirus. *Nature*, 436(7049), 401.

Negrete, O. A., Wolf, M. C., Aguilar, H. C., Enterlein, S., Wang, W., Mühlberger, E., ... & Lee, B. (2006). Two key residues in ephrinB3 are critical for its use as an alternative receptor for Nipah virus. *PLoS pathogens*, 2(2), e7.

Negrete, O. A., Wolf, M. C., Aguilar, H. C., Enterlein, S., Wang, W., Mühlberger, E., ... & Lee, B. (2006). Two key residues in ephrinB3 are critical for its use as an alternative receptor for Nipah virus. *PLoS pathogens*, 2(2), e7.

Nor, M. M., Gan, C. H., & Ong, B. L. (2000). Nipah virus infection of pigs in peninsular Malaysia. *Revue Scientifique et Technique-Office International des Epizooties*, 19(1), 160-165.

Norment, A. M., & Littman, D. R. (1988). A second subunit of CD8 is expressed in human T cells. *The EMBO journal*, 7(11), 3433-3439.

Ober, B. T., Summerfield, A., Mattlinger, C., Wiesmüller, K. H., Jung, G., Pfaff, E., ... & Rziha, H. J. (1998). Vaccine-induced, pseudorabies virus-specific, extrathymic CD4⁺ CD8⁺ memory T-helper cells in swine. *Journal of Virology*, 72(6), 4866-4873.

Ong, S. T., Yusoff, K., Kho, C. L., Abdullah, J. O., & Tan, W. S. (2009). Mutagenesis of the nucleocapsid protein of Nipah virus involved in capsid assembly. *Journal of General Virology*, 90(2), 392-397.

O'sullivan, J. D., Allworth, A. M., Paterson, D. L., Snow, T. M., Boots, R., Gleeson, L. J., ... & Bradfield, J. (1997). Fatal encephalitis due to novel paramyxovirus transmitted from horses. *The Lancet*, 349(9045), 93-95.

Pallister, J., Middleton, D., Wang, L. F., Klein, R., Haining, J., Robinson, R., ... & Chan, Y. P. (2011). A recombinant Hendra virus G glycoprotein-based subunit vaccine protects ferrets from lethal Hendra virus challenge. *Vaccine*, 29(34), 5623-5630.

Palomares, K., Vigant, F., Van Handel, B., Pernet, O., Chikere, K., Hong, P., ... & Mikkola, H. K. (2013). Nipah virus envelope-pseudotyped lentiviruses efficiently target ephrinB2-positive stem cell populations in vitro and bypass the liver sink when administered in vivo. *Journal of virology*, 87(4), 2094-2108.

Pager, C. T., Craft Jr, W. W., Patch, J., & Dutch, R. E. (2006). A mature and fusogenic form of the Nipah virus fusion protein requires proteolytic processing by cathepsin L. *Virology*, 346(2), 251-257.

Parashar, U. D., Sunn, L. M., Ong, F., Mounts, A. W., Arif, M. T., Ksiazek, T. G., ... & Othman, G. (2000). Case-control study of risk factors for human infection with a new zoonotic paramyxovirus, Nipah virus, during a 1998–1999 outbreak of severe encephalitis in Malaysia. *The Journal of infectious diseases*, 181(5), 1755-1759.

Parisien, J. P., Bamming, D., Komuro, A., Ramachandran, A., Rodriguez, J. J., Barber, G., ... & Horvath, C. M. (2009). A shared interface mediates paramyxovirus interference with antiviral RNA helicases MDA5 and LGP2. *Journal of virology*, 83(14), 7252-7260.

- Paton, N. I., Leo, Y. S., Zaki, S. R., Auchus, A. P., Lee, K. E., Ling, A. E., ... & Sng, I. (1999). Outbreak of Nipah-virus infection among abattoir workers in Singapore. *The Lancet*, 354(9186), 1253-1256.
- Pasquale, E. B. (2008). Eph-ephrin bidirectional signaling in physiology and disease. *Cell*, 133(1), 38-52.
- Pescovitz, M. D., Lunney, J. K., & Sachs, D. H. (1984). Preparation and characterization of monoclonal antibodies reactive with porcine PBL. *The Journal of Immunology*, 133(1), 368-375.
- Piccioli, D., Sbrana, S., Melandri, E., & Valiante, N. M. (2002). Contact-dependent stimulation and inhibition of dendritic cells by natural killer cells. *Journal of Experimental Medicine*, 195(3), 335-341.
- Piriou-Guzylack, L., & Salmon, H. (2008). Membrane markers of the immune cells in swine: an update. *Veterinary research*, 39(6), 1.
- Playford, E. G., McCall, B., Smith, G., Slinko, V., Allen, G., Smith, I., ... & Field, H. (2010). Human Hendra virus encephalitis associated with equine outbreak, Australia, 2008. *Emerging infectious diseases*, 16(2), 219.
- Pernet, O., Pohl, C., Ainouze, M., Kweder, H., & Buckland, R. (2009). Nipah virus entry can occur by macropinocytosis. *Virology*, 395(2), 298-311.
- Pelkmans, L., & Helenius, A. (2002). Endocytosis via caveolae. *Traffic*, 3(5), 311-320.
- Poliakov, A., Cotrina, M., & Wilkinson, D. G. (2004). Diverse roles of eph receptors and ephrins in the regulation of cell migration and tissue assembly. *Developmental cell*, 7(4), 465-480.
- Pulliam, J. R., Epstein, J. H., Dushoff, J., Rahman, S. A., Bunning, M., Jamaluddin, A. A., ... & Daszak, P. (2012). Agricultural intensification, priming for persistence and the emergence of Nipah virus: a lethal bat-borne zoonosis. *Journal of the Royal Society Interface*, 9(66), 89-101.
- Piriou-Guzylack, L., & Salmon, H. (2008). Membrane markers of the immune cells in swine: an update. *Veterinary research*, 39(6), 1.
- PyMOL The PyMOL Molecular Graphics System, Version 2.0 Schrödinger, LLC.
- Rawlings, J. S., Rosler, K. M., & Harrison, D. A. (2004). The JAK/STAT signaling pathway. *Journal of cell science*, 117(8), 1281-1283.
- Reddy, N. J., Borgs, P., & Wilkie, B. N. (2000). Cytokine mRNA expression in leukocytes of efferent lymph from stimulated lymph nodes in pigs. *Veterinary immunology and immunopathology*, 74(1-2), 31-46.

- Reynes, J. M., Counor, D., Ong, S., Faure, C., Seng, V., Molia, S., ... & Sarthou, J. L. (2005). Nipah virus in Lyle's flying foxes, Cambodia. *Emerging infectious diseases*, *11*(7), 1042.
- Razani, B., Woodman, S. E., & Lisanti, M. P. (2002). Caveolae: from cell biology to animal physiology. *Pharmacological reviews*, *54*(3), 431-467.
- Rodriguez, J. J., Parisien, J. P., & Horvath, C. M. (2002). Nipah virus V protein evades alpha and gamma interferons by preventing STAT1 and STAT2 activation and nuclear accumulation. *Journal of virology*, *76*(22), 11476-11483.
- Rodriguez, J. J., & Horvath, C. M. (2004). Host evasion by emerging paramyxoviruses: Hendra virus and Nipah virus v proteins inhibit interferon signaling. *Viral immunology*, *17*(2), 210-219.
- Rodriguez, J. J., Cruz, C. D., & Horvath, C. M. (2004). Identification of the nuclear export signal and STAT-binding domains of the Nipah virus V protein reveals mechanisms underlying interferon evasion. *Journal of virology*, *78*(10), 5358-5367.
- Rockx, B., Brining, D., Kramer, J., Callison, J., Ebihara, H., Mansfield, K., & Feldmann, H. (2011). Clinical outcome of henipavirus infection in hamsters is determined by the route and dose of infection. *Journal of virology*, JVI-00473.
- Rockx, B., Bossart, K. N., Feldmann, F., Geisbert, J. B., Hickey, A. C., Brining, D., ... & Long, D. (2010). A novel model of lethal Hendra virus infection in African green monkeys and the effectiveness of ribavirin treatment. *Journal of virology*, *84*(19), 9831-9839.
- Rota, P. A., & Lo, M. K. (2012). Molecular virology of the henipaviruses. In *Henipavirus* (pp. 41-58). Springer, Berlin, Heidelberg.
- Sánchez, C., Doménech, N., Vázquez, J., Alonso, F., Ezquerra, A., & Domínguez, J. (1999). The porcine 2A10 antigen is homologous to human CD163 and related to macrophage differentiation. *The Journal of Immunology*, *162*(9), 5230-5237.
- Satterfield, B. A., Cross, R. W., Fenton, K. A., Agans, K. N., Basler, C. F., Geisbert, T. W., & Mire, C. E. (2015). The immunomodulating V and W proteins of Nipah virus determine disease course. *Nature communications*, *6*, 7483.
- Singh, M., Berger, B., & Kim, P. S. (1999). LearnCoil-VMF: computational evidence for coiled-coil-like motifs in many viral membrane-fusion proteins¹. *Journal of molecular biology*, *290*(5), 1031-1041.
- Shiell, B. J., Gardner, D. R., Cramer, G., Eaton, B. T., & Michalski, W. P. (2003). Sites of phosphorylation of P and V proteins from Hendra and Nipah viruses: newly emerged members of Paramyxoviridae. *Virus research*, *92*(1), 55-65.

- Shaw, M. L., Cardenas, W. B., Zamarin, D., Palese, P., & Basler, C. F. (2005). Nuclear localization of the Nipah virus W protein allows for inhibition of both virus-and toll-like receptor 3-triggered signaling pathways. *Journal of virology*, 79(10), 6078-6088.
- Shaw, M. L., García-Sastre, A., Palese, P., & Basler, C. F. (2004). Nipah virus V and W proteins have a common STAT1-binding domain yet inhibit STAT1 activation from the cytoplasmic and nuclear compartments, respectively. *Journal of virology*, 78(11), 5633-5641.
- Sleeman, K., Bankamp, B., Hummel, K. B., Lo, M. K., Bellini, W. J., & Rota, P. A. (2008). The C, V and W proteins of Nipah virus inhibit minigenome replication. *Journal of General Virology*, 89(5), 1300-1308.
- Smith, I., Broos, A., de Jong, C., Zeddeman, A., Smith, C., Smith, G., ... & Tachedjian, M. (2011). Identifying Hendra virus diversity in pteropid bats. *PLoS One*, 6(9), e25275.
- Stachowiak, B., & Weingartl, H. M. (2012). Nipah virus infects specific subsets of porcine peripheral blood mononuclear cells. *PloS one*, 7(1), e30855.
- Summerfield, A., Rziha, H. J., & Saalmüller, A. (1996). Functional characterization of porcine CD4+ CD8+ extrathymic T lymphocytes. *Cellular immunology*, 168(2), 291-296.
- Summerfield, A., & McCullough, K. C. (2009). The porcine dendritic cell family. *Developmental & Comparative Immunology*, 33(3), 299-309.
- Saha, K., Zhang, J., Gupta, A., Dave, R., Yimen, M., & Zerhouni, B. (2001). Isolation of primary HIV-1 that target CD8+ T lymphocytes using CD8 as a receptor. *Nature medicine*, 7(1), 65.
- Saalmüller, A., Pauly, T., Höhlich, B. J., & Pfaff, E. (1999). Characterization of porcine T lymphocytes and their immune response against viral antigens. *Journal of biotechnology*, 73(2-3), 223-233.
- Smit, J. M., Moesker, B., Rodenhuis-Zybert, I., & Wilschut, J. (2011). Flavivirus cell entry and membrane fusion. *Viruses*, 3(2), 160-171.
- Srouf, E. F., Leemhuis, T., Janski, L., Redmond, R., & Jansen, J. (1990). Cytolytic activity of human natural killer cell subpopulations isolated by four- color immunofluorescence flow cytometric cell sorting. *Cytometry: The Journal of the International Society for Analytical Cytology*, 11(3), 442-446.
- Stabel, T. J., Bolin, S. R., Pesch, B. A., & Rahner, T. E. (2000). A simple and rapid flow cytometric method for detection of porcine cell surface markers. *Journal of immunological methods*, 245(1-2), 147-152.
- Shiue, L. I. L. Y., Gorman, S. D., & Parnes, J. R. (1988). A second chain of human CD8 is expressed on peripheral blood lymphocytes. *Journal of Experimental Medicine*, 168(6), 1993-2005.
- Sun, J., & Kavafhas, P. B. (1997). Comparison of the Roles of CD8aa and CD8aP in Interaction With MHC Class I'.

Talekar, A., DeVito, I., Salah, Z., Palmer, S. G., Chattopadhyay, A., Rose, J. K., ... & Porotto, M. (2013). Identification of a region in the stalk domain of the Nipah virus receptor binding protein that is critical for fusion activation. *Journal of virology*, JVI-01646.

Tamin, A., Harcourt, B. H., Ksiazek, T. G., Rollin, P. E., Bellini, W. J., & Rota, P. A. (2002). Functional properties of the fusion and attachment glycoproteins of Nipah virus. *Virology*, 296(1), 190-200.

Tan, K. S., Tan, C. T., & Goh, K. J. (1999). Epidemiological aspects of Nipah virus infection. *Neurol J Southeast Asia*, 4(1), 77-81.

Tan, C. T., & Tan, K. S. (2001). Nosocomial transmissibility of Nipah virus. *The Journal of infectious diseases*, 184(10), 1367-1367.

Tan, C. T., Goh, K. J., Wong, K. T., Sarji, S. A., Chua, K. B., Chew, N. K., ... & Thayaparan, T. (2002). Relapsed and late-onset Nipah encephalitis. *Annals of neurology*, 51(6), 703-708.

Taub, D. D., Anver, M., Oppenheim, J. J., Longo, D. L., & Murphy, W. J. (1996). T lymphocyte recruitment by interleukin-8 (IL-8). IL-8-induced degranulation of neutrophils releases potent chemoattractants for human T lymphocytes both in vitro and in vivo. *The Journal of clinical investigation*, 97(8), 1931-1941.

Travers, P., Walport, M. J., Janeway, C., & Murphy, K. P. (2008). *Janeway's immunobiology*. Garland Science.

Trinchieri, G. (1989). Biology of natural killer cells. In *Advances in immunology* (Vol. 47, pp. 187-376). Academic Press.

Uppal, P. K. (2000). Emergence of Nipah virus in Malaysia. *Annals of the New York Academy of Sciences*, 916(1), 354-357.

Vivier, E., Tomasello, E., Baratin, M., Walzer, T., & Ugolini, S. (2008). Functions of natural killer cells. *Nature immunology*, 9(5), 503.

Vogt, C., Eickmann, M., Diederich, S., Moll, M., & Maisner, A. (2005). Endocytosis of the Nipah virus glycoproteins. *Journal of virology*, 79(6), 3865-3872.

Wang, L. F., Michalski, W. P., Yu, M., Pritchard, L. I., Crameri, G., Shiell, B., & Eaton, B. T. (1998). A Novel P/V/C Gene in a New Member of the Paramyxoviridae Family, Which Causes Lethal Infection in Humans, Horses, and Other Animals. *Journal of virology*, 72(2), 1482-1490.

Wang, H. U., Chen, Z. F., & Anderson, D. J. (1998). Molecular distinction and angiogenic interaction between embryonic arteries and veins revealed by ephrin-B2 and its receptor Eph-B4. *Cell*, 93(5), 741-753.

Wang, L. F., Harcourt, B. H., Yu, M., Tamin, A., Rota, P. A., Bellini, W. J., & Eaton, B. T. (2001). Molecular biology of Hendra and Nipah viruses. *Microbes and infection*, 3(4), 279-287.

- Wang, Y. E., Park, A., Lake, M., Pentecost, M., Torres, B., Yun, T. E., ... & Lee, B. (2010). Ubiquitin-regulated nuclear-cytoplasmic trafficking of the Nipah virus matrix protein is important for viral budding. *PLoS pathogens*, 6(11), e1001186.
- Weatherman, S., Feldmann, H., & de Wit, E. (2018). Transmission of henipaviruses. *Current opinion in virology*, 28, 7-11.
- Wierda, W. G., Johnson, B. D., Dato, M. E., & Kim, Y. B. (1993). Induction of porcine granulocyte-mediated tumor cytotoxicity by two distinct monoclonal antibodies against lytic trigger molecules (PNK-E/G7). *The Journal of Immunology*, 151(12), 7117-7127.
- Weingartl HM (2015). Hendra and Nipah viruses: pathogenesis, animal models and recent breakthroughs in vaccination. *Vaccine: Development and Therapy*.5: 59-74.
- Weingartl, H. M., Berhane, Y., Caswell, J. L., Loosmore, S., Audonnet, J. C., Roth, J. A., & Czub, M. (2006). Recombinant nipah virus vaccines protect pigs against challenge. *Journal of virology*, 80(16), 7929-7938.
- Weingartl, H., Czub, S., Copps, J., Berhane, Y., Middleton, D., Marszal, P., ... & Czub, M. (2005). Invasion of the central nervous system in a porcine host by Nipah virus. *Journal of virology*, 79(12), 7528-7534.
- Whitman, S. D., & Dutch, R. E. (2007). Surface density of the Hendra G protein modulates Hendra F protein-promoted membrane fusion: role for Hendra G protein trafficking and degradation. *Virology*, 363(2), 419-429.
- Wong, K. T. (2000). Emerging and re-emerging epidemic encephalitis: a tale of two viruses. *Neuropathology and applied neurobiology*, 26(4), 313-318.
- Wong, K. T., Shieh, W. J., Kumar, S., Norain, K., Abdullah, W., Guarner, J., ... & Goh, K. J. (2002). Nipah virus infection: pathology and pathogenesis of an emerging paramyxoviral zoonosis. *The American journal of pathology*, 161(6), 2153-2167.
- Wong, K. T., & Tan, C. T. (2012). Clinical and pathological manifestations of human henipavirus infection. In *Henipavirus*(pp. 95-104). Springer, Berlin, Heidelberg.
- Wu, Z., Yang, L., Yang, F., Ren, X., Jiang, J., Dong, J., ... & Jin, Q. (2014). Novel henipa-like virus, Mojiang paramyxovirus, in rats, China, 2012. *Emerging infectious diseases*, 20(6), 1064.
- Xu, K., Chan, Y. P., Rajashankar, K. R., Khetawat, D., Yan, L., Kolev, M. V., ... & Nikolov, D. B. (2012). New insights into the Hendra virus attachment and entry process from structures of the virus G glycoprotein and its complex with Ephrin-B2. *PLoS One*, 7(11), e48742.
- Xu, D., & Ma, H. M. (2016). Molecular characterization and tissue expression profile of porcine Ephrin-B2. *Genetics and molecular research: GMR*, 15(1), 15017463-15017463.

- Xue, L. C., Jordan, R. A., El-Manzalawy, Y., Dobbs, D., & Honavar, V. (2011, August). Ranking docked models of protein-protein complexes using predicted partner-specific protein-protein interfaces: a preliminary study. In *Proceedings of the 2nd ACM Conference on Bioinformatics, Computational Biology and Biomedicine* (pp. 441-445). ACM.
- Xue, L. C., Dobbs, D., & Honavar, V. (2011). HomPPI: a class of sequence homology based protein-protein interface prediction methods. *BMC bioinformatics*, *12*(1), 244.
- Xue, L. C., Jordan, R. A., Yasser, E. M., Dobbs, D., & Honavar, V. (2014). DockRank: Ranking docked conformations using partner-specific sequence homology-based protein interface prediction. *Proteins: Structure, Function, and Bioinformatics*, *82*(2), 250-267.
- Yamaguchi, M., Kitagawa, Y., Zhou, M., Itoh, M., & Gotoh, B. (2014). An anti-interferon activity shared by paramyxovirus C proteins: inhibition of Toll-like receptor 7/9-dependent alpha interferon induction. *FEBS letters*, *588*(1), 28-34.
- Yob, J. M., Field, H., Rashdi, A. M., Morrissy, C., van der Heide, B., Rota, P., ... & Ksiazek, T. (2001). Nipah virus infection in bats (order Chiroptera) in peninsular Malaysia. *Emerging infectious diseases*, *7*(3), 439.
- Yoneda, M., Guillaume, V., Sato, H., Fujita, K., Georges-Courbot, M. C., Ikeda, F., ... & Kai, C. (2010). The nonstructural proteins of Nipah virus play a key role in pathogenicity in experimentally infected animals. *PLoS One*, *5*(9), e12709.
- Yu, G., Luo, H., Wu, Y., & Wu, J. (2003). Mouse ephrinB3 augments T-cell signaling and responses to T-cell receptor ligation. *Journal of Biological Chemistry*, *278*(47), 47209-47216.
- Yu, G., Luo, H., Wu, Y., & Wu, J. (2003). Ephrin B2 induces T cell costimulation. *The Journal of Immunology*, *171*(1), 106-114.
- Zamoyska, R. (1994). The CD8 coreceptor revisited: one chain good, two chains better. *Immunity*, *1*(4), 243-246.
- Zhang, Y., Wallace, D. L., De Lara, C. M., Ghattas, H., Asquith, B., Worth, A., ... & Macallan, D. C. (2007). In vivo kinetics of human natural killer cells: the effects of ageing and acute and chronic viral infection. *Immunology*, *121*(2), 258-265.
- Zhu, Q., Biering, S. B., Mirza, A. M., Grasseschi, B. A., Mahon, P. J., Lee, B., ... & Iorio, R. M. (2013). Individual N-glycans added at intervals along the stalk of the Nipah virus G protein prevent fusion, but do not block the interaction with the homologous F protein. *Journal of virology*, JVI-03084.
- Zhu, Z., Bossart, K. N., Bishop, K. A., Cramer, G., Dimitrov, A. S., McEachern, J. A., ... & Dimitrov, D. S. (2008). Exceptionally potent cross-reactive neutralization of Nipah and Hendra viruses by a human monoclonal antibody. *The Journal of infectious diseases*, *197*(6), 846-853.

Zuckermann, F. A., Pescovitz, M. D., Aasted, B., Dominguez, J., Trebichavsky, I., Novikov, B., ... & Lunney, J. K. (1998). Report on the analyses of mAb reactive with porcine CD8 for the second international swine CD workshop. *Veterinary immunology and immunopathology*, 60(3-4), 291-303.

Zamora, D. O., Babra, B., Pan, Y., Planck, S. R., & Rosenbaum, J. T. (2006). Human leukocytes express ephrinB2 which activates microvascular endothelial cells. *Cellular immunology*, 242(2), 99-109.